

Hybridized Biomass-driven Combined Heat and Power Systems  
Optimization

Considering Reliability, Availability, and Maintainability Criteria

Masoud Rezaei

A Thesis

In the Department

of

Building, Civil, and Environmental Engineering (BCEE)

Presented in partial fulfillment of the requirements

for the degree of

Doctor of Philosophy (Civil Engineering) at

Concordia University,

Montreal, Quebec, Canada

August 2025



## **Abstract**

### **Hybridized Biomass-driven Combined Heat and Power Systems Optimization Considering Reliability, Availability, and Maintainability Criteria Masoud Rezaei, Ph.D. Concordia University, 2025**

Despite the increasing use of renewables for energy supply and considering the history of using them for energy generation purposes, new challenges associated with their utilization emerge. For biomass-powered energy systems, issues such as seasonality, supply chain problems, heat content of resources, weather pollution, environmental contamination, and energy conversion limitations put the availability and affordability of such systems into question. The optimization of energy systems considering their reliability, availability, and maintainability (RAM) parameters and constraints could considerably affect system design and operation.

This research proposes and develops an integrated RAM-optimization methodology for hybrid biomass-powered energy systems. The methodology handles nonlinear single or multi-objective functions that minimize costs and emissions while satisfying RAM constraints. The methodology empowers designers to account for fuel and pollution chemical compositions, feedstock logistics and modular system configurations. Multiple Criteria Decision-Making (MCDM) techniques, such as TOPSIS, are used to help in the identification of optimal values based on system performance criteria.

Three progressive models were proposed and developed as part of the methodology. The first model integrates biomass and geothermal modules for heat-only applications at a single-building scale. The second extends to biomass-based combined heat and power (BCHP) systems at the district level based on the building model of the first case, explicitly integrating RAM function as constraints. The third model adds hydrogen production to heat and electricity generation, illustrating the framework's ability to be a trigeneration system for district-level deployment. Case studies, defined for Kuujuaq in Northern Québec, Canada, help to validate the methodology's application under real conditions.

Sensitivity analysis of such methodology and model is performed by scenarioizing and via scenarios considering biomass chemical compositions, distance from consumption areas, and RAM parameters for a single building or a complex of buildings. Validation of the results was performed by several activities such as expert feedback, optimization method features, and their results' comparative analysis.

## ACKNOWLEDGMENTS

I would like to express my sincere gratitude to Concordia University and my dear Supervisor Dr. Nasiri for supporting me and providing the exceptional environment and resources that have contributed significantly to my academic journey. The support and guidance from the faculty and staff have been invaluable throughout this process.

I would like to acknowledge the Natural Sciences and Engineering Research Council of Canada (NSERC) and BBA company for their generous financial and technical support, which made this research possible. Their funding has played a crucial role in enabling me to pursue and complete my PhD studies.

I dedicate this research to my Parents, notably my deceased Father that inspired me for continuing my field in academia, research and science.

## List of publications

- Masoud Rezaei, and Fuzhan Nasiri (2019). The Technology Selection Analysis Based on Bi-Level Enviro-economic Optimization of a Biomass-Powered CHP'' In Proceedings of *International Association for Energy Economics (IAEE) Conference*, May 29 – June 01, MONTRÉAL, QC, Canada. [https://symposia.gerad.ca/iaee2019/en/schedule/view\\_document/8217](https://symposia.gerad.ca/iaee2019/en/schedule/view_document/8217)
- Masoud Rezaei, Mohammad Sameti, and Fuzhan Nasiri (2021). Biomass-fuelled combined heat and power: integration in district heating and thermal-energy storage *Clean Energy*, 5(1), 44–56. <https://doi.org/10.1093/ce/zkaa031>
- Masoud Rezaei, Mohammad Sameti, and Fuzhan Nasiri (2021). An enviro-economic optimization of a hybrid energy system from biomass and geothermal resources for low-enthalpy areas, *Energy and Climate Change*, 2, 100040. <https://doi.org/10.1016/j.egycc.2021.100040>
- Masoud Rezaei, Mohammad Sameti, and Fuzhan Nasiri (2024). An enviro-economic RAM-based optimization of biomass-driven combined heat and power generation, *Biomass Conversion and Biorefinery*, 14, 24427–24442. <https://doi.org/10.1007/s13399-023-04713-9>
- Masoud Rezaei, Mohammad Sameti, and Fuzhan Nasiri (2024). Design optimization for an integrated tri-generation of heat, electricity, and hydrogen powered by biomass in cold climates, *International Journal of Thermofluids*, 22, 100618. <https://doi.org/10.1016/j.ijft.2024.100618>

This thesis contains extractions of the data and information of these publications such as cases, methods or methodologies and results in its chapters.

The above listed journal articles were published in collaboration with co-authors. It should be noted that the second author, Dr. Mohammad Sameti, assisted by reviewing and editing the manuscripts for publication purposes. The main research ideas, model development, methodological framework, and scientific contributions of all four articles were entirely conceived and conducted by Masoud Rezaei. Accordingly, the authorship reflects editorial and supervisory support, while the intellectual and scientific ownership of the research belongs to the doctoral candidate.

I, Masoud Rezaei, gratefully acknowledge the contributions of Dr. Mohammad Sameti to the published papers, particularly for his careful editing, revisions, and assistance in refining the manuscripts.

I also sincerely appreciate the support of Dr. Fuzhan Nasiri, the third author of the papers, for his supervision and guidance during my PhD studies.

## *Table of Contents*

<b>1. Chapter 1: Introduction.....</b>	<b>1</b>
1.1 Background .....	1
1.2 Problem Statement .....	4
1.3 Research Objectives .....	5
1.4 Thesis Organization.....	8
<b>2 Chapter 2: Literature Review .....</b>	<b>11</b>
2.1 DHS .....	11
2.2 Biomass Energy Systems .....	14
2.3 CHP .....	22
2.4 Optimization Approaches: DHS.....	30
2.5 CHP Optimization .....	40
2.6 CHP Reliability Analysis .....	50
2.7 Integration of Energy Storage .....	51
2.8 Green Hydrogen Production.....	59
2.9 Biomass-Based Hydrogen Energy Systems .....	63
2.10 Biomass-Based Hybrid Energy Systems Optimization.....	65
2.11 CHP-DHS Optimization Challenges and future.....	67
2.12 Research Gap Analysis.....	68
<b>3 Chapter 3: Methodologies .....</b>	<b>71</b>
3.1 Background .....	72
3.2 Formulation of Reliability, Maintainability and Availability .....	73
3.2.1 Reliability .....	73
3.2.2 Maintainability .....	76
3.2.3 Availability.....	77
3.2.4 Weibull function applicability.....	78
3.3 Proposed and developed Models.....	80
3.3.1 Model 1: Bio-Geo Hybrid System .....	82

3.3.2	Model 2: Biomass for CHP Application - BCHP .....	93
3.3.3	Model 3: BCHP-Hydrogen generation.....	100
3.4	Summary of the Proposed and developed Methods .....	107
<b>4</b>	<b>Chapter 4: Case Studies, Results, and Discussions .....</b>	<b>110</b>
4.1	District Heating Load Calculation.....	111
4.1.1	Kuujuaq Weather .....	115
4.1.2	Building Modeling .....	120
4.1.3	Building Energy Analysis .....	122
4.2	Case 1: Bio-Geo Hybrid System for Only Heating Approach .....	126
4.3	Case 2: CHP From Biomass.....	131
4.4	Case 3: Heat, Power, and Hydrogen Triple Generation.....	141
4.5	Chapter Summary.....	152
<b>5</b>	<b>Chapter 5: Conclusions.....</b>	<b>155</b>
5.1	Summary .....	155
5.2	Contributions .....	157
5.3	Limitations .....	158
5.4	Future Research Directions .....	160
<b>6</b>	<b>References .....</b>	<b>162</b>

## *List of figures*

<b>Figure 1</b> .....	2
<b>Figure 2</b> .....	3
<b>Figure 3</b> .....	7
<b>Figure 4</b> .....	13
<b>Figure 5</b> .....	14
<b>Figure 6</b> .....	32
<b>Figure 7</b> .....	33
<b>Figure 8</b> .....	83
<b>Figure 9</b> .....	85
<b>Figure 10</b> .....	96
<b>Figure 11</b> .....	96
<b>Figure 12</b> .....	103
<b>Figure 13</b> .....	104
<b>Figure 14</b> .....	109
<b>Figure 15</b> .....	114
<b>Figure 16</b> .....	114
<b>Figure 17</b> .....	116
<b>Figure 18</b> .....	120
<b>Figure 19</b> .....	123
<b>Figure 20</b> .....	123
<b>Figure 21</b> .....	124
<b>Figure 22</b> .....	124
<b>Figure 23</b> .....	127
<b>Figure 24</b> .....	128
<b>Figure 25</b> .....	129
<b>Figure 26</b> .....	130
<b>Figure 27</b> .....	131
<b>Figure 28</b> .....	133
<b>Figure 29</b> .....	133
<b>Figure 30</b> .....	134
<b>Figure 31</b> .....	135
<b>Figure 32</b> .....	136
<b>Figure 33</b> .....	136
<b>Figure 34</b> .....	137
<b>Figure 35</b> .....	137
<b>Figure 36</b> .....	142
<b>Figure 37</b> .....	142
<b>Figure 38</b> .....	142
<b>Figure 39</b> .....	142
<b>Figure 40</b> .....	143
<b>Figure 41</b> .....	143
<b>Figure 42</b> .....	143
<b>Figure 43</b> .....	143
<b>Figure 44</b> .....	144
<b>Figure 45</b> .....	144
<b>Figure 46</b> .....	145
<b>Figure 47</b> .....	145
<b>Figure 48</b> .....	146

<b>Figure 49</b> .....	146
<b>Figure 50</b> .....	147
<b>Figure 51</b> .....	147
<b>Figure 52</b> .....	148
<b>Figure 53</b> .....	148
<b>Figure 54</b> .....	149
<b>Figure 55</b> .....	149
<b>Figure 56</b> .....	150
<b>Figure 57</b> .....	150
<b>Figure 58</b> .....	151
<b>Figure 59</b> .....	151
<b>Figure 60</b> .....	152

***List of tables***

<b>Table 1</b> .....	15
<b>Table 2</b> .....	17
<b>Table 3</b> .....	18
<b>Table 4</b> .....	23
<b>Table 5</b> .....	26
<b>Table 6</b> .....	39
<b>Table 7</b> .....	40
<b>Table 8</b> .....	44
<b>Table 9</b> .....	89
<b>Table 10</b> .....	92
<b>Table 11</b> .....	113
<b>Table 12</b> .....	117
<b>Table 13</b> .....	125
<b>Table 14</b> .....	127
<b>Table 15</b> .....	127
<b>Table 16</b> .....	130
<b>Table 17</b> .....	138
<b>Table 18</b> .....	139
<b>Table 19</b> .....	139
<b>Table 20</b> .....	139

## *Nomenclature*

A	Availability
AMTD	Arithmetic mean temperature difference
BLD	Base load design
BCHP	Biomass combined heat and power
CAD	Canadian Dollar
CC	Capital cost (CAD)
CHP	Combined heat and power
C <sub>op</sub>	Operation cost
DoE	Department of Energy
EES	Engineering equation solver
el(ec)	Electrical
FC	Final cost (CAD)
GA	Genetic algorithm
GEX	Ground heat exchangers
GSHP	Ground source heat pump
GMTD	Geometric mean temperature difference
GT	Gas turbine
HHV	High heat value
HHVW	High heat value woods
HPES	Hydrogen penetrated energy system

ICE	Internal combustion engine
i	Interest rate
LCA	Life cycle assessment
LCC	Life cycle cost
LHS	Latent heat storage
LHV	Low heat value
LHVW	Low heat value woods
LMTD	Logarithmic mean temperature difference
MCWB	Moisture content of wet biomass
MILP	Multi-integer linear programming
MHV	Medium heat value
MHVW	Medium heat value woods
MTBF	Mean time to failure (h)
MTTF	Mean time to failure
MTTR	Mean time to repair/restore (h)
MINLP	Multi-integer nonlinear programming
N	Number of maintenances
NLP	Non-linear programming
NHV	Net heat value
OC	Operation cost (CAD)

P	Rated power
$P_{el}$	Electrical module rated capacity (kW)
$P_{in}$	Compressor inlet pressure (bar)
$P_{out}$	Compressor outlet pressure (bar)
PCM	Phase change materials
PLD	Peak load design
Q	Hydrogen flow rate (kg/h)
R	Reliability
RAM	Reliability, availability, maintainability
R(t)	Reliability function
RCM	Reliability Centered Maintenance
SHS	Sensible heat storage
ST	Steam turbine
TES	Thermal energy storage
$\tau$	Usage (Utilization) times
$\tau_{el}$	Electrical module use time (h)
$\tau_{th}$	Thermal module use time (h)
$\tau_{hy}$	Hydrogen module use time (h)
T	Lifetime
$T_{(m)}$	Maintenance interval (h)

$T_{(m,el)}$	Maintenance interval for electrical module (h)
$T_{(m,th)}$	Maintenance interval for thermal module (h)
UHS	Underground hydrogen storage
UTES	Underground Thermal Storage
WEC	Wave energy converter
$\varphi$	Annuity factor
$\alpha$	Scale parameter
$\beta$	Shape parameter
m, n, x, y, z	Number of carbons, hydrogen, oxygen, nitrogen and sulfur atoms

## **1. Chapter 1: Introduction**

### **1.1 Background**

Biomass has long been used for energy generation. From direct burning in traditional furnaces to generate heat to using them along with steam boilers and turbines to cogenerate heat and electricity in district heating systems (DHSs), biomass is an option for supplying energy depending on the location. Biomass has also gained attention anew thanks to global environmental problems such as climate change and recently defined approaches such as combined heat and power (CHP), smart cities, hybrid energy generation, and technological advancements. However, using biomass for energy generation raises challenges concerning the supply chain, biomass processing, energy conversion efficiencies, environmental pollution, and contamination.

There are many parameters affecting the effectiveness of using biomass for energy generation. The seasonality of biomass feedstocks, stocking requirements, relatively lower content heat of biomass than fossil fuels, and low energy conversion efficiencies have deterred operators from relying solely on biomass-powered energy systems, especially when various types of energies are required at the same time.

Biomass exists in solid, liquid, and gaseous forms and has applications in other fields such as biofuel production and nutrients for animal or poultry breeding (Hassan et al., 2020).

Figure 1 shows the application of biomass in the energy and byproduct sectors.

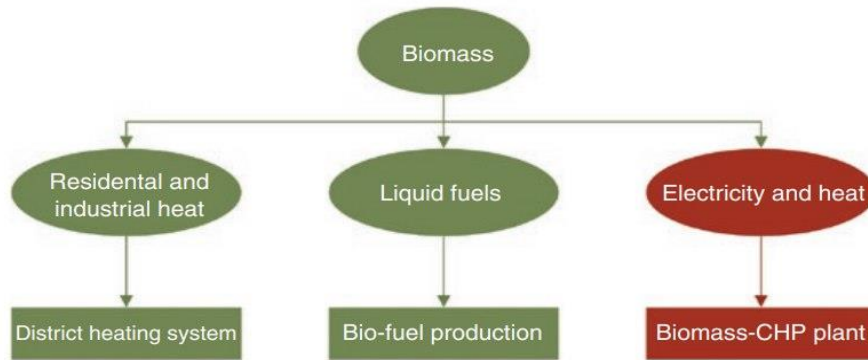


**Figure 1**

*Traditional Applications of Biomass as a Source of Energy*

Today, issues such as providing affordable energy resources for societies and climate change have encouraged employing biomass with the CHP concept via DHS. Despite problems, some features, such as a low or zero purchase price and its abundance in off-grid rural zones, still make biomass a viable option for delivering distributed or centralized energy (Brandoni et al., 2015).

The main parts of a biomass-powered CHP (BCHP) installation are feedstock receiving and preparation, biomass conversion, and power and heat production modules. Via a heat recovery module, the heat can be distributed through distributing networks to consumers such as a building complex (Figure 2).

BCHP systems can produce heat or steam for applications in industrial processes such as paper and pulp factories and for building an energy supply and district heating demands via a distribution network. The cofiring of biomass with other fuels in large CHP power plants has become increasingly common because of its higher efficiency compared to only generating heat.

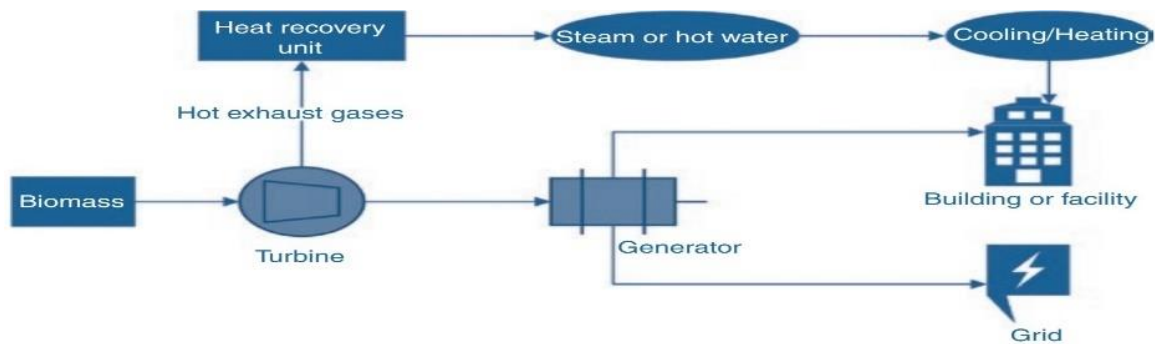


**Figure 2**

*Main Components of a Biomass-Driven CHP Connected to Grids and Buildings*

Cofiring in the BChP domain could have different meaning from CHP. Whereas cofiring in the energy generation sector is typically translated into the simultaneous generation of various sorts of energy, notably heat and electricity, cofiring in the biomass-powered systems sector means mixing biomass with fossil fuels (typically coal or natural gas) to be burned, substituting some portions of fossil fuels. It is one of the solutions for making up for low heat content or biomass wetness that reduces the generated energy or increases the leftovers that contaminate the air or environment. In this regard, cofiring uses an in-situ installation for a fossil fuel-powered system, with a slight modification for biomass handling and processing to provide biomass products for use in conjunction with fossil fuel. This approach is increasingly employed globally, and approximately 55 GW of coal-fired capacity is accompanied by biomass cofiring in North America and Europe (de Jong et al., 2012).

Possible configurations of cofiring in biomass-fired CHP setups are direct, parallel and indirect cofiring modes. In direct cofiring, biomass and another, usually fossil, fuel are supplied to the CHP boiler. The burners or CHP boiler may be shared or separated for biomass and the second fuel modules. In these configurations, solid biomass could be directly burned or converted into gas inside the gasification reactor and burned together with the second fuel.

In a parallel setup, biomass produces steam in a separate CHP boiler, and generated steam is fed into the coal-fired boiler. Woody biomasses, pulp and paper wastes, and agricultural residues are the three main biomass resources used in cofiring.

## **1.2 Problem Statement**

Biomass resources, combined heat and power (CHP) systems, and district heating (DH) networks involve multiple variables that affect energy efficiency, system cost, and the reliability and availability of energy supply and service quality. When these systems are integrated, their performance parameters often differ—and may even conflict—in terms of requirements and constraints. This makes a rigorous optimization approach essential to ensure dependable, reliable, and cost-effective operation.

Current analyses of biomass-powered systems (economic, techno-economic, LCC and LCA analyses that evaluate the total cost of an energy system and examine the environmental impacts across all life cycle stages respectively and enviro-economic analyses that try to balance economic and environmental objectives through optimization techniques) for design phase have two main limitations. First, they typically overlook or only partially address the reliability, availability, and maintainability (RAM) characteristics of energy resources (e.g., biomass, geothermal) and energy systems. Second, they rarely incorporate RAM parameters analytically into optimization frameworks to build a constrained RAM-optimization model. As a result, designers often rely on simplified redundancy strategies—such as oversizing components, adding backup modules, or maintaining unused energy pathways—to guarantee reliability and availability. These approaches lead to system overdesign and higher operation and maintenance costs.

A review of the literature on biomass-powered CHP, DH systems, and hybridized energy resources indicates that cost optimization in the presence of explicit, time-dependent reliability constraints remains underexplored. Few studies integrate RAM metrics—such as

mean time between failures (MTBF), hazard rate profiles, or mean time to repair/restore (MTTR)—into optimization models. Yet these parameters are critical, as they often interact in conflicting ways. For example, extending equipment usage time can improve cost efficiency, but it simultaneously reduces reliability and availability—an unfavorable trade-off for ensuring reliable energy service. This limitation highlights the need for an enviro-economic methodology that explicitly couples RAM analysis with optimization of biomass-based hybrid systems.

Furthermore, no established framework currently addresses the optimization of biomass-fired energy systems while integrating RAM criteria, feedstock chemical properties, hybridization with other renewables, and modular system configurations. The lack of reliable RAM data (e.g., MTBF, MTTF, MTTR) for biomass-powered energy systems further underscores the need for a structured methodology that unifies technical, economic, and reliability considerations in the design phase. This issue is especially significant in remote areas with harsh climates, where the infrastructure required for repairing and maintaining components and equipment is often unavailable.

### **1.3 Research Objectives**

This thesis aims to develop a more comprehensive, systematic, and technically robust methodology for the design, modeling, and optimization of hybrid biomass-powered energy systems, particularly for remote and off-grid communities with harsh climates. The primary goal is to integrate environmental, economic, technical, and reliability considerations into a joint RAM-optimization framework that supports cost-effective and reliable system operation. The specific objectives are as follows:

Objective 1: Develop a joint RAM-optimization methodology for biomass-powered systems

- Propose a methodology that simultaneously considers enviroeconomic criteria (fuel and pollution costs), system performance, and RAM metrics.
- Incorporate fuel and pollution chemical compositions (e.g., heat content, hydrogen, carbon, oxygen) and transportation distances as explicit input parameters in the optimization.
- Demonstrate that the methodology delivers system designs that balance cost efficiency with acceptable levels of reliability and availability, particularly in scenarios where repair and maintenance resources are limited.

Objective 2: Formulate and integrate RAM indicators and metrics

- Define probabilistic, time-dependent reliability functions (e.g., Weibull distribution) for system components.
- Consider maintenance strategies, such as ideal scheduled maintenance and maintenance intervals, as part of the optimization problem.
- Include key RAM indicators, including mean time to failure (MTTF), mean time between failures (MTBF), mean time to repair and restore (MTTR), and availability, ensuring that they serve as explicit constraints in the cost and performance optimization.
- Perform sensitivity and trade-off analyses between cost, reliability, and availability to account for these competing objectives.

Objective 3: Design a modular and flexible hybrid energy system framework

- Develop a modular design structure capable of incorporating or replacing system modules, including biomass, geothermal, hydrogen, solar, and wind components.
- Ensure the framework can adapt to different scales and configurations, such as building-level systems or district heating networks.
- Enable hybridization of energy products (heat, electricity, hydrogen) either individually or simultaneously, supporting multi-vector energy production.

Objective 4: Apply and validate the methodology in remote, off-grid community

contexts

- Conduct a case study for Kuujuaq, Northern Canada, to evaluate the feasibility of biomass-geothermal hybrid systems.
- Extend the methodology step by step to include heat-only, combined heat and power (CHP) configurations, and hydrogen hybridization (hydrogen, geothermal), demonstrating the broader applicability of the framework for remote or harsh climates with limited maintenance infrastructure.

Objective 5: Demonstrate the contribution of joint RAM-optimization to system design

- Show how integrating RAM metrics into optimization allows designers to obtain good-enough estimates of system performance parameters while minimizing costs.
- Highlight the advantages of explicitly modeling maintenance, fuel, and pollution costs in conjunction with RAM constraints.

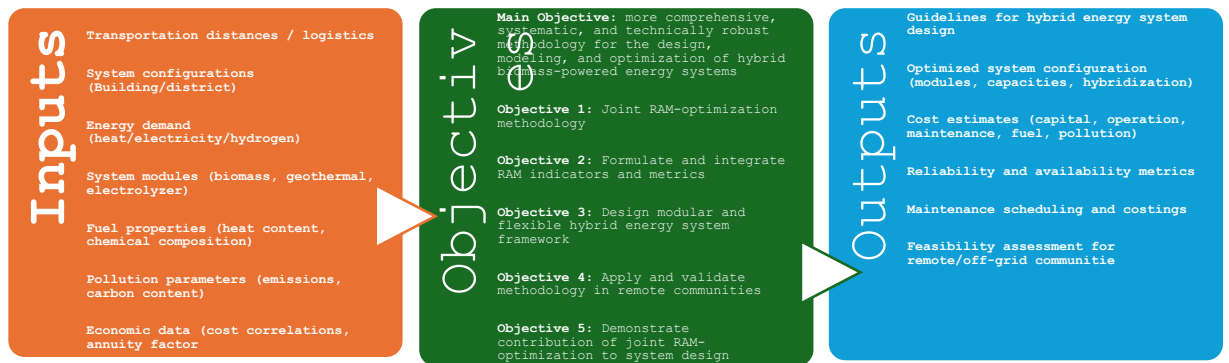


**Figure 3**

*Research Objectives and Their Linkage to Research Inputs and Outputs*

The proposed optimization approaches cover mostly the capital, fuel, and installation cost formulations or correlations, whereas operational, maintenance, or even pollution costs are either covered by LCC approaches or approximations.

## **1.4 Thesis Organization**

Chapter 2 provides a systematic review of the literature relevant to DHS, biomass-powered energy systems, energy generation concepts and technologies (including cogeneration and hybrid systems), thermal energy storage, and their design, optimization, and reliability assessment. It reviews the main concepts, methods, and approaches, and traces the historical development of systems and ideas in the field. In chapter 2, the most significant contributions in each domain are identified and existing methodologies for modeling, optimization, and performance assessment are evaluated. Particular emphasis is placed on works addressing DHS, biomass types and processing, cogeneration and hybrid generation, optimization frameworks, system modularity, RAM analyses, and applications in remote or off-grid communities. By addressing these topics and synthesizing the relevant findings, this chapter highlights the gaps and limitations of current approaches and establishes the theoretical foundation upon which the proposed research methodology is built.

In Chapter 3, the research methodology and case studies are proposed, formulated, and explained in detail. The chapter begins with background on the main research objective and the theoretical framework underpinning the integration of RAM indicators into optimization models for a B CHP system.

This is followed by the introduction and explanation of RAM variables, their definitions, and formulations. The extendable methodology and its associated case studies are then elaborated, beginning with a heat-only approach for a single building in the first case study, moving to a CHP approach for a district in the second case, and finally extending to a CHP–hydrogen generation approach for a district-level optimization problem. The scenario definitions and system configurations for each case study were guided by conclusions from previous case results as well as expert feedback.

For all three case studies, the optimization approaches and algorithms—including optimization and RAM analysis methods, assumptions, input data, objective functions, constraints, decision variables and performance parameters are presented. Methodological particularities and novelties are highlighted, such as the joint optimization approach that couples RAM analysis with enviro-economic assessment for second and third case studies, as well as the modular system design principles that allow for flexible configurations across multiple energy sources (biomass, geothermal, hydrogen). Furthermore, this chapter discusses the algorithms, tools, and methods employed, the data requirements for objective functions and constraints, and the rationale behind the chosen methodological pathways. The aim is to provide a clear and transparent framework that can be applied to different contexts and further analyzed in the next chapter.

In Chapter 4, the results, applicability, and effectiveness of the proposed methodologies through defined case studies are demonstrated. The case studies focus on Northern Canada because its isolated communities, severe weather, logistical costs, and reliability challenges, making it a relevant testbed for the application of a biomass-powered hybrid energy system. Each case study reflects its geographical, environmental, and configuration context, with particular emphasis on remote and off-grid communities where energy reliability and resilience are critical. For each case, the chapter presents the data and assumptions used (fuel properties, logistics, demand profiles, and constraints), the applied methodology, and the resulting optimized system configurations. Sensitivity analyses are carried out under different scenarios to compare and highlight the advantages of the proposed methods. The results provide insights into cost-effectiveness, pollution generation and reliability levels, energy generation profiles with optimal rated capacities and operating times, maintenance strategies, and availability performance. Taken together, the three case studies

demonstrate the flexibility, adaptability, and transferability of the methodologies and predictions, while also illustrating their practical relevance in real-world scenarios.

Chapter 5 serves as the final and concluding chapter synthesizing the findings of the research, extracting the major conclusions, and discussing their implications for both theory and practice. Key contributions include the integration of RAM into optimization, the application of a joint RAM–optimization approach to hybrid energy system design, the application of this methodology to a biomass-powered energy system, the formulation of modular frameworks for diverse energy mixes, and the demonstration of practical feasibility in remote areas with harsh climates. Beyond these contributions, this chapter also addresses the limitations of the research, such as assumptions in data availability, the generalizability of applications, and validation constraints. Finally, it highlights candidate subjects and issues for future research, including potential extensions to emerging energy carriers and demands, integration with smart grid technologies, and the modeling of dynamic transient behavior in such systems.

## **2 Chapter 2: Literature Review**

This chapter provides a review of the research and studies that frame the foundation of the proposed work. It begins by reviewing DHS, followed by biomass-based energy systems, and then a detailed discussion of CHP technologies. The chapter then presents optimization approaches for the design of DHS and CHP systems. The review expands to include research about reliability analyses, the integration of thermal energy storage and green hydrogen production. Attention is also given to the methodological and practical issues in hydrogen generation from biomass and in optimizing hybrid DHS–CHP systems. By synthesizing the studies and evaluating their contributions, this chapter identifies research gaps and limitations that motivated the development of a RAM-integrated optimization methodology proposed and developed in the subsequent chapters.

### **2.1 DHS**

A DHS is a system that carries energy for multiple applications in one or more buildings. The energy is carried by hot water, steam, oil, and the like for the purposes of domestic hot water supply, heating, or cooling demands. The distribution network consists of a network of pipes and pump houses for carrying heat from a plant to substations, which are the heat exchangers used to extract energy from the working fluid for select purposes (Hassan et al., 2020).

Energy demands or load profiles of the consumers normally determine the steps toward the system design, configuration, sizing, and optimization. From the design approach point of view, the peak load criterion is used to ensure the reliable performance of the system and available energies in case of maximum load demand. ASHRAE or other regional standards specifically determine the procedures to follow for calculating the peak load and applying the peak load design (PLD) approach (Jie et al., 2015; Nussbaumer et al., 2016). Usually, an oversizing factor is applied to peak energy demand to ensure supply reliability of systems for

unprecedented or unexpected circumstances. For example, pump sizing optimization is typically performed based on PLD (de Jong et al., 2012).

However, sometimes, the base load design (BLD) is used as the main approach for the DHS sizing, notably when DHS is coupled with CHP; BLD is the favorable criterion for the cost efficiency of such systems because it lowers the system capital costs. Furthermore, via this criterion, the system works on its full-load capacity close to its maximum nominal efficiency, which also helps the operator gain better control over the operation of the system and reduces operation and maintenance costs (Jie et al., 2015; Kalina 2016).

Base and PLD criteria have their own respective advantages and disadvantages. For example, systems designed by BLD criteria are unreliable during emergency events and even some peak demand hours and do not consider future energy demands. Vallios et al. (2009) performed a profound analysis of design, based on these measures.

The heat exchanger sizing is one of the DHS component parameters that is influenced directly by heat demand analyses. Heat exchanger type, dimensioning, localizations, required installation spaces, and hydraulic requirements are all derived from heat load analyses. For consumers' side radiators, using radiative and convective heat dissipation mechanisms is more widespread. Various methods are used for sizing consumer heat exchangers. As (Kays et al. 1960) outlined, the most used methods for sizing and dimensioning heat exchangers include the logarithmic mean temperature difference (LMTD), arithmetic mean temperature difference (AMTD), geometric mean temperature,  $\epsilon$ -NTU, and fixed pinch point methods. Logarithmic mean, geometric mean, and arithmetic mean are widely used methods in sizing and designing heat exchangers (Kays et al., 1960).

Besides component design and sizing, DHS installations are designed by modeling the entire system network as a set of substations, pipes, and building clusters, notably for hydraulic specifications (Madsen et al., 1990; Vesterlund, 2015). Network modeling deals

with the design of the entire system and is generally represented by a set of nodes denoting substations connected by lines illustrating pipes. The node model is a suitable approach for time-dependent modeling of the DHS systems to trace the response delays of the systems. Technical specifications such as substation rated capacities and pipe sizing can be depicted in the network model (Vallios et al., 2009). Nodes, as illustrated schematically in Figure 4, represent the connection points of lines and are assigned by weights or numeric values representing energy, pressure loss, or mass flow (Lund et al., 2016). Designers typically use graph theory to model DHS networks and their features such as mass flow, energy demands, substations, and pipe sizing, with notations as configured in Figure 5.

Graph theory aims to design and optimize the pattern of the heating network and equipment characteristics hydraulically or thermodynamically. It further aids in calculating and sizing technical parameters such as pump rated power based on the required energy for each line that is supplied or consumed by the nodes. Graphs consider the geographical and geotechnical constraints for DHS development and design. The slopes, the drilling or excavation requirements, the space required for localization, the geology of the soil, and the elevation of the pipes and pumps are considered. Graphs are also used for scheduling and delivery delay analyses for time-dependent DHS behavior, and they enable designers to optimize heat or mass flow rates and specify a suitable plant location. Weighted links and nodes assist in developing the financial attributes of the DHS networks. Karschin et al. (2015) used the net present value (NPV) of the pipes and buildings as the weight for calculations.

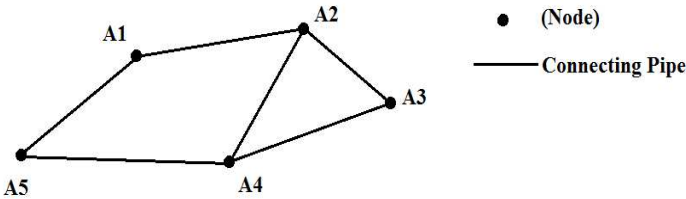


**Figure 4**

*Schematic of the Node and Lines Used for DHS System Modeling*

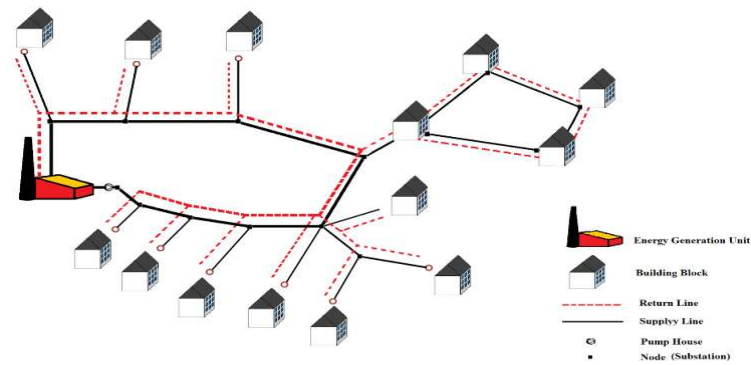


**Figure 5**

*Graph Model Representing Nodes, Lines, and Clusters of a DHS*

## 2.2 Biomass Energy Systems

Global climate change has triggered fundamental transformations and evolutions in all sectors of human activities and dramatically affected energy generation and distribution. Energy generation and distribution is one of the main contributing sectors to climate change and its subsequent outcomes (Lund et al., 2016; Østergaard et al., 2020). Therefore, despite a long history of using renewables as a resource for energy generation, some issues such as the variable nature of renewables (wind or solar resources) and direct burning and pollution of the environment through biomass triggered modifications and evolutions in renewable-powered energy concepts, related technologies, and domains, facilitating the transition from using fossil fuels to biomass (Ferrari et al., 2013; Powell et al., 2016; Rivarolo et al., 2016). Table 1 offers a brief review of transitional processes from conventional energy generation and distribution approaches toward more recent or modern approaches such as smart energy systems (Lund et al. 2010, 2016).

In this regard, biomass has gained attention in recent years for supplying energy demand thanks to such features as an abundance of resources in some areas, competitiveness of costs, and availability in the vicinity of energy generation plants (Williams et al., 2008).

**Table 1***Energy Generation and Distribution Approaches, Concepts, and Technologies*

Approach	Conventional	Modern
Resource	<ul style="list-style-type: none"> <li>▪ Fossil fuels</li> </ul>	<ul style="list-style-type: none"> <li>▪ Renewables</li> </ul>
Energy generation concept	<ul style="list-style-type: none"> <li>▪ Single energy module</li> <li>▪ Combined heat and power</li> </ul>	<ul style="list-style-type: none"> <li>▪ Multi-generation</li> </ul>
Technologies	<ul style="list-style-type: none"> <li>▪ Centralized energy conversion</li> <li>▪ Combustion-based cycles</li> <li>▪ Waste-heat recovery</li> </ul>	<ul style="list-style-type: none"> <li>▪ Decentralized energy conversion</li> <li>▪ Noncombustion-based cycle</li> <li>▪ Storage</li> <li>▪ Hybrid</li> </ul>
Energy distribution concepts	<ul style="list-style-type: none"> <li>▪ On-site grids</li> <li>▪ Centralized</li> </ul>	<ul style="list-style-type: none"> <li>▪ Off-grid</li> <li>▪ Decentralized</li> </ul>

Biomass is any organic, typically plant-based, matter, available on a renewable or recurring basis. Biomasses involve many types of matter such as forestry, agricultural or mill residues, agricultural crops, animal food and other industrial wastes, and aquatic or fast-growing trees and plants. The millennia-old traditional use of biomass has been for burning wood and agricultural residues for heat generation. Some characteristics of biomasses, such as low (or zero) purchase prices, make it attractive to designers and operators aiming to deliver distributed or centralized energy generation (Biomass CHP Catalog, 2007). Biomass as an energy resource was primarily intended for small-scale applications in farms, wood mills, remote villages, or off-grid small societies. They were suitable for areas and cases where there was a huge supply of unused biomasses or where biomass feedstocks were close to energy consumption areas. In recent years, biomasses have gained popularity in remote and isolated communities either lacking energy infrastructure and transportation facilities or dealing with high energy prices (Pfeifer et al., 2016; Sameti et al., 2018). Biomass's varying chemical composition and heat contents, proximity to plant areas, yield rates, and seasonality of alternative uses in other sectors other than energy dramatically affect biomass use and subsequently energy generation reliability. Table 2 shows a comparison of examples of biomasses, their advantages or disadvantages for energy generation uses, and their typical

heat content (Caputo et al., 2019; Girones et al., 2017; Kalina 2016). Biomass resources can be categorized based on their rural and urban sources. For rural applications, biomass sources are mainly forests, crop residues, and animal manure. Urban biomass sources are often wood mill residues, landfill gases (LFGs), food processing facilities, and wastewater facilities (Basu et al., 2013; Williams et al., 2008).

The biomass energy system can be characterized based on the capacity of the processing system for biomass preparation. Biomass preparation installations can be categorized based on their biomass processing capacities, which range from very small installations intended for processing a few tons per day to small-scale ones intended for processing 10–50 tons per day, intermediate-scale ones intended for processing 50–100 tons, and large-scale ones intended for processing more than 100 tons per day (Coelho et al.2015).

Besides being used in its solid state and being directly burned for generating heat or electricity, biomass can be processed and converted to other states for better transportation or less pollution. For biomass conversion, adopted technologies and processing methods matter for effective and efficient exploitation of the heat content. Coupling the conversion technologies and methods with various types of biomasses could deliver energy in different ranges of quantities, each appropriate for specific applications (Table 3; Coelho et al., 2015; Windeknecht et al., 2015).

The biomass processing system incorporates activities such as separation, sizing, removal of metals, refinement of impurities or other noncombustible materials, and size reduction methods before biomass conversion. For gaseous biomass, biogas and syngas fuel preparation includes biogas generation or syngas gasification, gas collection, and gas treatment, which entails gaseous biomass (biogas or syngas) readiness for injection into the combustion chambers (Basu et al., 2013; Li H et al., 2017; Prakash M et al., 2017).

**Table 2.***Categorization of Biomass Feedstocks Based on the Resources and Typical Heat Contents*

<b>Type</b>	<b>Source</b>	<b>Examples</b>	<b>Advantages</b>	<b>Disadvantages</b>	<b>Typical heat content (THC)</b>
Residues	Forestry	Forest thinning	Easily cofired No harvest fees	Costlier than coal because it requires more processing activities: Collecting Transportation Stumpage	5,140 (wet) < THC < 8,570 Btu/lb (dry)
	Mill	Sawmills Pulp and paper mills. other millworks such as lumber, pulp, vener, wood fiber	Typically, zero cost because of penalties for disposal	Competing applications in sectors such as mulch and bedding	8,570 Btu/lb
	Livestock	Manure biogas	Reduces odors and pathogens	High dependency on manure source and collection type	600 < THC < 800 Btu per standard cubic foot (scf)
	Agricultural	Rice husks Wheat straw Crop stalks Bagasse Corn stover Cobs	Zero purchase cost Environmental improvements	Seasonality High alkali and chlorine content Competing usage in animal feeding, compost, and animal bedding	Corn stover (Btu/lb) 5,290 (wet) < THC < 7,560 Wheat straw: 5,470 Btu/lb (wet) < THC < 6,840

Energy crops	Agriculture Forestry Aquatic plants	Hybrid poplars Hybrid willows Switchgrass	Less moisture content	Relatively higher overall costs than fossil fuels	Hybrid poplar and willows: 4,100(Btu/lb) < THC < 8,200 (Btu/lb) Switchgrass: 6,060 (Btu/lb) < THC < 8,670 (Btu/lb)
Waste	Woody	Yard trimmings Construction and demolition Site clearing wastes Wood packaging Furniture	Lower fuel costs than other forms of biomass	Higher levels of chemical impurities than other biomasses	4,600 Btu/lb < THC < 6,150 Btu/lb
	Municipal	Landfills	Zero or very low purchase costs	High dependency on landfills' site size Impurities such as hydrogen sulfide Varying compositions	Ranging from 350 to 600 Btu/scf 500 Btu/scf for: 50% methane and 50% CO <sup>2</sup>
	Wastewater	Wastewater facilities	Opportunity fuel	High dependency on facility's size and site and varying compositions	Ranging from 550 to 650 Btu/scf

**Table 3**

*Categorization of Biomass-Powered Energy Systems Based on Biomass Sources and Power Ranges*

Conversion concept	Conversion technology	Biomass source	Power range
Direct fired boiler Fixed bed Fluidized bed	Steam turbine	Sawdust, bark, chips, hog fuel, shavings, end cuts, sander dust, wood residue, peat,	4–300 MW (most in the 20–50 MW range) Cofiring up to 1000 MW

Cofiring			
Gasification processes	Fixed bed: Gas turbines—simple cycle	Chipped wood or hog fuel, rice hulls, shells, sewage sludge	Up to 50 MW
Fixed bed	Fluidized bed Gas turbines—combined cycle Large internal combustion (IC) engines	Most wood and agricultural residues	Up to 25MW
Fluidized bed			
Modular direct combustion technology	Small steam turbine Organic Rankine cycle Hot air turbine	Wood, crop waste, animal manure, and LFG	5–10 MW
Modular gasification technology	IC engine Micro-turbine Fuel cell Stirling engine		5–10 MW
Anaerobic digesters	Combined heat and power	Internal combustion engine Micro-turbine Gas turbine Fuel cell Stirling engine	Animal waste or wastewater

Biomass processing, besides removing the impurities or contaminations affecting the efficiency of energy generation, transforms solid biomass into a biofuel in liquid or gaseous forms, reducing transportation or stocking problems. Pyrolysis, Fischer-Tropsch synthesis, synthetic natural gas production, and torrefaction are among the biomass processing or conversion methods (Farahani et al., 2020; Li et al., 2022).

Biomass gasification systems operate by heating biomass in an environment where the solid biomass breaks down and forms a flammable gas. The gas produced, which is called synthesis gas or syngas, can be cleaned, filtered, and then burned in a gas turbine (GT) in a simple or combined cycle. (Williams 2008).

Biogas generation is the anaerobic digestion of organic matter, such as biomass, manure, sewage, etc. in oxygen-free conditions. This process produces biogas (mainly methane and carbon dioxide), which can be used for heat and CHP generation. (Coelho et al. 2015, Mudasar et al. 2017).

Conventionally, biomass with higher moisture content is suitable for biochemical conversion using some enzymes to produce biofuel, and biomass with lower moisture content is suitable for thermochemical conversion (e.g., pyrolysis or gasification) to produce fuels and chemicals. Solid biomass can be processed into competitive productions such as biogas and biofuel fluids (Basu et al., 2013; Moret et al., 2016; Prakash et al., 2017).

Another processing method for biomass conversion is modular hybrid gasification/combustion, in which gas is produced in a chamber at a lower temperature between 550°C and 800°C and then combusted in a hot chamber at up to 1300°C. This process reduces the need for gas cleaning and provides higher combustion quality (Farahani et al., 2020; H. Li et al., 2022).

The advantages of modular systems are the simplicity of combustors, the higher quality of gasification processes, and the possibility of using lower heat-value biomass such as forest thinning and wood chips in remote areas. The disadvantages are low electricity efficiency, low electricity-to-thermal ratios, high costs, and a higher installation area compared to gas-fired peer systems (Farahani et al., 2020; H. Song et al., 2021).

The performance parameters of biomass processing methods are other determining factors in such systems' design and operation. For example, for a thermochemical process, heating temperatures and the presence or absence of oxygen affect the quality and quantity of gases, biochar, and bio-oil. Pyrolysis is a thermochemical process where biomass is heated in oxygen's absence and within a temperature range of 400–600°C to produce a vapor, which is then cooled and condensed into bio-oil. The waste products are noncondensable gases and biochar (Basu et al., 2013; Prakash et al., 2017; Rolfsman et al., 2004).

Contrary to pyrolysis, gasification occurs in the presence of a limited supply of oxygen or air (less than the stoichiometric amount) and can produce a considerable amount of syngas. The gasification method that produces syngas employs high temperatures for its processing so that excessive heat can be recuperated and used in a steam power cycle to generate super-hot steam electricity. The temperature range of gasification is 800 to 1,200°C (Basu et al., 2013; Proskurina et al., 2017).

Gaseous products resulting from biomass processing are typically of low heat content compared to fossil fuels, primarily because of their mixture with carbon products. Therefore, these gaseous products (biogas or syngas) are cofired with natural gas, coal, or other fossil fuels to overcome their lower heat content compared to fossil fuels (Wang et al., 2017).

Studies have been carried out on the biomass conversion domain, including conversion pathways from the resource to the feedstock or storage sites (Ahmadi et al.2013). Environmental

evaluations have been conducted based on CO<sup>2</sup> emissions and the abatement potential for different pathways (Girones et al., 2017, Moret S et al., 2016).

Pretreatment of solid biomass can improve its quality for energy-generating purposes and its competitiveness compared to fossil fuels or renewables. For example, torrefied wood's energy content (caloric value) is comparable to coal's and greater than wood pellets. Torrefaction is a mild thermal pretreatment process in which biomass is heated to 200–300 °C in an oxygen-deficient atmosphere for approximately 2 hours. The torrefied biomass has a lower ash content and fewer net greenhouse gasses than fossil fuels (Goh et al., 2013; Nunes et al., 2014; Proskurina et al., 2017). Li et al. (2017) analyzed the possibility of cofiring torrefied biomass. They concluded that torrefied biomass would provide maximum efficiency and minimum emissions. Prakash et al. (2017) developed a process model for the gasification of biomasses.

The diversity of parameters and sensitivity of biomasses to these parameters, such as feedstock, heat content, supply sources, conversion conditions and used technologies, storage conditions and moisture levels, transportation requirements, pollution, hybridization with other fuels, and energy-generating technologies, pose disadvantages or advantages for biomass resources and justify their optimization for energy generation applications.

### **2.3 CHP**

The CHP generation concept, namely the simultaneous generation of heat and electricity on site, has been used for a long time and has demonstrated resilient behavior and remarkable performance in meeting energy demands. The CHP concept has considerably positive characteristics ranging from adaptability of integration to various fuels and technologies for energy generation to flexibility to various energy demand profiles (U.S. DoE CHP, 2019).

Known CHP concept applications date back to the early 20th century in industries such as wood and paper mills, alumina, petroleum, and food processing, which produced considerable

quantities of unused steam. In such industries, there was a large ratio of unused heat to generated heat or produced product, and by employing CHP, their efficiency was considerably increased. To make them even more efficient, the CHP concept was integrated into DHSs. After a decline in the 1950s and 1960s, the global economic crisis due to rising oil prices in the 1970s restarted the application of the CHP concept for generating energy. This occurred most notably in Europe first and then across the world (Coelho et al., 2015).

Many programs such as the Energy Efficiency Research and Development Scheme and the Energy Efficiency Demonstration Scheme in the United Kingdom were launched to reduce reliance on fossil fuels. The development and advancement of new technologies more appropriate for fuels with lower heat-to-power ratios also helped with the revival and penetration of CHP concept use in the energy sector (Brown et al., 1996). The development of technologies such as combustion engines working on Brayton, Otto, or Rankine cycles, which delivered higher electricity, and the introduction of fuel cells capable of exploiting fuels with lower energy content for micro- or small-sized applications encouraged further use of the CHP concept for meeting energy demands. (Pantaleo et al. 2020). Using these technologies along with other design and operation parameters highlighted optimization and reliability studies for CHP uses (Ahmadi et al., 2016).

Biomass is an energy resource that can be used to deliver energy based on the CHP concept. It is adaptable for integration with CHP technologies to meet a wide range of energy demands. Table 4 provides a summary of CHP concepts and their specifications with various forms of biomass.

**Table 4**

*Used Technologies, Rated Capacities, and Fuel Types Used in Biomass CHP Systems*

Technology	Steam turbine	Gas turbine	Micro-turbine	Internal combustion engine (ICE)	Fuel cell	Stirling engine
Rated capacities	< 250 MW	< 40 MW	< 250 kW	<5 MW	< 1 MW	< 200 kW
Fuel type	Biomass/ Biogas	Biogas	Biogas	Biogas	Biogas	Biomass /Biogas

A B CHP installation’s main components are a feedstock receiving and preparation module, biomass conversion module, and power and heat production unit. Despite its advantages, using biomass in CHP applications is problematic notably because of biomass supply chain seasonality, biomass processing, and CHP energy conversion technologies. There are many parameters affecting the B CHP concept’s effectiveness for biofuel production intended for energy generation and distribution (Hassan et al. 2020).

The field of system configuration has fascinated scholars, who have highlighted the ability to meet energy demand and reliability as important components. Micro CHP configuration or modular systems have been significantly investigated for configuration optimization analysis. Small packaged systems as scaled-down versions of larger conventional biomass cofired CHP energy systems generating less than 5 MW are typically called modular CHP systems (Basu et al. 2013).

Analyses of the impacts of different configurations of prime movers or technologies on CHP system performance have been conducted in numerous studies. Their sizing, operating and performance parameters, integration modalities, operating cycles, and so on have been the subject of research. Researchers have analyzed thermodynamic cycles such as the Rankine cycle in CHP systems (Drescher et al. 2007; Invernizzi et al. 2016, Mavrou et al. 2015, Moharamian et al. 2017, Pantaleo et al. 2020).

The prime mover for biomass-powered systems has been the subject of analyses aiming to justify biomass as an appropriate fuel for energy supply. For example, steam turbines (STs) in

extraction, back-pressure, or condensing types; GTs in single or combined cycles; reciprocating engines in internal and external combustion models; and fuel cells in phosphoric acid fuel cells or proton exchange membrane fuel cell types are among the technologies used for this purpose.

Prime movers are available in demonstrated or commercialized states for both large- and small-scale applications. Table 5 shows the taxonomy of the characteristics of prime movers used in biomass-powered systems and their comparison (Goh et al. 2013)

**Table 5***Taxonomy of Biomass CHP and Energy Conversion Technologies and Ranges*

Prime mover	Range	Integrated system	Output	Advantages	Challenges
Steam turbine Condensing boiler Extraction turbine Back-pressure turbine	50 kW–250 MW	Boilers Absorption chillers	Electricity Thermal power Steam Hot water Hot air	Fuel versatile Size versatile	Lower efficiencies and higher costs
Gas turbines Simple cycle Combined cycle	0.5–40 MW		Chilled water Mechanical power Compressors Pumps Fans	Lower costs Higher efficiencies	Inlet temperature limitation due to turbine blade material strength Lower air-to-fuel mixture for biogas than natural gas Proposed for landfill and wastewater
Micro-turbine	30–250 kW	Recuperator		Simple design	Lower electrical efficiencies than larger gas turbines Reduced maintenance compared to reciprocating engines Alternators to process electricity frequency
Reciprocating internal combustion engine (ICE)  Spark ignition Engines Compression ignition	Smaller than 5 MW	Desiccants Engine-driven chillers		Low necessary modification Less cleanup Less expensive Fuel diversity	Emergency standby or limited duty-cycle service Air emission concerns (NO <sub>x</sub> and particulates) High wear and tear Higher operation and maintenance cost Complex heat recovery Not commercially developed for low Btu gases
Reciprocating ICE Stirling engines	Smaller than 200 kW			High thermal efficiency Low emission Low noise	Small capacities Low electricity efficiency

<p>Fuel cells</p> <p>Phosphoric acid fuel cells (PAFC)</p> <p>Proton exchange membrane fuel cell (PEMFC)</p> <p>MCFC</p> <p>SOFC</p>	<p>50 W–2 MW</p>		<p>Electricity</p>	<p>High electrical efficiency (up to twice ICE)</p> <p>Low emissions</p> <p>No combustion</p> <p>Very quiet</p>	<p>Very high cost</p> <p>Low durability</p> <p>Difficult maintenance</p> <p>Cleanup technology for fuel cell in early stages</p> <p>No experimental results</p> <p>High cleanliness levels</p> <p>PAFC: High-hydrogen rich, no methane</p> <p>PEMFC: Less than 10 ppm CO</p> <p>Early stage for commercialization</p>
--	------------------	--	--------------------	---	---

Murugan et al. (2016) surveyed the technologies and fuels widely used in CHP systems from coal boilers to fuel cells and GTs. Studies have also focused on small or micro-CHP systems supplying energy for a small single building (Verhaert et al. 2016, Adams et al. 2014), up to large-scale systems (Girones et al. 2017).

Other researchers used Aspen Plus software to optimize hybrid CHP systems (Kaushal et al. 2017; Prakash et al. 2017; Proskurina et al. 2017).

In addition to technology adoption, thermodynamic, mechanical, fuel chemical, and environmental issues emerge in CHP design. In this regard, some researchers have focused on fuels and energy conversion processes. Used fuels for CHP purposes range from fossil fuels such as natural gas, diesel, oil, or coal and renewable sources such as solar, wind, and biomass. Studies have also targeted the impact of fuel selection on CHP systems' design and operation (Martinez et al. 2017, Pirkandi et al. 2016, Volkova et al. 2020). A CHP plant with photovoltaic cells was modeled for a residential complex in Austin, Texas (Ondeck et al. 2015). The authors identified the best operational schedules for the system subject to variable electricity prices in the grid.

In line with the concept of smart grids linked to hybrid energy systems, CHP has the flexibility to incorporate energy storage systems to deliver a more resilient system to operators and more energy availability to customers (Chidambaram et al. 2011; Ferrari et al. 2019; Kaygusuz et al. 2013).

Researchers investigated the impact of various fuels and technologies on CHP systems' performance (Connolly et al. 2010). They found that in the case of energy production for district networks, the choices for technologies and fuels are limited because of complexities such as the additional design and configuration constraints that emerge during hybridization and the coupling of economic and technical parameters.

In the thermo-economic approach, thermodynamic properties are coupled with economic parameters to design systems economically. Web-based economic cogeneration modular program software was developed to introduce a thermo-economic model for plant configuration targeting smart poly-generation from natural gas (Rivarolo et al. 2016).

The engineering equation solver (EES) was used to solve a mathematical model to identify the thermodynamic properties of a CHP system (Moharamian et al. 2017). Researchers modeled solar energy as the primary source of heat production (Wang et al. 2015). Designers at Ecole Polytechnique Fédérale de Lausanne developed OSMOSE software to process integration and optimization of CHP systems costs. This was followed by a sensitivity analysis to arrive at the best set of design parameters (Buoro et al. 2014; Ziebig et al. 2012). The CHP concept integrated into DHS and renewables has gained momentum in the realm of smart energy system research and practice. Smart energy generation, first defined in Denmark, where it focused on the transportation sector and bioenergy, is a holistic and cross-sectoral energy system with characteristics such as 100% renewable energy, storage synergies across energy subsectors, and exploitation of low-value energy sources (Lund et al. 2016, Østergaard et al. 2020, Sameti et al. 2018). Emerging smart energy systems have storage and predictive controls, and their integration into DHS enables system operators to take advantage of renewable energy sources (RESs) considered infeasible or inefficient because of technical issues or lack of on-time availability of resources. Energy storage is considered a solution for increasing a CHP system's reliability and versatility in normal and emergency situations, notably those that arise when working with renewables (Connolly et al. 2010; Lund et al. 2016, 2018, Østergaard et al. 2020; Rivarolo et al. 2013; Rolfsman et al. 2004).

Verda et al. (2011) examined the potential for implementing heat storage in a CHP-DHS configuration to reduce fuel consumption. Franco et al. (2017) used a model that they developed

for sizing and scheduling a CHP-DHS system equipped with a thermal energy storage (TES) system. They considered several scenarios for energy demand and system efficiency to identify the start/turn-off pattern for thermal storage. Haeseldonckx et al. (2007) investigated the operational behavior of CHP systems equipped with thermal storage to mitigate carbon emissions.

## **2.4 Optimization Approaches: DHS**

As mentioned, a typical DHS grid could range from a housing scheme connected to a few houses or an entire community, city, or area (Lund et al. 2016; Ferrari et al. 2013; Østergaard et al. 2020; Powell et al. 2016; Rivarolo et al. 2016).

The CHP concept can also vary from single small burners, furnaces, or combustors to large power plants using complex technologies and thermodynamic cycles, and from the exploitation of one exclusive biomass fuel to hybrid systems exploiting various kinds of biomasses or other renewables like solar, wind, or geothermal resources. Many researchers of the first generation of the cogeneration concept focused on one aspect or domain within a DHS grid or CHP plant without considering interrelated parameters for sizing the grids or plants, to avoid overdesign and derive technical specifications of such systems (Brown et al. 1996; Tran et al. 2017).

In the second round of DHS design optimization, cost optimization of DHS-CHP systems mainly using coal as fuel was performed in the 1990s. Research in this area involved the energetic analysis analyses of systems and technical specifications like network topology or configuration and hydraulic or thermo-dynamical parameters (Brown et al. 1996). Most research in this period was carried out using thermodynamic and hydraulic optimization approaches. In the next decade, during the third round of CHP and DHS design evolution, the optimization research trend was oriented towards optimizing system operation and control strategies to manage

operational costs. In this era, energetic analyses of DHS-CHP systems focused on the systems' cost optimizations. Exergetic analyses dealing with the quality of delivered energy and the cost affordability of energy conversion further highlighted thermo-economic approaches to the optimization of costs (Mazhar et al. 2018). Decarbonization and energy supply reliability are considered in new approaches. Diversification of used technologies, energy resources and delivered energy types, and energy storage parameters and transfer of energy and data between customers and operators were among the optimization topics studied (Lund et al. 2016, 2018; Mazhar et al. 2018, Østergaard et al. 2020). Wei et al. (2010), using the fuzzy approach, analyzed, compared, and ranked seven available technologies for heat generation. They ranked their heat generation costs as follows: CHP, gas boilers, water source heat pumps, coal boilers, ground source heat pumps (GSHP), solar energy heat pumps, and oil boilers. In recent generations, DHSs are characterized by decentralized generation, the use of storage capacities to achieve flexible energy usage and storage (with hourly-based scenarios), long-term planning, smart control, and exploitation of existing energy systems with novel distribution mechanisms (Østergaard et al. 2020, Lund et al. 2016, 2018, Sameti 2017).

DHS optimization can be categorized as synthesis, design, and operation optimization, as illustrated in Figure 5 (Mongibello et al. 2014). The synthesis level of optimization refers to configuring the system and the components within it. The system's layout (e.g., linear, radial, loop, mesh network, or tree shaped) has been illustrated by different models. The geographical and geotechnical constraints facing a DHS network are considered in design phase, accounting for excavation, required space, trench depth, pipe elevation, and energy source (Wang et al. 2015).

Design begins with system sizing and dimensioning using thermodynamic, mechanical, or hydraulic design approaches for technical criteria characterization. This practice is part of the

first level of efficient DHS network optimization (Vallios et al. 2009, Hammer et al. 2004). Designers have employed the source location network flow method to optimize heat flows or energy pathways and specify the plant location based on the optimum heat flow patterns. Operation or control optimization is the next phase. It is accomplished after the system-sizing optimization phase. It deals with optimally dispatching the technically optimized system output (energy) in efficient sequences. For DHS, at this phase, the models address the varying energy demand profiles, required temperature ranges, or circulating fluid flows in the networks (Nussbaumer et al. 2016, Vallios et al. 2009). These characteristics have been well-researched, with analytical tools being used to demonstrate how various operation scenarios are integrated to meet energy service demands under various operation circumstances (Weber et al. 2011). Figure 6 illustrates the sequences, levels, and cycles of DHS modeling optimizations.

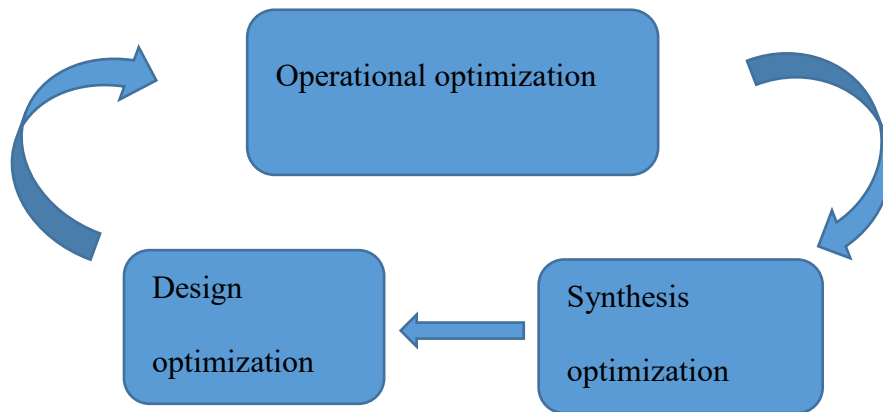


**Figure 6**

*Sequences, Levels, and Cycles of Energy System Optimization*

Figure 7 shows how sensitivity analysis is conducted by examining technology adoption, fuel selection, and equipment configuration. Various approaches are used to model heat demand, and the accuracy of this modeling has an impact on the optimization of DHSs. Meeting the

demand involves determining the sizing of DHS components such as pumps, pipes, and operational scenarios, including pump house schedules. Different methods such as sinusoidal-shaped, discrete decomposition, representative days, representative blocks, and representative hours are employed to specify network heat demands. Werner’s study involved analyzing heat load as a sinusoidal-shaped pattern, defining the amplitude, minimum, and maximum values for the yearly range (Werner 1984;).

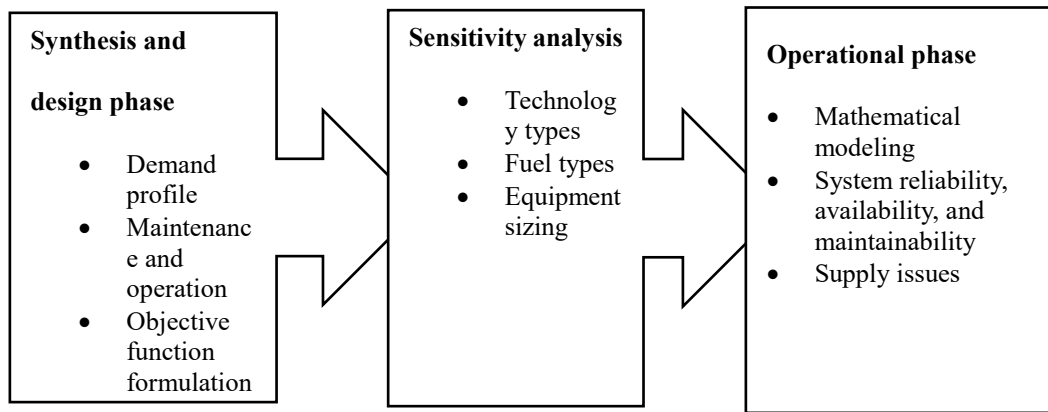


**Figure 7**

*The Modeling Characteristics of DHS System Optimization*

Heat demand modeling is accomplished using various approaches, and the exactness of the modeling affects DHS optimization. It involves meeting energy demands, determining the sizing of DHS components like pumps and pipes, and envisioning operational scenarios including pump house schedules.

Sartor et al. (2014) used geometric modeling and performed a steady-state two-dimensional simulation to identify heat loss patterns. On that basis, they provided the optimized use time for a biomass power plant serving a DHS. This optimization resulted in the selection of temperature and flow rate profiles for dispatching control of a DHS.

Karschin et al. (2015) used the NPV method and graph theory for pipes and buildings as the weights for calculating the delivered energy cost. Using this approach, the configurations and layouts of the heating network, the number of user's connections to CHP plant, and locations were optimized. To model DHS, they implemented Steiner nodes to account for the construction costs of the heating network and the revenue from selling heat to the connected nodes.

Historically, most scholars on the design of DHS used a reduction strategy for optimization and focused on the sizing of the system piping. The design criteria for these networks are typically those employed for water supply networks.

In this regard, instead of the whole system, only certain parts are subjected to optimization. However, despite the simplicity of this approach, the accuracy of reduction strategy analyses is low. This is because the whole scale's modeling is neglected and interactions between various components are not considered (Marconcini et al. 1979). Moreover, although water supply networks have been widely referenced for DHS pipe sizing, their design is less challenging than that of district heating networks due largely to a lack of consideration of heat loss issues (Stoner et al. 1974). The sizing of the pipes in conventional methods of DHS sizing is based on the pressure loss and the maximum allowed velocity in the network (Sameti et al. 2018, 2019). Heat exchanger modeling in both supply and consumer substations is another area largely focused on in research. The most used heat exchangers are tubular, tube fin, helical coil, spiral plate, shell and tube, shell and plate, and spiral coil types. Parallel, cross, and mixed flow are among the patterns used in heat exchanger design concepts (Phetteplace 1981, Böhm 1986, Frederiksen 1982, Kalina 2016, Martinez et al. 2017, Jie et al. 2015).

Aamot et al. (1976) introduced a new approach to DHS design based on the ratio between heat loss and power cost. After reaching the minimum amount of this ratio, optimization of the system is carried out by obtaining the most economical pipe diameters and by considering

investment and fuel costs. This method, however, lacks the holistic approach toward DHS system behavior because it just focuses on a segment of the pipe instead of the whole network.

Szepe et al. (1979) also applied a reduction strategy to a single segment of a pipe using geometric programming. Like Aamot's strategies, this strategy neglected the time-dependent and dynamic behavior of networks with varying energy demand profiles.

Phetteplace (1981) closed this gap by considering fluctuating annual loads while still taking into account just a single segment of the pipe. McDonald and Bloomster (1977) introduced the "simple search" method for cost optimization of DHS network sizing, fed by geothermal energy.

The general layout of the network is arranged using this method, and the pipe diameters are determined by minimizing the sum of the annual capital, heat loss, and pumping costs. Annual load variations and their impacts on system design and behavior, however, were missing from their research. Böhm (1986) indicated that the traditional approaches to finding the pipe diameters, subject to the minimum sum of the pipe lengths and the minimum capital cost, result in overpressure occurring in the heating plant. To prevent this, the Munster method was recommended, in which the total pressure loss in the network is distributed based on a proposed formula to deliver the pipe diameters. This approach also reduces the minimum capital sum, heat loss, and pumping costs by avoiding unnecessary overpressure in the network.

Operating fluid is an important item that can drastically affect the efficiency and optimization of DHS when it is used with CHP (Mavrou et al. 2015; Stijepovic et al. 2016). Many costly factors such as corrosion, clogging, and thermal conductivity depend on the operating fluid. The impact of the working fluid on energy systems' efficiency and performance is analyzed to specify the proper working fluid type for each application. The working fluid is selected

according to its thermodynamic, environmental, and economic features. It should be cost-efficient, nonflammable, chemically stable, and low in toxins (Drescher et al. 2007).

Water, as the most widely used working fluid, is often mixed with anti-corrosion and/or anti-freezing fluids. In cold climates, steam and oil-derived substrates are also employed extensively. Stoner (1974) devised models that worked both with steam and water and noted the sensitivity of the models' operation to mechanical and hydraulic characteristics of the system. These models were unable to provide the optimum pipe diameters and did not consider the cluster of the pipes.

Different working fluids and operating conditions for a particular heat source have been investigated in the literature to analyze the cost, pollution, or operation they give rise to (Qiu 2012; Victor et al. 2013; Stijepovic et al. 2016).

Pressure drop within the network helps determine and optimize the network pumping and piping layout, sizing, and subsequent cost (Stoner. 2016; Sameti et al. 2019; Noussan et al. 2014). The conventional methods in this field are based on the maximum pressure loss and the permissible fluid velocities in the network (Noussan et al. 2014; Sartor et al. 2018; Volkova et al. 2018).

Heat consumption can dramatically recast optimally designed DHS specifications. The heat consumption and exchanger capacities for delivery of required heat, the space required for their installation, the hydraulic requirements, and the associated maintenance problems can drastically affect the heat exchanger optimization. It also can affect the overall energy system efficiency through its impact on return temperature profiles. Therefore, the modeling design of the heat exchanger can then become a constraint on the return temperature (Kays, 1960, Soumerai 1987).

DHS research has focused on the performance of heat exchanger types in substations and consumer sites. LMTD is the most widely used heat exchanger modeling method; however, there are some restrictions on its use on different applications. For example, deriving precise and explicit correlations for return and supply temperatures could be problematic and affect optimizations (Phetteplace 1981).

Soumerai (1987) proposed AMTD as an approximation for the logarithmic mean method. The AMTD provides correlations for the supply and return temperatures. The arithmetic mean method provides the upper bound for the logarithmic mean, which leads to overestimating the actual heat transfer and oversizing the heat exchanger.

The geometric mean temperature difference (GMTD) is another alternative to the logarithmic mean temperature difference method. Like arithmetic, it uses an explicit correlation based on the temperature parameter. It also can deliver a less overestimated approximation for the logarithmic mean temperature difference compared to the AMTD (Kays et al. 1960, Phetteplace 1981).

Frederiksen (1982) optimized intermediate substations by focusing on the behavior of heat exchangers and their pipelines. The focus of this research was on conducting a suitable sizing and performance evaluation of heat exchangers while the distribution network modeling was cut to a single supply and return line.

Marconcini et al. (1979) proposed a model for a steam distribution network that considered flow rate, pressure, and temperature profiles as variables. However, their methodology lacked pipe diameter sizing and optimization.

As mentioned, a system's design depends on its technical properties, whereas in operation optimization, the operation regimes, modes, states, and control scenarios of the system are optimized. Component sizing resulting from design optimization is restricted by operational costs

and financial issues. They serve to develop the operating, maintenance, or repair-and-restore procedures of the system. However, technical optimization parameters derived from the design phase are not sufficient for the operation phase. Moreover, using the technical parameters derived from design optimizations by integrating them into their calculated values could conflict with the optimization of the system in the operation phase (Jiang-Jiang et al. 2010).

For example, the controlling mechanism in conventional DHS operation is based on dispatching mass flow rates and supplying required temperatures. However, meeting energy demands requires increasing the supply fluid flow and temperature simultaneously, resulting in more substantial pressure and energy loss, which inflicts cost (Stoner 1974, Morofsky 1979).

Therefore, unlike in the design phase, reduction strategies are not adequate for the optimization of the operation phase because of the other parameters important to the operation. Consequently, approaches, strategies, and even objective functions for optimization will be different and will consider various technical, economic, and environmental parameters and their associated constraints. Like many other optimization methods, objective functions may conflict. They can include technical or operational functions like minimum length, or diameter, maximum reliability, and availability. Some of the objective functions and their relations were summarized in Table 6. Morofsky (1979) conducted an economic analysis where the author introduced a cost tool for district energy configuration. The total (maximum allowed) pressure difference was used as a decision parameter to optimize the cost. Designers have integrated the concept of heat storage into a DHS to improve its performance in terms of flow rate and supply temperature, mainly when it is supplied with CHP to derive the storage sizing and their operation scheduling (Sartor et al. 2018). DHS and heat storage with a dynamic programming approach have been investigated to identify the best time sequences for heat storage charging/discharging (Powell et al. 2016).

Optimization strategies are categorized based on varying flow rates and temperature profiles. Jie et al. (2015) investigated four different strategies based on fixed or variable flow rates to minimize the sum of annualized costs. They used a static approach in which the provision of energy to consumers was based on fixed and predetermined supply temperatures.

In a static approach dealing with fixed temperatures, implicit optimization of cost as an objective function is performed (Eriksson 1988; Lurid et al.1989; Svensson et al.1989, Uotila 1989).

In the dynamic approach, designers consider varying supply temperatures in their proposed models (Madsen et al. 1990; Sogaard et al.1988) to investigate the impact of supply temperature reduction on the operation of the system and, subsequently, the cost of the system. They proposed a statistical approach for analysis of the system subject to supply temperature variations.

Lurid et al. (1989) and Nuorkivi (1989) also presented dynamic programming models that considered temperature as a decision variable. Benonysson et al. (1995) used the sum of the costs associated with fuel and electricity (for pumps and boilers) as well as the likely income from selling electricity to the grid as objective optimization functions. Koskelainen (1980) developed a linear programming method to determine the pipe diameters of a branched DHS network. By considering linear objective function and constraints, some authors proposed an algorithm for DHS sizing. They considered five functions and constraints with a linear programming algorithm.

**Table 6.**

*Interrelation Between Objective Functions of DHS Design*

	Minimum length	Minimum operation cost	Minimum storage capacity	Minimum heat loss	Maximum availability	Maximum reliability	Minimum cost
Minimum length	-	S	C	D	C	C	S

<b>Minimum operation cost</b>	S	-	D	S	C	C	S
<b>Minimum storage capacity</b>	C	D	-	C	D	D	C
<b>Minimum heat loss</b>	D	S	C	-	C	C	C
<b>Maximum availability</b>	C	C	D	C	-	S	C
<b>Maximum reliability</b>	C	C	D	C	S	-	C
<b>Minimum cost</b>	S	S	C	C	C	C	-

C: Conflicting, D: Depending, S: Satisfactory

## 2.5 CHP Optimization

Detailed optimization would be required of a CHP plant integrated into a DHS network (Kayo et al. 2014; Prato A. Pini et al. 2012). CHP optimization problems deal with various models and approaches reflected in objective functions, constraints, and decision variables. Constraints on CHP optimization can include various balance equations for energy, exergy, and mass flows. There are also constraints on equipment operations or performance capacities as well as on control mechanisms (Vallios et al. 2009). The objective functions for CHP systems can be conflicting, depending, or satisfactory. They can include economic, technical, or operational functions like initial or capital cost, pollution, and storage size. Table 7 summarizes some of the objective functions and their relations. Table 7 lists the objective functions used in the operational optimization of CHP systems. The relationships between these objectives can be of a conflicting, supporting, or dependent nature.

**Table 7.**

*Interrelationships Among Objective Functions in CHP Design*

	<b>Minimum Initial Cost</b>	<b>Minimum Pollution</b>	<b>Maximum Renewables</b>	<b>Minimum Storage Size</b>	<b>Maximum Availability</b>	<b>Maximum Usage Time</b>	<b>Minimum Operational Cost</b>

<b>Minimum initial cost</b>	-	C	C	S	C	C	S
<b>Minimum pollution</b>	C	-	S	C	D	C	C
<b>Maximum renewables</b>	C	S	-	C	D	D	C
<b>Minimum storage size</b>	S	C	C	-	C	C	C
<b>Maximum availability</b>	C	D	D	C	-	D	C
<b>Maximum usage time</b>	C	C	D	C	D	-	C
<b>Minimum operational cost</b>	S	C	C	C	C	C	-

C: Conflicting, D: Depending, S: Satisfactory

The heat tracking approach aims to adjust the system to provide heat and electricity at the required level or above. Fixed-point operation is based on rated or nominal values designed for maximum efficiency, and the hybrid operation strategy is a combination of the two (Franco et al. 2017). Today's pressing issues, such as global climate change, have highlighted the need for integration of renewables into energy systems to create hybrid energy systems in energy management concepts, particularly the development of smart energy systems via district heating (Ferrari et al. 2013; Kaygusuz et al. 2013; Moradi et al. 2013).

Fuel resources for CHP systems are varied and include a wide range of resources, from conventional fossil fuels such as oil, gas, diesel, or coal to renewable sources such as solar, wind, wave, and biomass. Table 8 offers a summary of optimization research on CHP systems. They are categorized based on energy sources, used technologies, and generated energy types. Murugan et al. (2016), Maghanki et al. 2013, and Verhaert et al. 2016 reviewed the technologies and fuels widely used in CHP energy concepts. These technologies range from simple coal boilers to sophisticated fuel cells and GTs.

Early researchers of the CHP concept dealt with supplying heat and electricity energy for single buildings or small communities (Barbieri et al. 2012, Brandoni et al. 2015, De Paepe et al. 2006, Murugan et al. 2016,). Like optimization approaches for the DHS concept, in these studies, the optimization approach for CHP were mostly the synthetic optimization approach for determining the proper adopted technologies or fuels.

The next wave of researchers in the synthetic design phase focused on energy production in large quantities and for district networks where the system had to provide energy for more than one building. These researchers faced greater challenges such as more objective functions and constraints. There were also fewer available technologies or resources for meeting larger energy demands, typically because of constraints imposed on the technologies' capacities for energy generation or on the energy content of some fuels (Girones et al. 2017).

For the optimized design of a CHP system in a small ecotown in the United Kingdom, Weber et al. (2011) used a tool based on a method for achieving the best combination of different technologies from both renewable and nonrenewable sources. In the second phase of optimization, namely design optimization, optimization aims to optimize the thermo-economic properties of the system components. These types of optimization problems have been solved analytically, statistically, or numerically via simulation software (Jørgensen et al. 2016; Ruan et al. 2008). Li et al. (2017), after using process simulation software and analyzing the possibility of cofiring torrefied biomass, concluded that 100% torrefied biomass usage with acceptable levels of efficiency and minimum emissions is technically possible.

Rivarolo et al. (2016) used W-ECOMP, which their research group developed for thermo-economic time-dependent smart poly-generation analysis and optimization. It works on a modular approach to facilitate construction of complex plant configurations. Additionally, EES applies a mathematical model to CHP design and derives the operating parameters used for

thermodynamic analysis of each energy or flow path based on mass, energy, and exergy balances (Moharamian et al. 2017, Ziebig et al. 2012). Along with DHS, CHP studies have also compared the performance of different working fluids under various conditions in terms of cost and pollution (Invernizzi et al. 2016; Mavrou et al. 2015; Qiu et al. 2012; Stijepovic et al. 2016; Victor et al.).

Mavrou et al. (2015) and Stijepovic et al. (2016) analyzed the impact of working fluids on the total efficiency and performance of heat-generating sources. Qiu et al. (2012) researched different fluids under diverse energy-generating cycles in a CHP system. Invernizzi et al. (2016) proposed titanium tetrachloride as a novel working fluid. They showed that despite some operation, design, and maintenance issues due to using titanium tetrachloride and water, it is stable up to 500°C.

**Table 8.***A Summary of the Key Literature on CHP-DHS Systems and Their Characteristics*

Approach	Energy source	Technology	Purpose	Authors
Thermo-economic	Biomass Electricity Geothermal	Boiler Steam turbine Gas turbine Ground source heat pump (GSHP)	Heat Electricity	Li et al. (2017)
	Geothermal Sunlight	GSHP Solar	Heat Cooling	Trillat-berdat et al. (2006)
	Biomass	Boiler Absorption chiller Organic Rankine Cycle (ORC) turbine	Heat Electricity Hydrogen	Ahmadi et al. (2018)
	Biomass Natural gas	Boiler Steam turbine	Heat Electricity	Sartor et al. (2014, 2018)
			Cooling	Noussan et al (2014)
		Boiler Steam turbine Gas turbine	Heat Electricity	Moharamian et al. (2017)
			Heat Electricity	Prakash et al. (2017) Ren et al. (2008)
	Biomass	Boiler Steam turbine	Heating Electricity Cooling	Lian et al. (2010)
			Heat Electricity	Ziebig (2012)
	Typical fossil fuel	Steam boiler Turbine	Heat Electricity	Ziebig (2012)
Sunlight Natural gas Electricity	Boiler Steam turbine Photovoltaic (PV) cell Chiller	Cooling Heat Electricity	Ruan et al. (2009)	
Biomass Natural gas Diesel	Micro-turbine	Heat Electricity	Pirkandi et al. (2016)	
Linear programming	Natural gas	Internal combustion engine (ICE) Gas turbine Chiller	Cooling Electricity	Ünal et al. (2016)

	Natural gas Solar	Chiller Gas turbine PV cells	Cooling Heat Electricity	Ondeck et al. (2015)
	Biomass Natural gas Heavy oil Solar	Boiler Steam turbine Gas turbine	Heat Electricity	Wang et al. (2018)
	Natural gas Electricity	ICE Steam boiler	Heat Electricity	Franco et al. (2017)
	Air (hydrogen) Electricity	Fuel cell Chiller	Cooling Heat Electricity	Weber et al. (2006)
Multi-integer linear programming	Natural gas Wind Electricity	Chiller Steam turbine Boiler Solar PV cell Wind turbine Heat pump	Cooling Heat Electricity	Weber et al. (2011)
	Restored heat	ORC cycle	Heat	Stijepovic et al. (2016)
	Natural gas Electricity	ICE Microturbine Chillers	Heat Electricity Cooling	Rivarolo et al. (2013, 2016)
		Microturbine Steam boiler ICE	Heat Electricity	Casisi et al. (2009)
	Fossil fuel Geothermal	GSHP Biomass Fossil fuel	Heat Electricity	Moret et al. (2016)
	Biomass	Boiler Gas turbine Bottoming Rankine cycle	Heat Electricity	Jørgensen et al. (2016)
		Back-pressure steam turbines Gas engines Gas turbines in combined cycles	Heat Electricity	Fazlollahi et al. (2013)

	Sunlight Natural gas Chillers	Solar Boiler	Heat Electricity Cooling	Buoro et al. (2014)
Nonlinear programming	Natural gas Electricity	Gas boiler Gas turbine Fuel cell Steam boiler Electric and absorption chillers	Heat Electricity Cooling	Jing et al. (2012)
	Gas Coal	Steam turbine Boiler	Heat Electricity	Benonysson et al. (1995)

To develop optimization methods, different techniques in holistic analyses have been used ranging from fuzzy programming to sensitivity analysis (Nieto-Morote et al. 2011). These methods have also been combined with the life-cycle assessment concept (Moret et al. 2016; Mavrou et al. 2015; Singh et al. 2023).

The intricate nature of these techniques highlights the necessity of using analytical software for the operation phase of CHP systems. Other methods for holistic analysis have been used in the optimization of CHP systems, such as linear programming, pure integer linear programming, quadratic planning, pure integer quadratic planning, nonlinear planning, pure integer nonlinear programming, multi-integer linear programming (MILP), and multi-integer nonlinear programming (MINLP). Besides using methods and tools such as the simplex method, Microsoft Excel solver or Visual Basic, designers have proposed methods for solving nonlinear problems such as the Broyden–Fletcher–Goldfarb–Shanno algorithm or the Monte Carlo method (Girones et al. 2017; Rivarolo et al. 2016; Luenberger, 2008). Decomposing nonlinear functions into several linear elements, called piecewise linearization, is another approach to nonlinear operational optimization problems that is widely used by the GAMS/LINGO platforms. Linearization of nonlinear equations via piecewise methods is carried out through unbounded and bounded function approaches or stepwise methods. The unbounded approach guarantees global optimum solutions, but it is limited to objective functions with concave maximum or convex minimum points. In contrast, the bounded approach ensures only local optima without restrictions on the existence of concave maximum or convex minimum points (Ondeck et al. 2015; Weber et al. 2011).

Because of the complexity of CHP nonlinear optimization problems, numerical methods are used to provide an estimation of optimal solutions. MILP is a common approach to solving CHP operational optimization problems with binary decision variables using techniques such as

branch and bound. The CPLEX and Xpress suites are optimization solvers especially developed for linear programming and MILP methods (Fazlollahi et al. 2013; Wei et al. 2010; Wu et al. 2023).

Multi-objective optimization, which considers several financial, technical, and environmental objectives, is also used in CHP system optimization (Pirkandi et al. 2016; Stojiljković et al. 2014). Gerber et al. (2013) used a MILP approach to formulate a multi-objective optimization problem with environmental and economic objective functions during the system life cycle.

Solving such problems requires powerful solvers with more intricate approaches. If the objective functions are of considerably different scales, normalization of objectives can be carried out (Franco et al. 2017). Designers have widely implemented the genetic algorithm (GA) and its decomposition techniques in multi-objective optimization. They have used GA to construct a Pareto front by iteratively finding global or local solutions (Rivarolo et al. 2016).

They can also employ life-cycle assessment or cost assessment for system analysis and optimization. The use of LCC in the optimization of CHP systems has been extensively reported in the literature (Adams et al. 2014; Luenberger et al. 2008). With LCC, the total annualized costs for the whole service life of a system are calculated using NPV, the discounted payback period, the internal rate of return, or annuity factors (Kaushal et al. 2017; Kayo et al. 2014; Wu et al. 2006).

The mean annual profit technique is used to formulate an economic performance indicator for CHP optimization. This method estimates the profit from the operation of a CHP system compared to the separate production of heat and electricity. Ziebig et al. (2012) used an annual profit function as the objective and a hot-water-to-space-heating load ratio as the decision

variable. This allowed them to identify the optimal allocation of energy generation between the back-pressure ST module and the cogeneration unit.

Gasification's overall advantages over direct combustion of solid biomass are efficient cleanup, lower heat loss in syngas generation, lower corrosion or slagging risks, better heat recovery from the reaction zone or exhaust flue gas, and higher efficiencies once integrated into CHP systems. Meanwhile, the disadvantages are issues like sensitivity to biomass feedstock moisture content, more complex equipment for activities such as gas cleanup to make it suitable for burning in modules such as GT units, and higher operation and maintenance costs (U.S. DoE CHP, 2019).

Members of academia and industry aiming to achieve a balance between the advantages and disadvantages of gasified biomass and make it an appropriate option for the CHP-DHS concept have focused on the optimized gaseous products of biomass (Ferrari et al. 2013; Wei et al. 2010; Williams et al. 2008; Windeknecht et al. 2015, Kaushaul et al. 2017).

The implicit optimization of biomass gasification via indicators has been the subject of several studies (Jing et al. 2012, Kaushaul et al. 2017, Prakash et al. 2017). Indicators for optimization can include operating parameters such as water-to-biomass ratio, syngas or gas mass flow rate, and reactor temperature.

Prakash et al. (2017) used indicators for optimization of gasified biomasses in CHP systems for supplying energy demands. The impact of the operating indicators (water-biomass ratio, total mass flow rate, the temperature of gasification) and 10 different biomasses readily available in India were compared for parameters such as hydrogen production, heat content, and power production from steam and organic Rankine cycles.

## 2.6 CHP Reliability Analysis

The proposed optimization approaches cover mostly capital, fuel, and pollution costs, and implicitly cover operational costs based on the approximations for maintenance and operation costs (Adams et al. 2014; Gerber et al. 2013; Girones et al. 2017). LCC analysis that addresses maintenance and operation costs cannot address the reliable configurations of systems in the design phase.

Reliability, availability, and maintainability (RAM) are essential parameters in the development, operation, and performance of current complex systems. They are some of the most important design parameters and are considered from the very beginning of the design phase of units, components, subsystems, and systems (Postnikov 2022; Milovanovic 2012).

Traditional RAM analyses are based on available dependable data from the designer and operator side. A long history of employing equipment and components in generic or specific applications, notably for electric, electronic, or electromechanics components in military, nuclear, aviation, or railway sectors led to the development of a multitude of handbooks, standards, and regulations for RAM analysis (Cornvall 2011).

RAM analysis can identify the critical item list of components that are important not only for the availability of the services or products but also for system safety. An RAM analysis in the design phase identifies critical failure modes and causes of unavailability. It helps to provide a baseline for predicting system behavior and selecting appropriate design, operation, and even supply requirements to ensure their optimized performance (Tol et al. 2015).

Regarding the reliability and availability of energy systems, the analyses were conducted more for energy generation plants or electricity generating modules. Operation cost analysis for electricity energy generation systems has been conducted for large electrical power plants by RAM concepts (Sikos 2010).

Felea et al. (2013) analyzed the reliability of the boiler structures used in a CHP system. Distribution function identification and random variables, such as time between failures or corrective maintenance, repair, and restore, were examined in a study based on failure data. Critical subsystems and components such as electrical power plant modules have been the subject of studies using diverse methodologies (Milovanovic 2012; Valdma et al. 2007).

Valdma et al. (2007) evaluated the reliability of thermal and electric power from wind plants. The authors use probabilistic models with numerical methods to analyze the reliability of such energy systems. Carazas et al. (2009) conducted GT reliability and availability evaluation of two F-series GTs using the reliability centered maintenance concept and historical failure database.

Dewangan et al. (2014) determined the reliability of a ST thermal power plant by analyzing the historical failure database of two turbines using functional tree development and by conducting failure mode and effects analysis (FMEA).

Rezaei et al. (2024) studied the integration of RAM analysis with the optimization of a biomass cogeneration production to derive the optimal values for the sizing of the modules of this system.

## **2.7 Integration of Energy Storage**

Recent generations of DHS systems and smart energy generation concepts, including poly-generation, energy storage, and particularly TES are of most interest. TES helps to economically justify and provide technically dependable CHP systems when integrated into renewable resources. The application of TES stabilizes CHP systems, particularly with intermittent renewables such as solar energy (Chidambaram et al. 2011). Among renewables, solar power and biomass are the most researched in combination with TES (Kabbara et al. 2016).

In addition to providing some level of reliability and stability to consumers, TES offers advantages such as saving energy and mitigating pollution. In Europe alone, it can save around 1.4 GWh and 400 million tons of carbon dioxide (CO<sub>2</sub>) per year (Sarbu et al. 2018).

Additionally, TES can be classified into three categories based on its heat transfer mechanism: sensible heat storage (SHS); latent heat storage (LHS), which is associated with phase change materials (PCM); and thermochemical storage (Al-Abbasi et al. 2017; Noro et al. 2014).

SHS usually operates in solid and liquid forms while LHS usually operates in three transient states (solid-liquid, liquid-gas, and solid-solid). SHS, as the simplest and least expensive storage option, is associated with technologies such as water tanks, underground storage, and packed-bed storage. LHS systems are used for solar heating/cooling of buildings, solar water heating, heat pump systems, and concentrated solar power plants. Compared to SHS, LHS using PCM, given its potential benefits and challenges, is a newer concept in energy storage, specifically when it is used with renewable energy. PCMs can retain energy with up to four times more significant heat density (Al-Abbasi et al. 2017; Sarbu et al. 2018). While hot tanks are associated with temperatures between 80 and 90°C, warm tanks are associated with temperatures between 40 and 50°C, and cold tanks are associated with temperatures between 7–15°C (Noro et al. 2014).

Researchers have performed comparisons between the advantages and disadvantages of each type, finding them capable of delivering optimal values for capacity, efficiency, storage period, and cost (Al-Abidi et al 2013; Noro et al. 2014).

Noro et al. compared liquid SHS and PCM used in a solar cooling energy plant. In their study, a simulation of a solar cooling plant with PCM TES storage was carried out to analyze storing materials' characteristics economically and technically. They optimized operating

parameters such as storage capacity, the efficiency of component operations, and energy consumption for space heating/cooling. Al-Abidi et al. (2013) conducted an economic analysis of LHS thermal storage with the aid of computational fluid dynamics analysis.

Heier et al. (2015) conducted a comprehensive review of the use of TES for meeting building energy demands. The researchers covered a range of subjects related to the different kinds of TES to be employed in the building. Tian et al. (2013) analyzed and compared accessible technologies, medium fluids, materials for heat transfer, active and passive storing techniques, structural building characteristics, less popular or limited use materials, and technologies such as thermochemical or snow storage. They studied the characteristics of PCM materials used as an LHS medium for heat transfer.

The heat transfer medium is an essential parameter, notably for PCM TES. It directly affects capacity specifications and optimal operation. Researchers have reviewed the most common solid and liquid mediums for SHS along with their physical, chemical, and thermodynamic characteristics (Ayyappan et al. 2016). The solid-state mediums that researchers have investigated are metal and nonmetal materials such as sand-rock minerals, reinforced concrete, cast steel, and magnesia fire bricks. The biggest disadvantage of solid-state mediums is that their heat capacities are rather low; their biggest advantage is their lower costs compared to other materials.

For technical and economic reasons, such as simplicity of use, lower costs, and flexibility of integration into renewable resources, water tanks have long been used as a storage medium. Researchers have closely studied their efficiency. Techniques such as water temperature stratification have been applied along with insulation to enhance water tanks' efficiency for CHP systems (Basecq et al. 2013; ECES Programme Brochure, 2016).

SHS hot water tanks have been widely used primarily in European DHSs. According to Smith et al. (2013), in Sweden, a large portion of the produced heat is stored in TES.

Water tanks help users to benefit from low electricity prices at off-peak hours. Users can store heat for use during peak hours, when electricity prices are higher. These water tanks typically have short-scale or a small-capacity TES, which makes them a better fit for building applications. Large-scale tanks are used in combination with a DHS and heat pumps because of the heat pump's ability to work at low temperatures. Basecq et al. (2013) reviewed and compared various methods for the design of short-term TES including water tanks. They specifically focused on their operation condition and performance. In particular, the active or passive nature of TES was examined, and a comparison analysis with PCM TES was performed.

Two more conventional renewables for integration with SHS and CHP concepts are solar energy and biofuels, especially for buildings (Al-abidi et al. 2013; Ayyappan et al. 2016; Chidambaram et al. 2011; Kabbara et al. 2016; Tian et al. 2013). In these configurations, solar collectors along with a biofuel-burning boiler are used to heat water and store it for domestic heating and space heating purposes (Al-abidi et al. 2013).

Underground storage in various forms has been studied in the context of SHS applications. Pipe array configurations, borehole ground heat exchangers (GEX), and aquifers are the most studied underground TES (UTES). (Novo et al. 2010) reviewed the various UTESs and analyzed the feasibility and difficulty of their use from a technical and economic point of view.

Paksoy et al. (2009) researched the use of UTES for meeting building energy demands. They compared two types of UTES, borehole storage and aquifers, and concluded that borehole TES is more efficient and economical than aquifers. Because of the nature of such storage, heat loss is the most critical parameter for the optimization of UTES.

Regarding packed-bed and pebble-bed storage, authors have studied fluids and bedding material the most for optimization purposes (Duffie et al. 2013; Nemš et al. 2017). Schumann (1929) developed the first simplified model for heat transfer in such storage. Researchers such as Nemš et al. (2017) performed thermo-hydraulic analysis. They mathematically analyzed a heating system equipped with an air-packed-bed TES that used ceramic bricks for bedding to store solar energy. The temperature ranges and air volumes were subjected to analysis for optimal economic performance. Authors have also conducted various types of mathematical modeling to examine thermodynamic behavior and thermo-hydraulic parameters like thermal conductivity or specific heat capacity.

Liu et al. (2016) conducted a survey of high-temperature LHS and SHS integration with concentrated solar panel power plants from technological and economic viewpoints. The survey included technologies and tactics for TES efficiency improvements. Thermochemical storage for large-scale applications has also been investigated by analyzing promising reactants and chemical reactions. Further, researchers have examined the corrosion problem arising from high temperatures and existing contaminants, which are common in this type of storage.

Sharma et al. (2009) split up solid-liquid PCMs into organic, inorganic, and eutectic materials; analyzed their chemical and physical specifications; and compared their advantages and disadvantages.

Kenisarin et al. (2016) analyzed and compared organic and inorganic PCMs like paraffin, fatty acids, and hydrated salts as part of the building structure for passive energy control. The materials they studied are among the most widely used PCMs. In their research, 15 full-size buildings containing PCMs were compared. The results showed that using PCM in buildings led to an increase in efficiency by mitigating air temperature variations and shifting peak demand hours.

Organic PCMs like sugar alcohols and polyols (Del Barrio et al. 2017; Gunasekara et al. 2016; Yuan et al. 2014) and inorganic PCMs like salty hydrates and metallic materials (Ge et al. 2013) have been explored.

Haoshan Ge et al. (2013) categorized PCMs based on their melting point. Their comparative research analyzed the characteristics of low melting point liquid metals and alloys that could be potentially used as smart PCMs. Higher conductivity, higher volumetric enthalpy of fusion and specific heat, and more stability compared to other conventional PCMs were identified and emphasized. However, challenges such as interaction with the container and corrosion of the container were also addressed.

Hassan et al. (2016) reviewed and addressed optimum micro-encapsulation methods and combinations of shell and core materials for optimal structural, energy, and safety performance of buildings. De Gracia et al. (2011) also researched encapsulated PCMs, conducting a numerical simulation with a finite volume method for a solar cooling system. They parametrically optimized encapsulated PCM inside an electrical hot water cylinder, which transferred heat to introduced cold water by melting the encapsulated PCM. They validated their results with experimental data for 57 vertical pipes. Agyenim et al. (2010) studied the heat transfer characteristics of RT58 PCM in a setting of a horizontal cylinder embedded by a finned tube. Experimental analysis with real data showed heat transfer coefficient increases with a rise of the fluid inlet temperature. The use of such a setting integrated into a heat pump to meet building heat demand led to a 30% increase in efficiency. Biomass is a renewable resource that has been used for supplying energy for TES. Researchers have studied the emissions of biomass-fueled systems equipped with storage. Emissions can be in gaseous, particulate, and organic forms. Advanced combustion technologies such as gasification and air/fuel staging are used for reducing emissions and increasing efficiency.

Noussan et al. (2014) thermo-economically analyzed the optimal configuration of a biomass-fired ORC system integrated into DHS. They conducted multiple parameter simulations and sensitivity analyses based on long-term operation scenarios and changes to the component size. Maximum heat storage capacity, primary energy saving, and payback period were the results for various configurations.

Volkova et al. (2018) tested the application of TES with CHP and DHS. Moreover, using a scenario-based analysis, they evaluated the influence of TES size on the performance of large-scale CHP-DHS systems. The authors showed that there is a strong relationship between electricity generation and subsidy policies.

Stritih et al. (2004) analyzed the performance optimization of a boiler with thermal storage. Via mathematical modeling in TRNSYS, the optimal values for storage volume, supply temperature, and boiler heating power were determined. The modeled system had three components: thermal storage, biomass boiler, and building.

Mongibello et al. (2014) conducted techno-economic analysis of two-storage systems intended for use in micro-CHP. The heat transfer medium was water and sodium acetate trihydrate as a PCM to save heat during electricity generation. Using a techno-economical approach, the researchers aimed to optimally size two SHS and LHS systems for micro-CHP systems in two residential buildings. Their results showed that using PCM storage resulted in larger heat exchangers than using SHS storage.

Wang et al. (2018), using a dynamic simulation methodology, examined the storage capacities for various boiler operational modes, such as boiler on-time, boiler off-time, and maximum boiler output temperatures. The heat storage capacities for low, medium, intermittent, variable, and high heat demand profiles were optimized.

In Pantaleo et al.'s (2020) study, a hybrid power system consisting of solar-biomass subsystems equipped with thermal storage for heat recovery was thermodynamically analyzed and techno-economically optimized. A wood chip biomass-fired boiler equipped with a bottoming ORC module and solar panels was integrated, and thermal storage was used as a link between the top and bottoming cycles. The size of TES via GA was optimized. The results showed that the hybrid biomass-solar system increased the system's efficiency and flexibility. However, it raised costs, highlighting the need for incentives and supportive tariffs.

In a techno-economic study, Sorrentino et al. (2018) analyzed the heat demand of a commercial building to optimize the configuration and size of a biomass-fired boiler coupled with ORC module and TES systems. The molten salt type of TES was added to decouple the boiler from the ORC module and avoid partial operation and low efficiency.

Pfeifer et al. (2016) focused on unused land in Croatia to evaluate the economic feasibility of biomasses for combined cooling, heating, and power purposes with heat storage. Based on defined scenarios, they analyzed the economic behavior of the biomass-fed poly-generation system that was feeding a 90°C TES with an efficiency of 80%. Heat generation up to 30 MW and electricity generation up to 15 MW were accounted for in system sizing (Pfeifer et al. 2016).

Krajačić et al. (2011) analyzed the impact of feed-in tariffs on various storage types used in European countries. They economically analyzed the sensitivity to technical parameters of various energy storage components such as pumped hydro storage, hybrid wind-pumped hydro storage, hydrogen storage systems, and batteries combined with PV systems. Their results were promising for the use of storage in renewable-fed grids.

Chen et al. (2007) worked on the "Renewislands" program with four work packages to verify the profitability of renewable supplies (biomass, biogas), hydrogen, and fuel cell modules.

They considered various case studies to evaluate the integration of renewables and decentralized power systems using energy storage. They delivered the main results for each work package.

Coelho et al. (2015) techno-economically analyzed the feeding of gasified biomass from wastewater treatment to a central receiver system for two base and hybrid cases in Portugal. They compared various hybridizations of the biomass and central receiver systems to find a case with a lower levelized cost. Simulation analysis for energy demand, solar fluxes, and air cycles was run to evaluate economy of scale using various software. The authors calculated the size for the central receiver system equal to 4 MW rated electrical capacity.

## **2.8 Green Hydrogen Production**

Although RESs could be one of the best alternatives to fuel-based systems, they are mainly uncontrollable and intermittent in natural sources. They can cause fluctuations in the outcome of RES-based systems. To stabilize them, energy storage systems have been developed with hydrogen as a carrier and underground storage (Mahmoud et al. 2021). Hydrogen energy storage systems, when combined with RESs in the grid, offer tremendous potential for energy generation and storage. They address the need for management of grid demand, contributing to the enhancement of overall energy sustainability (Arsad et al. 2022). Underground storage is one of the most effective methods for the practical large-scale use of hydrogen. This approach seamlessly integrates with intermittent green electricity-producing sources like solar and wind. Gas Infrastructure Europe highlighted the necessity for green underground hydrogen storage (UHS), which plays a pivotal role in maintaining balance and ensuring the resilience of the future energy system. This is of paramount importance, especially because the current energy landscape requires supply-and-demand equilibrium over various timescales. Furthermore, the European Hydrogen Backbone outlined the value that an extensive, integrated hydrogen transport infrastructure can bring to Europe's future energy system (Cihlar et al. 2021).

These integrated systems are instrumental in facilitating the widespread deployment of hydrogen as a versatile energy carrier. They not only contribute to the harmonization of RESs but also provide backup power and support various industrial processes. Underground storage is particularly appealing because of its considerable capacity and safety advantages. Regarding UHS's integration into hydrogen energy systems, Li et al. (2022) introduced an approach driven by deep deterministic policy gradients, framing energy management as a Markov decision process. This novel approach uses an actor-critic structure, which they validated through time-domain simulations to reduce network dependence.

Ongoing research endeavors are directed toward achieving improved convergence, adapting to renewable energy fluctuations, and exploring alternative optimization strategies. Building on this, Farahani et al. (2020) explored a 100% renewable energy system at Shell Amsterdam, where hydrogen is at the forefront as an energy carrier. Their efforts revolved around evaluating various scenarios, conducting cost analyses, and optimizing scheduling while safeguarding the integrity of electric vehicles and fuel cells. Their conclusions underscored the viability of an integrated energy and mobility system that leverages both electricity and hydrogen as energy carriers, stressing the need for essential infrastructure and incentives for successful implementation.

In a different domain, Song et al. (2021) delved into a hybrid system that combined offshore wind power with hydrogen storage in depleted oil reservoirs. Their study took a comprehensive approach, using a mathematical model that integrated components such as Weibull distribution, wind turbine power function, Faraday's law, continuity equation, Darcy's law, state equation of real gas, NPV, and levelling. Through their work, the authors emphasized the importance of renewable and carbon-free energy for sustainability, with a significant focus on the cost-effective use of renewable energy through hydrogen production and underground

storage. Notably, their findings revealed that wind speed significantly influences both the NPV of the system and the levelized cost of hydrogen.

In the broader context of China, Qiu et al. (2020) undertook an investigation of UHS within a hydrogen penetrated energy system (HPES), considering both salt caverns and depleted hydrocarbon fields. Their study unfolded as a multi-faceted analysis of three distinct Chinese regions to determine the feasibility of HPES implementation. The combination of salt cavern UHS with offshore wind power is promising, particularly on China's east coast. While the authors acknowledged longer payback periods in certain regions, their research underscored the enduring benefits of such systems. The effectiveness of salt cavern UHS shines through in terms of construction cost, cushion gas level, gas injection/withdrawal capability, and a shorter investment payback period.

Wu et al. (2023) advocated for a renewable energy system that seamlessly united wind and photovoltaic power with hydrogen storage in salt caverns. Their approach stands out for its use of an improved particle swarm optimization algorithm, which meticulously homes in on system optimization. They underlined the flexibility of hydrogen storage and comparatively reduced space requirements, reinforcing its economic viability and carbon emission reduction. It is crucial to note that hydrogen storage costs constitute a significant portion of operational expenses in this model.

The above studies provided valuable insights into the multifaceted realm of UHS, emphasizing the importance of technological innovation, economic viability, and sustainability. The next section will discuss the significance of hydrogen storage systems in depth. It will provide a comprehensive overview of these systems, examine both past and present research on them, and explore their prospects.

Okundamiya et al. (2021) argued that fuel cell technology is experiencing significant global adoption, particularly in domestic and commercial applications.

Integrated energy storage devices serve the specific purpose of addressing temporal imbalances in renewable energy generation. They possess the potential to maximize energy use and enhance the flexibility of both energy consumers and the grid (Zhang et al. 2020).

Energy storage systems typically consist of two key components: energy storage devices and power conversion systems. Integrated systems offer notable advantages in terms of scalability for larger capacities, operational flexibility, rapid response times, and environmental sustainability. However, they do have drawbacks such as reduced efficiency and specific technological limitations, particularly in the case of hydrogen-burning GTs (Gao et al. 2014).

Choosing the right storage form (e.g., compressed gas, liquid, ammonia) is a complex decision influenced by factors like geographical constraints, safety regulations, installation costs, storage volume, transportation logistics, and the intended end use. Each storage form has its distinct advantages and disadvantages compared to others (Schrotenboer et al. 2022).

The topic of integrating and, in some cases, substituting hydrogen storage within battery energy storage systems has been the subject of extensive research and analysis. This hybrid approach provides a cost-effective and high-performance solution, particularly for seasonal energy storage needs. Hybrid battery and hydrogen storage systems effectively address the limitations of standalone batteries, including cost, charge/discharge capacity, and environmental considerations (Yuksel et al. 2018).

This approach is well-suited for large-scale PV systems. While battery systems currently excel in terms of efficiency, they face limitations in scalability compared to hydrogen storage. Previous research has indicated that the most promising means of hydrogen generation is through

wind energy. Conversely, based on analytical findings, geothermal energy emerges as the pivotal external investment resource for electricity in hydrogen production (Yavuz et al. 2020).

Additionally, hydrogen energy offers a promising solution to tackle challenges in wave energy converter (WEC) systems. By directing generated electrical power toward hydrogen production instead of transmitting it to the mainland, the need for a lengthy power cable to connect the WEC system to the grid is eliminated. Moreover, the hydrogen produced can be safely stored underwater at low temperatures in the deep sea, reducing energy transfer losses associated with cable-based transmission and enhancing overall system efficiency (Yavuz et al. 2020).

Wind energy is cost-effective and clean but faces intermittency and potential visual or noise concerns. Hydropower is efficient but has environmental impacts and location restrictions. Geothermal energy is reliable but limited geographically. Biomass energy is versatile but raises emissions and land use issues. The selection of renewable sources depends on project objectives and local conditions, with hybrid systems emerging as a promising alternative.

## **2.9 Biomass-Based Hydrogen Energy Systems**

Optimization of biomass-powered systems is more problematic than that of fossil fuel systems. The reason for that is the uncertainties associated with biomass supply as well as technical issues such as biomass heat values, leftovers, maintenance, availability of resources, and feedstocks. To make biomass systems feasible for fuel and energy generation, researchers have explored different aspects of their integration into other systems, including their economics, technology, and environmental effects, through the phases of design, operation, and development (Stijepovic et al. 2016). There are three main techniques for generating hydrogen from biomass:

- a) The thermochemical technique
- b) Biological methods

c) Electrolysis from biomass electricity

The third method is achievable with other renewables as well, because 92.9% of the sources that are used in electrolysis are renewable sources. This method also provides the best environmental effect compared to the other two methods (Ju et al. 2018; Lin et al. 2018).

In this method, the biomass plant is designed to meet all the electricity demand for both the electrolysis (for generating hydrogen) and compression stages (to store it), with no extra external power requirement. The required energy is around  $4.2 \times 10^{12}$  joules to produce  $4.2 \times 10^{12}$  joules of equivalent hydrogen energy (Kalinci et al. 2009).

Research has shown that electrolysis is the most efficient method of green hydrogen production; the authors compared the effectiveness of numerous hydrogen-producing systems (steam reforming, biomass gasification, electrolysis, dark fermentation, and pyrolysis) and concluded that electrolysis with more than 70% recovery efficiency is the most efficient way, whereas fermentation has the lowest recovery efficiency at around 20% (Singh et al. 2023).

The gasification of biomass followed by the upgrading of the resultant gas is a method used to generate hydrogen from renewable resources that results in practically carbon-neutral hydrogen production. Cormos et al.'s (2023) study included a technical, financial, and environmental evaluation of several different green hydrogen generation pathways through the gasification of decarbonized biomass. They could reduce CO<sup>2</sup> emission by approximately 34% compared to other assessed pathways.

Valizadeh al. (2022) reviewed the feasibility of biomass valorization by gasification to produce green hydrogen for commercial and industrial applications. They concluded that green hydrogen from biomass is a promising technology to meet future energy demands. However, power cycles based on electricity generation and recovery of heat were not included in their research.

Oner et al. (2022) increased the overall efficiency of the solar and biomass energy-driven systems by integrating these systems.

A cogeneration system (electricity and hydrogen) at the microscale was based on biomass resources, and a comparison was made between gasification and digestion; however, the cost of storage and its effects were not considered in that study. The authors concluded that the gasification process is better in terms of economics because its cost is 21.6% lower compared to the digestion process (Cao et al. 2022).

## **2.10 Biomass-Based Hybrid Energy Systems Optimization**

Besides heat generation, CHP and trigeneration are more prevalent concepts in biomass-powered systems economics, specifically either in large-scale industrial energy generation (Proskurina et al. 2017) or in micro-CHP concepts for residential purposes and low enthalpy buildings and districts (Pirkandi et al. 2016).

In their first research, Rezaei et al. (2019) reviewed the various approaches in optimizing, hybridization and hydrogen generation approaches for making Biomass powered energy systems.

Rezaei et al (2021) then performed research and development on a combination of biomass and geothermal systems in cold climates to supply economically 171 kW rated heating capacity for a building, while only 44% to 56% of the total rated capacity is in use. Then Rezaei et al. (2024) researched on justifying biomass-powered systems to supply heat to remote north Canadian communities in reliable manner via a joint RAM-optimization method. By obtaining optimal results, authors concluded that the optimized sizing of components rated capacities is the most important parameter in minimizing cost and emissions.

By gasifying the biomass and considering the carbon conversion ratio as well as the warm water temperature, Li et al. (2017) improved the thermodynamic performance of the proposed system. They concluded that gasified biomass could economize such systems. Moreover, the

overall energy efficiency was improved to 72%, while the system efficiency of the CHP was reported to be 40%.

Lian et al. (2010) tried to analyze the thermo-economic optimization of a trigeneration system that provided cooling in addition to heat and electricity. They concluded that exergy destruction has the highest value in the furnace, amounting to almost 60%.

Noussan et al. (2014) thermo-economically analyzed a trigeneration biomass-powered system running on a ST and increased its efficiency by up to 8.6% through installation of TES. Based on the steam temperature for different operating fluids, using the MINLP formulation, Stijepovic et al. (2016) tried to optimize a trigeneration biomass-powered system running on a ST.

Using a nonlinear programming approach, Sartor et al. (2014) modeled a boiler-powered biomass system and simulated the performance of a biomass-natural gas hybrid system based on the CHP concept to feed a DHS. They concluded that decreasing the temperature of the hot water in the district distribution network by 40% can reduce half of the heat loss in the pipes.

Ünal et al. (2016) analyzed the operational optimization and management of a trigeneration. They found that the operation of a hybrid trigeneration system decreases the total annual costs in comparison with individual system under the same conditions.

Sameti et al. (2019) selected linear programming optimization for a trigeneration system comprising solar thermal and PV along with absorption chillers and thermal storage. Over 22% of carbon emission reduction was achieved after optimization compared to the normal cooperation of the integrated system.

Rezaei et al. (2024) performed the optimization of a biomass-based heat, power, and hydrogen trigeneration system using joint RAM and optimization approach and provided the results for optimal and reliable sizing for thermal, power, and hydrogen modules.

Regarding an integrated energy system, particularly for power plants, studies have largely addressed the reliability, availability, maintainability, and safety of the plants; the equipment in the systems or subsystems; and the components. For example, Shonin et al. (2017) stated that because of the faults in the operation of GTs, it is essential to improve their reliability for uninterrupted power generation. This in turn reduces the risk of more pollution. Similarly, using failure distribution functions, Felea et al. (2013) conducted a structural reliability analysis of boilers in a CHP system.

Based on statistical data, the empirical description of the boiler can be expressed using the Weibull and normal distribution functions. Postnikov (2022) studied the reliability of a hybrid energy wind and CHP-integrated system and used the availability criteria as the reliability factor. They calculated it according to the heat demand profile.

## **2.11 CHP-DHS Optimization Challenges and future**

To compensate for the relatively higher costs of DHS systems, authors have studied the topic of integrating them into CHP systems or product generator modules for a long time.

Another promising solution to offset the cost challenge in such systems is to increase the biomass share, replacing more fossil fuels with biomass in hybrid systems and integrating other byproduct-generating modules into biomass.

Energy dispatching control is another strategy for ensuring the affordability and efficiency of energy generation and distribution, given that many DHSs run with low temperature flows in supply and return networks to avoid heat loss at substations. To provide higher temperatures and better control of energy dispatching, thermal storage integration could be considered.

However, these cost reduction configurations and optimization requirements in the design phase result in higher final costs during the operation phase when the availability of energy generation and reliability of systems matter.

Challenges such as lower heat content or seasonality of renewables, variability of energy demands, extension of energy networks, and integration of new concepts such as newer technologies raise doubts about the availability and reliability of the results for renewable energy systems, notably in areas with harsh climates and remote communities. There is a lack of a dependable methodology to consider RAM criteria inherently during design optimization. In lack of such methodology and to ensure availability of services, overdesign of equipment or redundant components (more than needed) are considered that cause increasing system operation costs. There is an important need to integrate the reliability of energy supply into optimizations of solutions and scenarios during study or design phases. Addressing reliability during optimization could ensure the delivery of a smart, consistent, and responsive energy generation and distribution system that considers the seasonality of renewable resources, varying energy demands, and various network configurations or energy concepts.

## **2.12 Research Gap Analysis**

Despite the increasing popularity and availability of renewable energy systems worldwide including solar, wind, biomass, geothermal etc. which are integrated to deliver energy demands in various concepts and via multiple systems, and considering large number of the optimization efforts carried out to make them affordable, such renewable systems continue to face significant challenges in terms of energy reliability and availability, particularly in remote areas with harsh climates that suffer from limited resources and infrastructure, feasibility constraints, and cost-efficiency issues. Many communities in these areas rely on a single energy source, often supported by government subsidies, which still frequently fails to meet energy demands due to

intermittent availability, operational limitations, cost inefficiencies, or environmental impacts.

Current research has examined biomass-powered technologies and other renewable systems, such as geothermal and hydrogen generation.

However, research on hybrid biomass energy systems that take advantage of available local resources while explicitly accounting for reliability and availability constraints remains limited. In particular, the integration of biomass-powered systems within hybrid configurations for cold climates, such as those in Canada, has not been fully explored, especially regarding operational limitations and techno-economic and environmental implications in northern regions near the Arctic.

Recent advancements in hybrid energy system design have demonstrated technical feasibility, potential economic benefits, and reduced greenhouse gas emissions. Studies have also investigated optimization approaches for energy generation, supply and dispatch, energy storage, and system sizing.

In harsh climate regions such as northern Québec, the application of biomass-powered energy systems that function reliably and economically raises several key questions:

- Which hybrid combinations are most reliable?
- What factors most influence the likelihood of such systems being successfully implemented as resilient and reliable solutions in northern Canada?
- To what extent do RAM factors affect the design in terms of performance and techno-economic and environmental evaluations?

The need to answer these questions, in the absence of comprehensive research, is clear. Further development is required in several areas:

Designing flexible and modular biomass-powered hybrid energy systems capable of operating reliably under various energy generation and demand profiles in isolated communities in harsh climates.

Integrating RAM metrics into optimization frameworks to evaluate associated costs, assess feasibility, quantify system performance, and consider environmental implications under operational uncertainties.

This thesis aims to bridge the gaps by proposing and developing a RAM-integrated optimization methodology for biomass-powered hybrid energy systems intended for harsh climates, notably in northern Canada. This research analyzes how reliability constraints influence system design and affect both operational modes and environmental outcomes. Using a modular and flexible framework with a joint RAM-Optimization approach, the research evaluates different hybrid combinations for energy sources or products (e.g., biomass, geothermal and hydrogen generation) and provides guidance on their applicability (or other resources) for heating and electrifying remote communities in Canada. By explicitly integrating a probabilistic RAM analysis to system optimization, this work addresses the gap in designing reliable, resilient, and financially viable hybrid energy systems, particularly for biomass-based configurations.

### 3 Chapter 3: Methodologies

In this chapter, three different models used biomass as a source of energy to generate heat, power, and hydrogen by incorporating RAM constraints. Several key assumptions were made to ensure a coherent and effective evaluation of the models. First, it was assumed that the biomass feedstock was available and sustainable, with a consistent supply chain. Next, the models assumed that the operational environment for biomass conversion systems was stable, and any external factors, such as weather or market fluctuations, would not significantly disrupt energy production. The RAM constraints were integrated into models under the assumption that the necessary technical and maintenance infrastructure are not easily available in place to support heavy repairs and maintenance or overhauling. It was further assumed that the systems being evaluated can go rapidly to the failure rate hazard increasing phase of its service life, due to harsh climate it is working, namely North Canada. Last, economic factors such as the cost of biomass, infrastructure, and the technology's overall life cycle were considered stable and predictable within the context of this study in Canada. These assumptions were fundamental to the methodology's ability to accurately assess each model's viability and efficiency in real-world applications. All other assumptions and a detailed methodology flowchart were provided for each model separately.

The methodology was defined as a step-by-step methodology depending on the model. At the first step of optimization, besides achieving the optimal (minimum) values for cost, the optimal system sizing, including the rated capacities for modules or their use times, was obtained and used as an input in the second phase either for optimizing the remaining technical parameters such as GSHP boreholes or for RAM parameters. Before providing the details of each model, the background and formulation of the reliability analysis were described.

### 3.1 Background

Classical reliability analysis employs data derived from real tests and inspections to evaluate systems. This applies to RAM analysis in the domain of long-established industries such as aviation, nuclear, military defense, and even fossil fuel energy generation. This study was novel because it incorporated optimization and RAM analyses into a joint RAM optimization approach in the design phase, delivering values for system performance parameters while keeping the cost at an assured minimum level and reliability and availability at acceptable higher levels.

However, renewable energy systems, because they are rather new compared to other systems, suffer from a rarity of dependable test data or specific standards.

Because of the particularities associated with such systems, namely their capability of being integrated into new modules and delivering a varied basket of energies, enough data may not be accessible for extracting the necessary parameters with a reasonable level of confidence.

Attempts at gathering renewable energy systems' RAM data, such as inherent or operational availability levels and failure rates, or developing prediction methodologies at the subsystem level are not usually successful or are sufficient because of the characteristics of such systems, notably systems with mechanical component modules. For example, using a constant failure rate distribution may not apply to such components because of wear, fatigue, and other stress-related failures and degradations that result in more complicated data collection.

Estimating effective design life or using time of equipment is another difficult task. Numerous life-limiting failure modes such as corrosion, erosion, creep, and fatigue operate on the component at the same time and have a synergistic effect on reliability.

Using methods such as FMEA that were developed primarily for electronic equipment evaluation is not completely appropriate for renewable energy systems because of a lack of data about the probability of occurrence of each identified failure mode of mechanical and electrical

components. Therefore, the application of traditional RAM analyses in a dependable manner was not possible, and theoretical or design optimization were considered for RAM analysis instead.

Because the RAM analysis was carried out early in the design phase to aid in design assessment; cost reduction for installation, operation, and maintenance costs; and formulation of a maintenance plan for assuring system availability, it was an integral part of the system optimization and would be performed jointly with it.

## **3.2 Formulation of Reliability, Maintainability and Availability**

### **3.2.1 Reliability**

Reliability is the probability that the system will perform its intended function for a specified interval of time under stated conditions.

The three steps for reliability analysis were carried out below: (a) system reliability modeling, (b) reliability analysis, and (c) result analysis and interpretation.

System reliability modeling is performed simultaneously with optimization modeling based on the modularization of the energy system and splitting of the system into constituent elements, notably heat, electricity and hydrogen modules. In this phase, considering the lack of accurate and available data, system breakdown to the lower levels (parts and units) was not carried out and system reliability modeling remained at the module level.

For model reliability analysis, calculation of reliability performance indices of each module (block) and reliability functions and RAM parameters were performed simultaneously while optimization calculations were performed via the coupling of the decision variables, notably modules use times.

In the third phase, by considering the desired reliability level of availability and obtained reliability and maintainability parameters, it was decided whether the results obtained were

practical enough or not. It was done by a mix of expert feedback, sensitivity analyses and optimization methods comparisons.

Instantaneous failure rate,  $\lambda(t)$ , or hazard rate function, is a reliability measure. It is derived from the distribution function of the time to failure. The expression  $\lambda(t) \Delta t$  is approximately equal to the conditional probability of failure during the time interval  $(t, t + \Delta t)$  given not failing of that item during the interval  $(0, t)$ .

Reliability function  $R(t)$  with  $R(0) = 1$ , and conditional reliability  $R(t, t + x | t)$ , when no failure has occurred in time  $(0, t)$ :

$$R(t) = \exp\left(-\int_0^t \lambda(x) dx\right) = 1 - \int_0^t f(x) dx \quad (1)$$

$f(x)$  is the probability density function of the time to failure of the item, and  $\lambda(x)$  is the instantaneous failure rate of the item.

$$\lambda_{(t)} = \frac{f(t)}{R(t)} = \lim_{\Delta t \rightarrow 0} \left( \frac{n_s(t) - n_s(t + \Delta t)}{n_s(t) \Delta t} \right) \quad (2)$$

$n_s(t)$  is the number of items that are still operational at the instant of time  $t$  ( $n_s(0) = n_0$ ).

$n_s(t) - n_s(t + \Delta t)$  is the number of items that fail in the time interval  $(t, t + \Delta t)$ .

The estimated value of the failure density function  $f(t)$ , at time  $t$ , is given by the following:

$$f(t) = \lim_{\Delta t \rightarrow 0} \left( \frac{n_s(t) - n_s(t + \Delta t)}{n_0 \Delta t} \right) \quad (3)$$

Conditional reliability,  $R(T, T+t)$ , is defined as the conditional probability that an item can perform a required function for a given time interval  $(T, T+t)$ , provided that the item survived during  $(0, T)$ :

$$R(t|T) = \exp\left(-\int_T^{T+t} \lambda_{(t)} dt\right) \quad (4)$$

The expected value of the continuous random variable called time to failure is mean time to failure (MTTF). In many practical situations, knowledge of MTTF is enough to assess the quality and usefulness of a certain component, subsystem, module, or system.

$$\text{Mean (operating) time to failure MTTF} = \int_0^{\infty} R(t) dt = \int_0^{\infty} t f(t) dt \quad (5)$$

When  $\lambda(t) = \lambda$  for all values of  $t$ ,

$$f(t) = \lambda e^{-\lambda t} \quad (6)$$

$$R(t) = e^{-\lambda t} \quad (7)$$

$$\text{MTTF} = \frac{1}{\lambda} \quad (8)$$

If the time to failure of an item has a Weibull distribution with scale parameter  $\alpha > 0$  and shape parameter  $\beta > 0$ , then

$$\lambda(t) = \frac{\beta * t^{\beta-1}}{\alpha^{\beta}} \quad (9)$$

$$R(t) = e^{-\left(\frac{t}{\alpha}\right)^{\beta}} \quad (10)$$

$$f(t) = \frac{\beta * t^{\beta-1}}{\alpha^{\beta}} e^{-\left(\frac{t}{\alpha}\right)^{\beta}} \quad (11)$$

Mean failure rate for the items is calculated as follows:

$$\underline{\lambda}(t_1, t_2) = \frac{1}{t_2 - t_1} \int_{t_1}^{t_2} \lambda(t) dt = \frac{1}{t_2 - t_1} \ln \frac{R(t_1)}{R(t_2)} \quad (12)$$

For repairable items, modeling is based on the simple renewal process while restoration time may be neglected or the time to restoration may be nonzero. In this case, the item transits between an up state and a down state. The measure of reliability is the failure intensity derived from the expected value of the cumulative number of failures of a repairable item occurring during the time interval  $(0, t)$ .

### 3.2.2 Maintainability

Maintainability is the ability of a system, component, or unit to be retained or restored to a state where it can perform service under the conditions of use for which it is designed. Measures used in maintainability analysis are mean time to repair and mean time to restore which are the expected or mean values of the random variable called time to repair or time to restore.

Considering equipment that is subjected to regularly scheduled maintenance, such maintenance is considered ideal when it takes little time to maintain equipment (compared to the time between incidences of maintenance) and to restore components to a “like-new” state. This concept is intended for components such as mechanical components or electrical components that rely on mechanical parts, especially when their failure rates increase.

$f_T(t)$  = failure density function after maintenance

$T_M$  = Fixed time interval between maintenance

$$f_1(t) = f_T(t) \text{ for } 0 < t \leq T_M \quad (13)$$

Density function for equipment after maintenance consideration is written as follows:

$$f_T^*(t) = \sum_{k=0}^{\infty} f_1(t - kT_m) R^k(T_m) \quad (14)$$

The function  $f_T^*(t)$  after every maintenance is scaled down by a scaling factor equal to  $R(T_m)$  of the function in the previous phase before maintenance.

The ideal maintenance density function of the lifetime of equipment shows an exponential behavior, and in this case the value of MTTF with maintenance included is calculated as follows:

$$\text{MTTF}^* = \int_0^{\infty} t f_T^*(t) dt. \quad (15)$$

The time is assumed to be put up for restoring the equipment to a new state, but after the happening of failure in an unpredictable time. Ideal repair can be modeled as zero time to repair. The best example of ideal repairs is the replacement of faulty or failed equipment.

Like maintenance time, zero time for repair is a relative concept and can be considered as the required time for repair compared to the time to failure of equipment.

### **3.2.3 Availability**

For conventional energy systems, the productivity of a system or energy plant is measured by a combination of indicators that are influenced by their availability and magnitude, frequency, and duration of outages as well as their costs.

Availability analysis is a methodology that results in improving the productivity of a plant or system. This analysis in its terminology ranges from cost-availability, cost-benefit analysis or trade-off evaluations based on the system's operational and environmental parameters to theoretical or pure mathematical analysis considering design technical parameters. Solutions for optimizing plant productivity are recommended based on the results of availability analysis. Availability helps to balance compromises carried out between maintainability and reliability against each other to minimize overall cost.

Conflicting measures, parameters, and technical, economic, or environmental constraints appear at every phase of a system's life, and each influences the optimal operation of such a system. Thus, availability goals shall be evaluated at the design phase and the cost shall be estimated to be minimized before proposing solutions to improve the productivity of a plant.

The availability of a system  $A(t)$  is the probability that the system is operating successfully at time  $t$ .

Availability is a function of reliability denoted by MTBF or MTTF and maintainability that is designated by MTTR as follows:

$$A_{(t)} = \frac{MTTF (MTBF)}{MTTF (MTBF) + MTTR} \quad (16)$$

If the time to repair/restore is very low compared to the time between failures, the MTBF could be said to be the same as MTTF, and the two terms could be used interchangeably.

In this study's methodology, which was developed for the biomass-powered hybrid energy system, the hazard rate profiles, failure distribution, or reliability functions were unknown in many cases. The time-dependent reliability function with Weibull distribution was incorporated as a constraint to the time-dependent cost objective function of the whole system. The Weibull distribution function models the increasing hazard phase of the system life cycle inter-coupled by power module use times to the objective function, which is a correlation function of the rated capacities of thermal and electrical modules, their usage times, and biomass chemical composition. The cost and reliability function constraints conflict because minimizing cost requires increasing the module usage times. This leads to reducing the reliability level of modules, which is considered unfavorable for system economic behavior and operation.

Therefore, the thermal and electrical modules are constrained by a reliability function with Weibull distribution that delivers the scale and shape factors necessary for developing a failure distribution function based on equation 11. Due to lack of reliable data about the design architecture of the hydrogen module, the reliability constraint was not defined for hydrogen generating module. Knowing the reliability and failure distribution functions (equation 11) and setting the time interval between maintenance, MTTF after maintenance was derived from equation 15. By considering the predetermined availability levels, the maximum required mean times to restore MTTR were obtained from equation 16.

#### ***3.2.4 Weibull Function Applicability***

In this research, the Weibull distribution function was selected among other functions for reliability modeling to represent the reliability characteristics of the thermal and electrical modules. The Weibull distribution was chosen primarily because of its flexibility in representing

various failure behaviors through its shape and scale parameters, making it suitable for components in hybrid biomass-powered energy systems.

Although Monte Carlo and Markov or semi-Markov modeling were theoretically possible for this methodology, the Weibull function was preferred.

Monte Carlo simulation, commonly used for uncertainty analysis, requires a large number of input samples and well-defined probability distributions, which were highly uncertain for biomass-based components in remote applications, rendering it less practical under data-scarce conditions.

Furthermore, the Weibull distribution provides a direct and tractable way to characterize time-to-failure for non-repairable modules in harsh and isolated environments, which is the case for this research due to the remoteness of the studied communities, their low population density, and extreme climatic conditions. These modules were considered effectively non-repairable, reflecting the real challenges of mobilizing repair personnel and spare parts in such areas, where failed components are more realistically replaced than repaired. This also justifies modeling an increasing hazard rate phase, which is typical for northern Canadian regions.

Markov models require detailed state-transition data, which were unavailable for emerging biomass-based technologies in northern Canada. In contrast, Weibull models can be parameterized with little or no time-to-failure data, which can be estimated from engineering knowledge.

For these reasons, the Weibull distribution was selected as it provides a computationally tractable and widely accepted approach that integrates seamlessly into the RAM-constrained optimization methodology, ensuring consistency with reliability engineering practices for energy systems in remote areas. To avoid unnecessary computational complexity and because the two-

parameter Weibull function is sufficient, mathematically tractable, and adequately flexible to capture the expected increasing failure rate patterns, the two-parameter Weibull function was chosen.

### **3.3 Proposed and Developed Models**

Based on the system configuration and objective function modeling, the decision variables of this optimization process were thermal, electrical, or byproduct (hydrogen) producing modules' technical or performance parameters such as the modules' rated capacities and their use times, hydrogen mass flow rates, and reliability and failure distribution factors.

Depending on the number of objective functions (single or multi-objective optimization) and multiplicity of decision variables, the methodology was also flexible to adopt various multi-criteria decision-making (MCDM) techniques. In one studied case, a special MCDM technique called TOPSIS was used to demonstrate the capability of the methodology to model multi-objective optimization problems.

Three models were developed for the application of reliability analysis to three distinct systems with various heat, power, and hydrogen production applications.

The three models are proposed and developed to demonstrate how the research objectives are progressively realized.

#### **Model 1: Bio-Geo Hybrid System for Heat-Only Applications**

This model demonstrates the feasibility of hybridizing biomass-powered energy systems with other renewable resources by integrating biomass and geothermal modules for heat production. It establishes an optimization platform necessary for the joint RAM-Optimization methodology (**Objective 1**) under a single energy-vector approach (heat only), while accounting for

environmental and cost parameters. RAM role definition and RAM indicators embedding were carried out in this model. (Objective 2).

It highlights the modularity of system design (**Objective 3**) by showing the potential for hybridization of biomass with geothermal energy.

Its application to a single building in remote polar regions of Canada, such as Kuujuaq, provides an initial validation against **Objective 4**.

It also demonstrates the contribution of the optimization component of the methodology to building design trade-offs (**Objective 5**).

### **Model 2: Biomass for Combined Heat and Power (BCHP) Applications**

This model expands the methodology to pursue the hybridization approach by adding electricity generation to heat production through a CHP configuration.

It presents the joint RAM-Optimization methodology (**Objective 1**) by identifying optimization decision variables that are integrated into probabilistic reliability functions and metrics (**Objective 2**) and applying RAM indicators, including MTTF, MTTR, and availability, as explicit constraints in the optimization function and (**Objective 2**).

Its case study demonstrates how joint RAM-optimization delivers not only optimal energy production values but also reliable system operation for districts in harsh climate environments, directly validating **Objective 4**.

It further highlights the contribution of the joint RAM-optimization methodology to district-level design trade-offs (**Objective 5**).

### **Model 3: Hydrogen Production Integrated with BCHP**

The third model extends the methodology to a more hybridized system involving heat, electricity,

and hydrogen.

It verifies and validates the applicability of the joint RAM-Optimization methodology to a BCHP system enhanced with hydrogen production (**Objectives 1 and 2**), and embodies the scope of **Objective 3** by demonstrating modular expansion of the framework to incorporate hydrogen alongside CHP.

Reliability and availability metrics are embedded in the optimization (**Objective 2**) and used to evaluate system performance under harsh climate and economic conditions (**Objective 4**).

By explicitly modeling fuel, maintenance, and pollution costs alongside RAM constraints, this model illustrates the unique benefits of joint RAM-optimization in advanced hybrid energy design (**Objective 5**).

### ***3.3.1 Model 1: Bio-Geo Hybrid System***

The first developed methodology was established for a combined biomass-geothermal (bio-geo) system, as shown in Figure 8, to supply only heat for a single building in low enthalpy areas with an extremely cold climate. This methodology was intended to be a pilot methodology for verifying the applicability or feasibility of the predicted overall methodology for the next hybrid configurations. The optimization was a multi-objective nonlinear optimization where, because of its nature and delivery of a Pareto front of the optimal values, a MCDM technique was coupled with the optimization process to form a two-step optimization strategy. The purpose of this strategy was to achieve exploitable energy with the least pollution and cost possible. The reliability distribution function constraint was not applied to this methodology. Three nonlinear cost objective functions for optimization were used to minimize the heat generation cost and pollution for a modeled building in Kuujjuaq, Canada. Beside this model, other models are defined either for building or district applications in this area.

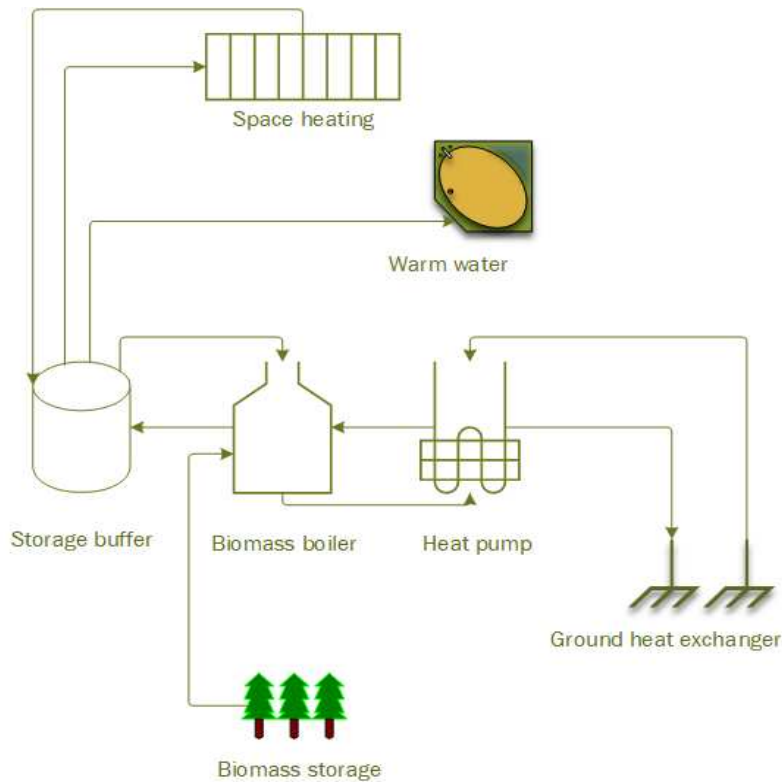


**Figure 8**

*Schematic View of the Subsystem Blocks and Their Configurations*

The bio-geo system was split into two parts: surface and subsurface. Twelve scenarios, including three wood pellet types in four distance ranges from pellet mills, were first defined. Scenario definition was done based on the available correlations for cost per biomass logistics distance for Canada. By modeling a building for heat demand analysis, the required building heat demand was obtained. Next, in the first step of optimization, the cost and pollution functions for surface parts were derived and optimized using GA to deliver Pareto fronts of optimal values. These were screened using TOPSIS to size the biomass and geothermal surface subsystems. In the second step, using the optimal sizing from the first step, the cost of the subsurface part, namely the geothermal GEX, was minimized.

12 scenarios were optimally configured in this way to be optimized to deliver minimum cost and pollution related to operational parameters, such as use time and rated powers. The developed methodology has capability for integration into other technologies, such as GT or ST, TES and other energy storages, or by-products like hydrogen. The optimization process, as its first step for minimizing the cost, optimized component sizing above the ground, including the biomass boiler for the defined case study. The second step addressed optimizing GSHPs and borehole settings for the geothermal module. As Figure 9 depicts, the steps are as follows:

**Step 1 of Optimization.** At this step, optimization was performed on the surface part based on two explicit functions, one for surface equipment costs and another for pollution. The cost objective functions for surface components were developed and correlated to technical parameters such as biomass boiler and geothermal heat pump capacities or biomass fuel compositions and pollution constituents. A GA code was developed in MATLAB to carry out the minimization of the surface part cost and pollution. The GA MATLAB code delivered a Pareto front of the optimal solutions for each scenario. That meant a set of solutions was delivered as a trade-off for cost and pollution. TOPSIS was then implemented at this step of optimization to find the optimal solution among the Pareto fronts using three criteria. The criteria were selected based on the system's technical parameters, namely generated heat powers, use times, and boiler efficiencies. The purpose was to deliver the maximum values for these three parameters while keeping the cost and pollution at the minimum level. The result of the first step was that the biomass boiler and geothermal heat pump achieved optimal sizing while delivering minimum cost and pollution.

**Step 2 of Optimization.** After minimizing the cost of surface components, at this step, the cost function for the equipment under ground, called the subsurface equipment, was targeted for

minimization. Optimization was performed for the subsurface cost as a function of the bore field specification namely borehole pipe (GHX) length (Tol et al. 2015).

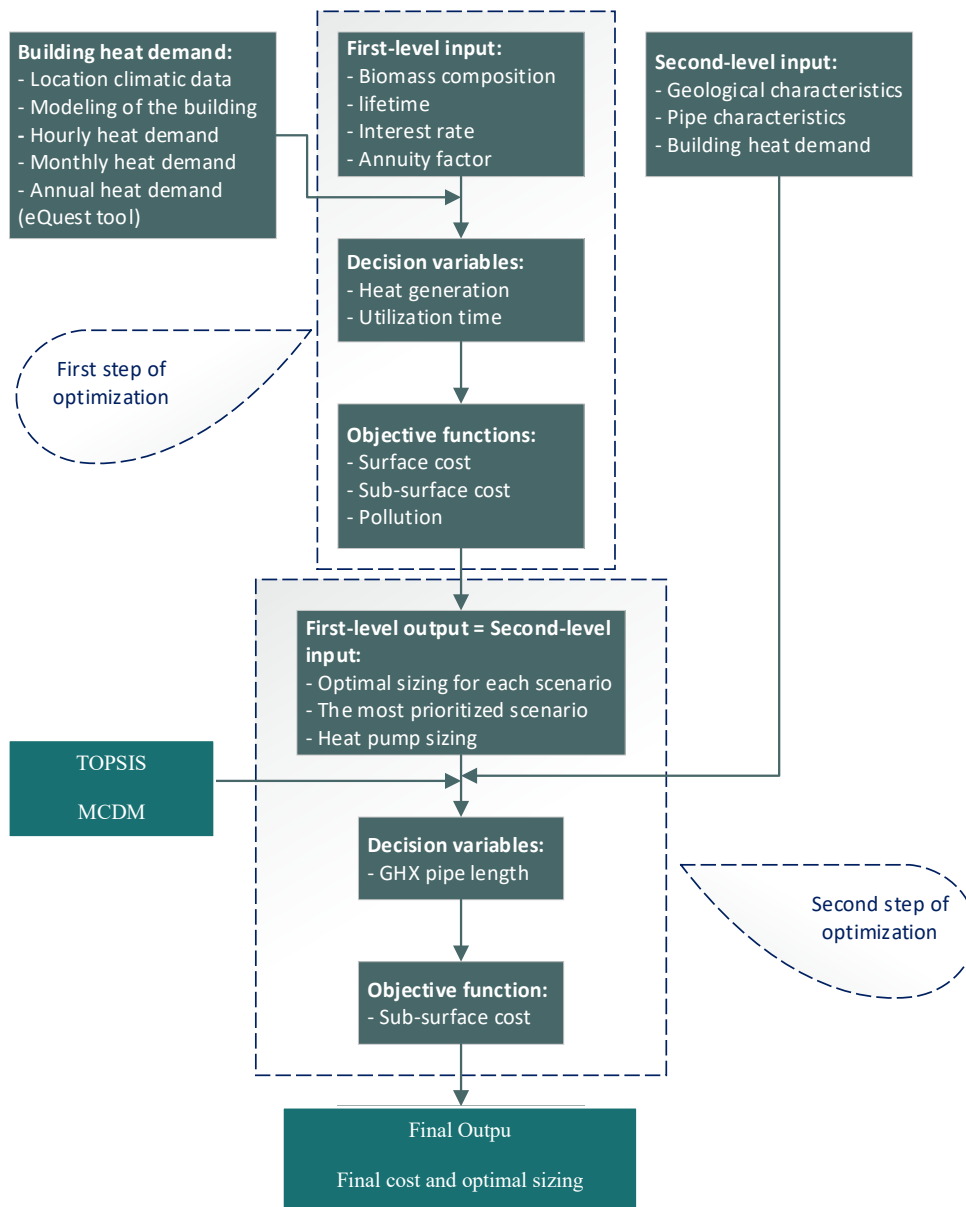


**Figure 9**

*Schematic View of the Subsystem Blocks and Their Configurations*

*Methodology Flowchart proposed for first model*

The bore field specifications, including total lengths, pipe types, aspect ratios, and pipe diameters, were restrained by the heat pump specifications in addition to the site geotechnical

characteristics (Philippe et al. 2010). The geotechnical characteristics of the region and ground load were derived from the geological and weather reports for Kuujjuaq, Canada (Belzile et al. 2017; Giordano et al. 2017).

**Scenarios.** Twelve scenarios were defined based on three biomass types and four distances from feedstock mills. The biomasses used in the research were high heat value (HHV), medium heat value (MHV), and low heat value (LHV) woods, which are abundant in Canada.

Four distances of 50, 150, 250, and 350 kilometers from the mills were considered for scenario definitions to conduct the sensitivity analysis of biomass logistics, including fuel cost and distance. These distances were the most common ranges of energy generation plants from feedstock resources and the cost correlations for such distances are more reliable. (Boukherroub et al. 2016).

**Formulation of Total Cost.** The cost function modeling of the bio-geo system was performed based on an annualized cost analysis (Sartor et al. 2014) for both surface and subsurface parts of the modeled system, considering their capital and operation (op) costs:

$$C_{tot} = C_{sur} + C_{subsur} \quad (17)$$

$$C_{sur} = (C_{cap} + C_{op})_{sur} \quad (18)$$

$$C_{subsur} = (C_{cap} + C_{op})_{subsur} \quad (19)$$

C : Cost

Sur : Surface

Subsur : Subsurface

Cap : Capital

Op: Operation

Next, the above formula was rewritten as follows where these costs were decomposed into biomass (bio) and geothermal (geo) modules:

$$C_{sur} = (C_{cap} + C_{op})_{sur\ bio} + (C_{cap} + C_{op})_{sur\ geo} \quad (20)$$

$$C_{subsur} = (C_{cap} + C_{op})_{geo\ subsur} \quad (21)$$

The capital costs for biomass and geothermal modules were correlated to the nominal capacities of each subsystem. The operation cost in this research consisted of the biomass purchase, transportation, and geothermal heat pump electricity consumption costs derived from the literature and surveys (Boukherroub et al. 2016; Croteau et al. 2015; Hassan et al. 2020; Tol et al. 2015, Vallios et al. 2009, Sartor et al. 2014). The cost objective function of surface parts considering operation costs as the percentage of capital cost was derived as follows:

$$C_{sur} = \frac{(11114P_{bio}^{0.67} + 38065P_{geo}^{0.4225})}{P_{bio}\tau_{bio} + P_{geo}\tau_{geo}} + \frac{0.0036(C_{feedstock} + 20 + 10(D - 50))}{\eta_{bio}NHV} + C_{elec} \text{ (CAD/kwh)} \quad (22)$$

In which  $\frac{0.0036(C_{feedstock})}{\eta_{bio}NHV}$  is the fuel cost,  $\frac{0.0036(20+10(D-50))}{\eta_{bio}NHV}$  is the transportation cost, and  $C_{elec}$  is the electricity cost for the operating geothermal module.

P: Module rated capacity (kW)

$\tau$ : Module use time (hr)

$\eta$ : Efficiency factor

*bio*: Biomass boiler

NHV: Net heat value

Elec: Electricity

$C_{feedstock}$  stands for biomass feedstock purchase price (CAD/ton) and  $\eta_{bio}$  is the biomass combusting efficiency. Pollution cost correlation was derived based on the NHV of the biomasses, the moisture content of wet biomasses (MCWB), the biomass module rated capacities and use times. MCWB of the biomass, expressed as the quantity of water per unit mass, ranges variably from 8% to more than 60%. The optimization considered various levels of MCWB during analysis for sensitivity analysis but for final results derivation, it was set to 30% (Demirbas et al. 2004).

For pollution, the CO<sub>2</sub> and sulfur dioxide (SO<sub>2</sub>) shares were considered the most detrimental pollutants in the gaseous state, and pollution was modeled as the sum of CO<sub>2</sub> and SO<sub>2</sub> pollutions. The pollution assigned to electricity necessary for running GSHP was added to these pollutions.

Biomass fuel was modeled as  $C_a m H_n O_x N_y S_z$ , in which:

Ca, H, O, N, and S indicate carbon, hydrogen, oxygen, nitrogen, and sulfur constituents of the modeled biomass and

m = Number of carbon atoms

n = Number of hydrogen atoms

x = Number of oxygen atoms

y = Number of nitrogen atoms

z = Number of sulfur atoms

$$Pollution = \frac{0,0036P_{bio}\tau_{bio}(44m + 64z)}{\eta_b NHV(12m + n + 16x + 14y + 32z)} + 1.2 \times 10^{-6} P_{elc} \tau_{geo} \text{ (ton)} \quad (23)$$

Where  $NHV = [34.1Ca + 101.98H - 9.85O + 6.3N + 19.1S][1 - 0.01MCWB] - 0.02452MCWB \left(\frac{MJ}{kg}\right)$  (24)

The numbers of elemental atoms were obtained from the biomass percentages. Table 9 shows the percentages for each type of biomass.

**Table 9.**

*Weight (Mass) Percent for Biomass Composition (Noussan et al.2014)*

<b>Fuel Type</b>	<b>Carbon</b>	<b>Hydrogen</b>	<b>Oxygen</b>	<b>Nitrogen</b>	<b>Sulphur</b>	<b>Ash</b>
<b>HHV Wood</b>	52.10%	5.7%	38.90%	0.20%	0.00%	3.10%
<b>MHV Wood</b>	52.00%	4.00%	41.70%	0.30%	0.00%	2.00%
<b>LHV Wood</b>	48.85%	6.04%	42.64%	0.71%	0.06%	1.70%

The pollution share for heat pump electricity was set to 1.2 grams per kWh of electricity generated in Kuujuaq, Canada, and its contribution to pollution was added to pollution from biomass burning in equation (23).

Based on the local utility company's (Hydro Quebec) data,  $C_{elec}$  was set to 0.0608 Canadian Dollars (CAD) per kWh.

Annuity factor  $\varphi$  for equivalent annualized cost calculation of one-time lump sum or capital costs was defined as follows:

$$\varphi = \frac{i}{1 - (1 + i)^{-T}} \quad (25)$$

where  $i$  stand for interest rate and  $T$  is the system service lifetime. If necessary, and in case the whole lifetime of a system is being considered, all the one-time fixed lump sum costs like capital costs are annualized and the recurring costs were considered on average to determine the uncertainty, seasonality or volatility of the markets and economic situations over time.

The economic parameters, such as service life and interest rates necessary for the annuity factor, were set to 30 years and 3.25%, respectively (“Bank of Canada”; “Canadian Biomass Magazine”). A ratio of 10% of capital cost has been considered to address the maintenance costs. This relatively high value for maintenance costs was chosen based on the particularities of a

system consisting totally of renewable sources in a remote area with harsh climate (Tol et al. 2015).

Biomass purchase prices were set to 250, 300, and 350 CAD per ton for LHV, MHV, and HHV woods, respectively. These values were yielded and estimated from the literature review and inquiries made throughout Canada (Boukherroub et al. 2016; Murugan et al. 2016).

A thermal conductivity of 2.29, a mass density of 2,540, a specific heat of 1,000, and a granitic thermal diffusivity of 0.10368 were used to size the geothermal GEX based on the ground and soil properties of the intended area (Belzile et al. 2017; Majorowicz et al. 2015).

The undisturbed ground temperature for the region was equal to 8. The operating fluid in the geothermal system was a solution composed of water and 40% ethylene glycol with a specific heat capacity equal to 3,472.72 (Majorowicz et al. 2015; Philippe et al. 2010).

The cost function at the second step included the subsurface costs, namely the costs associated with piping and drilling costs. The drilling cost was the main part of the geothermal subsurface formulation, and the contributions of other parts in the cost function could be neglected. The cost was extracted via the correlation below (Tol et al. 2015):

$$C_{subsur} = \frac{1.934 \times 10^{-7} L^2 + 1.664 \times 10^{-3} L + 0.38}{N(P_{bio}\tau_{bio} + P_{geo}\tau_{geo})} \text{ (CAD/kWh)} \quad (26)$$

where  $N$  stands for the number of bore holes,  $D$  is the drilling depth ( $m$ ), and  $L$  is equal to the total piping length in meter ( $m$ ). This cost was annualized.

The applied constraints to the cost objective function were as follows:

$$P_{bio} + P_{geo} = Q_{max} \quad (27)$$

$$0 \leq \tau_{geo}, \tau_{bio} \leq 7884 \text{ hr} \quad (28)$$

where the building heat demand after modeling a three-story building was fixed to 172,16 kW.

The use times of both biomass and geothermal modules considered the downtimes necessary for overhaul or heavy maintenance.

A GA method was employed to search for the optimal configurations at minimum cost. This optimization technique was adopted based on literature review and previous experiences in the field of hybrid energy system design optimization and because of its capabilities for global solution finding via its heuristic and random population generating features. (Alajmi et al. 2014).

The GA method obtained the optimized points after evolution of several generations from the initial population and after meeting the termination criteria for stopping further evolution. Individuals of each generation were selected based on selection functions or criteria such as randomness of selection, crossover, and mutation.

The parameters and criteria for running the GA code in MATLAB software are listed below:

- a) Population size: 250 (performed from 100 to 1000 with no change when exceeding 200)
- b) Creation function: Default (constraint dependent)
- c) Fitness scaling: Default (rank scale)
- d) Selection function: Default (Stochastic uniform)
- e) Elite count:  $0.05 \times$  population size
- f) Crossover fraction: 0.5, also tested with default (0.8)
- g) Mutation/Crossover function: Default (0.2)
- h) Migration direction: Forward (fraction: 0.2 intervals: 20 by default)
- i) Constraint parameters: Default (augmented Lagrangian)
- j) Stopping criteria: (stall generations: 50; function tolerance; constraint tolerance)

The GA code was run 60 times for each scenario to cover the solution spaces and to find as much as possible optimal solutions close to global ones. The results were then averaged, and

the outliers were screened for this purpose. For comparison results were compared to results of a gradient-based optimization code.

Note: Because the same code was used for the next model, Table 10 summarizes the objective functions, and the main parameters used in the GA code for optimization of all cases besides those used for the heat-only bio-geo system first case. This table was referenced when GA was used in future methodologies by changing some constraints or adding new parameters for reliability and maintenance. The main reasons for using GA for this study are listed below:

- a) It can handle a larger number of parameters, which is the case for methodologies, namely cost and reliability correlations as functions of numerous technical and performance parameters.
- b) It is less sensitive than other methods to objective function parameters such as variable types (discrete or continuous) via its evolutionary algorithm.
- c) It benefits from operation controls such as selection, crossover, and mutation to better ensure that the solution is not random by keeping the best solution in each generation of solutions.
- d) It has a great capability to be coupled with building energy simulation programs.

**Table 10**

*Summary of the Main Parameters, Variables, and Constraints in the Optimization Process*

Objective function	Final cost = Capital cost ( <i>Surface, subsurface, modules etc.</i> ) + Operation and maintenance costs (fuel, pollution, transportation) – Raised incomes (electricity, hydrogen)
Decision variables	Rated capacities for all three modules, their usage times, hydrogen mass flow rates, and reliability scale, shape factors, maintenance intervals and mean time to (between) failures.
Decision variables constraints	0,5MW < P <sub>el</sub> , P <sub>th</sub> < 10MW second case and 5MW < P <sub>el</sub> , P <sub>th</sub> < 50MW third case 1000 hr < τ <sub>el</sub> , τ <sub>th</sub> < 276000 hr second case and 20000 hr < τ <sub>el</sub> , τ <sub>th</sub> < 276000 hr 4000 hr < T <sub>MeI</sub> , T <sub>Mth</sub> < 20000 hr Minimum accepted reliability level > 40% for second case and > 40% for third case

	1 MW << P <sub>elc</sub> + P <sub>th</sub> < 20 MW second case and 10 MW < P <sub>elc</sub> + P <sub>th</sub> < 50MW third case
Parameters	Biomass purchase costs = (150 CAD/ton for LHVW, 250 CAD/ton MHVW and 350 CAD/Ton HHVW) Pollution costs = 30 CAD/Ton biomass weight (mass) percentages given in table 9 annuity factor parameters: system lifetime: 30 years, inflation (interest) rates: 3.25 % modules efficiencies defined for each case, etc.
Population	The population size is 250. It should be noted that increasing the population size after 200 does not change the optimization results.
Fitness function	Fitness function = $\left(\frac{\text{Reliability}}{10 \times (0.1 + \text{Cost})}\right)^2$ considering $0 < \text{Reliability} < 1$ The weighting factor (10) and translation parameters (0.1) are used in the formula. A weighting factor is used for the normalization of the cost compared to the reliability scale. A translation parameter of 0.1 is selected to raise income.
Mutation rate	The selected mutation rate is chosen through trial and error to balance fast convergence with sufficient exploration, preventing premature convergence. In MATLAB, the MutationFcn set to mutationgaussian applies Gaussian-distributed changes to several randomly selected genes in the population. Then, mutation uniform is used with the default value of “rate = 0.01.” It is corrected to 0.05 by trial and error. Finally, mutation uniform = 0.05 is selected for the current research.
Selection method	Both selection tournaments with a size of 10 and selection roulette are tested. A selection tournament with a size of 10 is preferred for this research.
Termination criteria	Termination criteria are applied by using MaxTime set to 1,200 seconds. The maximum number of iterations is 10,000.
Code running time	60 times for each GA and Gradient based method for sensitivity analysis and validation

### 3.3.2 Model 2: Biomass for CHP Application - BCHP

The methodology developed was for modeling a CHP system fed by biomass after analysis of the first model application on its case study, which was a heat-only bio-geo system. The primary purpose of formulating this methodology was to develop an enviro-economic optimization process for a CHP energy system subject to a minimum acceptable level of reliability. It was done after developing the first model and observing its capability to accept reliability function within optimization in conflict with cost objective function.

The methodology used in this case was still considered a two-step enviro-economic optimization approach, but unlike in the first methodology, its second phase was used for optimizing the MTTR and availability parameters of the system after deriving the optimal values for cost, technical parameters, and reliability parameters, namely MTTF.

Based on the results of modeling the first methodology, the multi-objective optimization was replaced by single objective optimization exposed to reliability function constraints by eliminating pollution as a second objective function, associating cost with it, and integrating it into fuel cost to form the operation cost function. It was performed based on the results of the first model application on to its case that demonstrated that results are sensitive to pollution and to give an estimation of pollution costs that shall be considered as part of whole system's costs.

Therefore, a nonlinear cost objective function was formulated consisting of capital cost, fuel costs, transportation and pollution costs. Fuel, transportation and pollution costs were characterized as previous methodologies based on the biomass specific heat values and their composition.

Reliability parameters used as constraints were those nonlinear functions of the Weibull distribution denoted in equations (10) and (11). The reliability and failure distribution functions in these equations were associated with both electrical and thermal modules by employing their use times in those functions. The optimization in this way, coupled with nonlinear reliability parameters and two constraints of reliability parameters (for electrical and thermal module), was defined for this work.

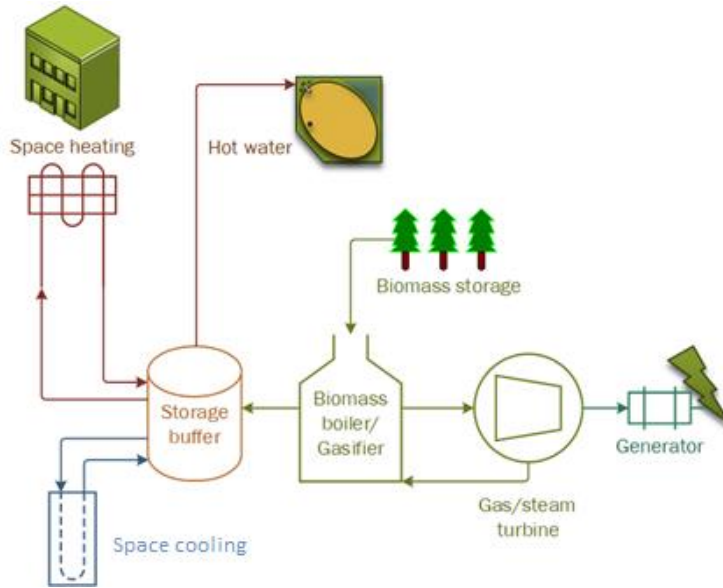
Regarding the pollution function, CO<sub>2</sub> and SO<sub>2</sub> pollutants were accounted for in the formulation for calculating costs as per Canadian-defined penalties per ton of the generated pollution (“Canadian Biomass Magazine”).

Figure 10 shows the schematics used for a biomass-driven CHP generation system. Steam and gas turbine ST/ GT (or other sorts of ICEs) operate along with a biomass boiler to provide electricity for the CHP concept. They are used in DHS in north Canada to provide heat for space heating, hot water services, or heat-driven cooling systems such as absorption refrigeration. However, cooling demand was out of the scope of the study. The estimation of heat and electricity demand of such district was based on extrapolation of building demand modeled for first model in Kuujuaq.

Figure 11 contains a flow chart of the proposed RAM-based methodology specific to this model, and the steps or phases followed for the analysis of such a system.

A genetics algorithm code was developed in MATLAB to carry out the minimization of the cost objective function. The results of the optimization were the biomass boiler and GT/ST sizing performance parameters and electricity and heat use times, reliability (failure times), scale, and shape factors for reliability and failure distribution functions.

For sensitivity analysis, six scenarios were defined with three biomass types as the previous methodology, namely HHV, MHV, and LHV woods, and two technologies, STs and GTs. They are denoted as HHVW-GT, HHVW-ST, MHVW-GT, MHVW-ST, LHVW-GT, and LHVW-ST. Because of results of the first model application to its case, that showed considerable sensitivity to logistics distance, all scenarios are considered for 50 km distance from feedstock biomass location.



**Figure 10**

*Configuration Schematic Used for a Biomass-Driven CHP Generation System*

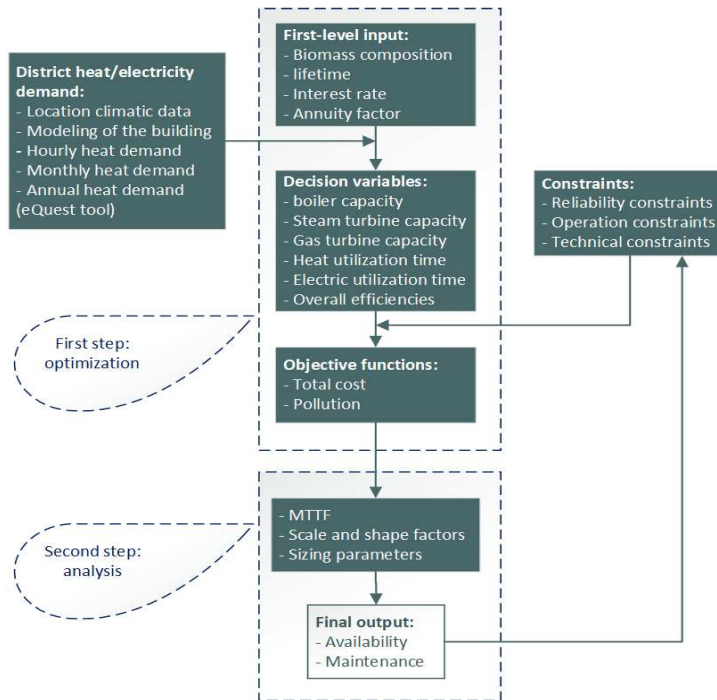


**Figure 11**

*Methodology Flowchart proposed for second model: Reliability-, Maintainability-, and Availability-Based Methodology*

Moreover, two configurations for energy generation were considered. In the first configuration, the gasifier unit gasified biomass and provided fuel to feed a GT compressor. The superheated exhaust gases from turbines were recuperated in the DHS substation heat exchangers and then supplied to DHS for heat demand meeting purposes. In the second configuration, the boiler was fed either by gasified biomass or by biomass feedstock directly. Boiler supplies required heat for STs, and STs like GTs provided both electricity and heat from recuperated exhaust gases in DHS substations. In both configurations, electricity for the system's main equipment was provided, and the extra electricity was sold to the grid. Both configurations could be integrated into a preheater intended for DHS if necessary. This preheater could play the role of an energy storage device in the form of an underground heat exchanger that could also be part of the borehole network of a geothermal system. The cost modeling of the biomass-powered system was carried out through an annualized cost analysis by decomposing the total cost into capital (cap) and operation (op) costs (Sartor et al. 2014):

$$C_{tot} = (C_{cap} + C_{op}) \quad (29)$$

$C_{cap}$  stands for capital costs associated with thermal and electricity modules,

$C_{op}$  stands for operational cost:

$$C_{cap} = (C_{cap \text{ thermal unit}} + C_{cap \text{ electrical unit}}) \quad (30)$$

The capital costs were correlated to the rated thermal (th)  $P_{th}$  and electricity (el)  $P_{el}$  capacities in kW of installed modules and their usage times,  $\tau_{th}$ ,  $\tau_{el}$  (Boukherroub et al. 2016; Croteau et al. 2015; Rivarolo et al. 2013; Sartor et al. 2014; Tol et al. 2015; Vallios et al. 2009).

For two system configurations using steam and GTs, the capital costs were calculated as follows:

$$C_{cap\ Config\ 1} = C_{cap\ Boiler} + C_{cap\ steam\ turbine} = (840P_{th}^{0.6} + 6400P_{el}^{0.778}) \quad (31)$$

$$C_{cap\ Config\ 2} = C_{cap\ Boiler} + C_{cap\ gas\ turbine} = (840P_{th}^{0.6} + 2420P_{el}^{0.872}) \quad (32)$$

As per the previous case, for equivalent annualizing of one-time lump sum costs, annuity factor  $\varphi$  was defined as that of equation (25) with the same parameters as those for the first model, namely service life equal to 30 years and interest rate equal to 3.25%.

Operation cost  $C_{op}$  consisted of biomass fuel purchase, transportation, maintenance, and pollution costs (Boukherroub et al. 2016; Tol et al. 2015; Vallios et al. 2009).

$$C_{op} = (C_{fuel} + C_{transportation} + C_{maintenance} + C_{pollution}) \quad (33)$$

$$C_{fuel\ (CAD/kwh)} = \frac{0.0036 * C_{feedstock}}{\eta_{bio\ (gaseous)} NHV} \quad (34)$$

In which  $C_{feedstock}$  stands for biomass feedstock purchase price (CAD/ton) and  $\eta_{bio\ (syn)}$  is the biomass conversion (heat or gaseous forms) efficiencies for direct combusting of biomass or its conversion to gaseous forms. Biomass purchase prices were set to 250, 300, and 350 CAD per ton for LHV, MHV, and HHV woods, respectively. These values were yielded and estimated from the literature review and inquiries made throughout Canada (Boukherroub et al. 2016; Murugan et al. 2016). NHV has the same definition as that for the heat-only bio-geo system.

Transportation cost as a function of distance to biomass feedstock location (D) was as follows (Boukherroub et al. 2016):

$$C_{transportation\ (\frac{CAD}{kwh})} = \frac{0.0036 * (20 + 10(D - 50))}{\eta_{NHV}} \quad (35)$$

In which  $D$  stands for feedstock storage distance to power plant (50 km).

The maintenance cost for each maintenance session of the electrical and thermal modules was set as equal to 2% of their initial capital costs for each maintenance. The aim was to consider the losses due to any probable halt of system use (Sartor et al. 2014).

Because the maintenance interval  $T_m$  for both electrical and thermal units was the parameter of optimization, the number of maintenance sessions  $N$  for each module was calculated as follows:

$$N_{th} = \frac{\tau_{th}}{T_{mth}} \quad (36)$$

$$N_{elc} = \frac{\tau_{el}}{T_{mel}} \quad (37)$$

Therefore, the maintenance costs for electrical and thermal units were as follows:

$$C_{maintenance} = C_{maintenance\ of\ thermal\ unit} + C_{maintenance\ of\ electrical\ unit} = N_{th} * 0.02 * (C_{cap\ boiler}) + N_{el} * 0.02 * (C_{cap\ steam\ or\ gas\ turbine}) \quad (38)$$

Therefore, for each configuration, the maintenance costs were calculated as follows:

$$C_{maintenance\ config\ 1} = N_{th} * 0.02 * (C_{cap\ Boiler}) + N_{el} * 0.02 * (C_{cap\ steam\ turbine\ module}) = \left( \frac{\tau_{th}}{T_{mth}} * 0.02 * 840P_{th}^{0.6} + \frac{\tau_{el}}{T_{mel}} * 0.02 * 6400P_{el}^{0.778} \right) \quad (39)$$

$$C_{maintenance\ config\ 2} = N_{th} * 0.02 * (C_{cap\ Boiler}) + N_{el} * 0.02 * (C_{cap\ gas\ turbine\ unit}) = \left( \frac{\tau_{th}}{T_{mth}} * 0.02 * 840P_{th}^{0.6} + \frac{\tau_{el}}{T_{mel}} * 0.02 * 2420P_{el}^{0.872} \right) \quad (40)$$

Pollution cost was taken into consideration based on the previous methodology as reflected in equations (23) and (24) and the pollution cost per ton was considered equal to 30 CAD/ton (“Canadian Biomass Magazine”).

For calculating the final cost, all the cost components were divided by the total delivered power (heat and electricity) given by  $P_{th} * \tau_{th} + P_{el} * \tau_{el}$ .

By varying reliability levels (represented by MTTF or MTBF) and maintainability levels (represented by MTTR), availability levels could be set based on the characteristics of equipment or operation requirements. Therefore, reliability levels could have variable values, and the system operator could compromise the time and frequency of the maintenance and repairs to restore the

components and keep the availability of the whole system at predetermined levels. Hence, minimum values for reliability levels could be compromised or decided by the system designers or operators.

To envision the minimum acceptable reliability levels for the operation of energy systems, inquiries were made among some energy operators, and a range of minimum values was used for the reliability constraint function in the optimization of both configurations (Postnikov 2022; Valdma et al. 2007).

Besides, the RAM parameters values could be decided at the design phase as an assumption or as input data, or they could be decided by the designer. For example, in the research by Sartor et al., they assumed an availability level equal to 98% (Sartor et al.). In this research case study, the minimum acceptable value for reliability was set at 40% for both thermal and electrical modules.

By deriving the shape and scale factors of the associated reliability function during optimization, the failure distribution function was derived. Then, using the equations (14) and (15), the optimal MTTF after maintenance was derived.

Considering the predetermined availability levels, using equation (16), the optimal values of MTTR were obtained. At this point, it could be said that the profile of operation of the system with minimum cost, assured minimum acceptable levels of reliability, and maximum availability levels were yielded with optimal values for all technical and RAM parameters like rated capacities, use times, and maintenance interval times.

### 3.3.3 *Model 3: BCHP-Hydrogen Generation*

The principal objective of the methodology developed for this model was to analyze a platform for an enviro-economic optimization of a biomass system and produce electricity and heat as well as hydrogen through electrolysis within acceptable levels of availability and reliability. Such a

system would contain three main modules, namely thermal, electrical, and hydrogen-generating modules, and include a boiler, TES, GT, electrolyser, compressor, and hydrogen tank that would be optimized to deliver affordable products such as heat, electricity, and hydrogen. To that end, a cost objective function was developed comprising thermal, electrical, and hydrogen-generating and storing modules using correlations that were derived from other studies. These correlations estimated costs based on each module's performance parameter. The cost function included both capital and operational costs. It incorporated the capital cost to purchase and install all modules. The income from selling extra electricity to the national grid or selling hydrogen was subtracted to yield the final cost of the system. Total cost, which was the objective function, was optimized using GA and a Gradient based optimization code to derive the optimal values for the minimum cost of such systems and through validation by the comparative analysis of both codes and methods results.

As the second model, such an objective function (cost) was constrained by a reliability function, which was modeled by a time-dependent ( $t$ ) Weibull distribution function. This function covers the decreasing, constant, and increasing hazard rate phases of the system by including a scale parameter  $\alpha$  and a shape parameter  $\beta$  as follows. For the reason of applying this model to a remote area district with harsh climate in north Canada, the increasing rate phase of such function was subjected to optimization.

The optimization of method settings in MATLAB or the averaging of results to derive the optimal results, and the use of parameters for reliability level constraints, were as the second model. The reliability function was kept as high as possible, while the total cost was attempted to be minimized. For system configuration, the hybrid system in this study was composed of three main thermal, electrical, and hydrogen-generating modules as follows:

1. GT provides electricity for running the hydrogen module and selling electricity to the grid. The electrical module capital and installation costs were modeled as a function of a GT power-rated capacity.

2. A biomass boiler was used for configuring the thermal module. The thermal module capital and installation costs were formulated via a correlation of biomass boiler capacities. The TES can be integrated into such configuration for energy management purposes.

3. The green hydrogen module consisted of an electrolyser, a compressor, and a hydrogen storage tank. The hydrogen module capital and installation costs were functions of the electrolyser, compressor, and hydrogen generation rated capacities.

The operational activities for running such a system, such as biomass purchase, transportation, storage, pollution and electricity consumption, maintenance, and sale of products (i.e., electricity and hydrogen), were also considered in the total costs referenced and calculated in previous models.

The electricity consumption and electricity selling incomes were calculated based on the unit price per kWh of generated or consumed electricity. The maintenance cost was considered for three modules, which was a function of maintenance intervals and the predefined costs for each maintenance activity.

For this model, just HHV wood was considered as the biomass resource with the characteristics addressed in Table 9. As Figure 12 illustrates, biomass was injected into the gasifier section of the biomass component. It was gasified to feed the GT along with air from the high-pressure compressor. Exhaust from the GT was directed to the heat recovery section to heat up the water for domestic applications in districts.

The residual char remaining from gasification was then combusted to produce heat and to supply district heating. Electricity generated in a GT provides the required amount for

electrolysis to produce hydrogen. Some of the electricity is transferred to the local grid to earn an income. The hydrogen is also sold to compensate for some expenses.

An unbounded increase in the size of the electrical module will eventually lead to higher total costs. There is an optimal size for the electrical module. At the same time, because both hydrogen and electricity are sold, an optimal combination of sales can be obtained as part of the solution to reliability constraints.

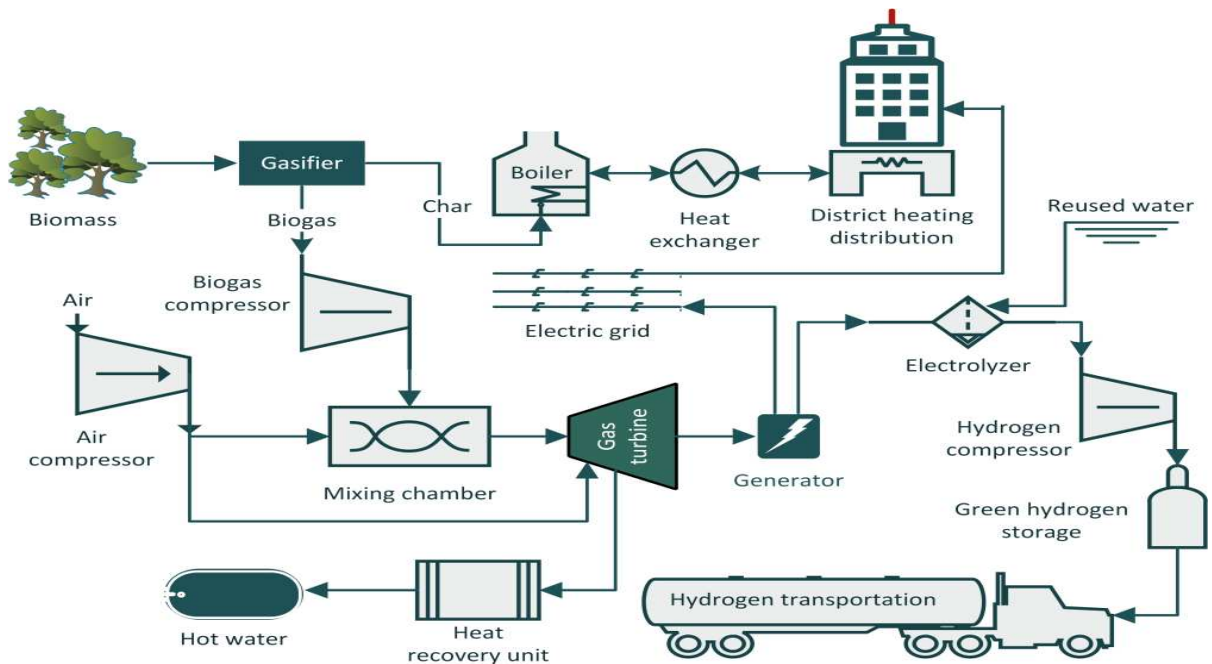


**Figure 12**

*The Biomass-Gasification Electricity-Electrolysis-Heating System*

The optimization process was carried out using a nonlinear algorithm to minimize the system cost as the objective function. It was constrained by the nonlinear reliability function, which was supposed to be maximized by considering maintenance interval times. Figure 13 provides a flowchart of optimization specific to this model.

A gradient-based constraint nonlinear multivariable optimization along with GA was carried out to determine and validate system performance parameters such as electricity, heat, and hydrogen capacities as well as RAM factors like maintenance intervals.

Decision variables of this optimization process were thermal, electrical, and hydrogen-generating modules' performance parameters such as rated capacities and their usage times, hydrogen mass flow rates, maintenance intervals, and other reliability factors.

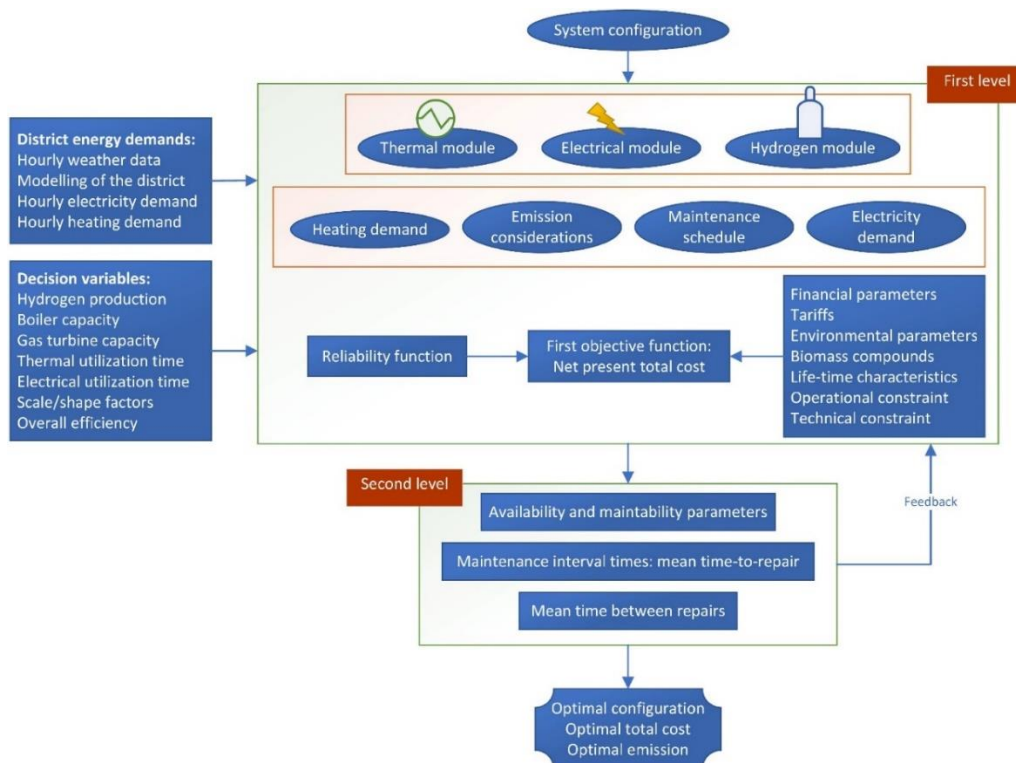


**Figure 13**

*Methodology Flowchart proposed for third model: Reliability-, Maintainability-, and Availability-Based Methodology for trigeneration (heat, power and hydrogen)*

The optimization code delivered the optimal values for the total cost. At the same time, it provided the dimensions necessary for module sizing and reliability indicators such as maintenance intervals. These optimal sizing performance parameters and reliability factors could

then be used to provide optimal configurations for maintainability and availability indicators such as MTTR and availability.

Modeling of the B CHP-hydrogen system was based on the equivalent annualization of capital and operation costs. While capital cost was associated with the installation of thermal, electrical, and hydrogen-generating modules, operation costs dealt with biomass purchase, transportation, maintenance, and pollution costs. All costs were calculated in CAD.

$$Final\ Cost\ (FC) = (Capital\ Cost\ (CC) + Operation\ Cost\ (OC) - income) \quad (41)$$

$$Capital\ Cost\ (CC) = (CC_{thermal\ module} + CC_{electrical\ module} + CC_{hydrogen\ module}) \quad (42)$$

$$CC_{hydrogen\ module} = CC_{Compressor} + CC_{electrolyzer} \quad (43)$$

$$Operation\ Cost\ (OC) = (OC_{biomass} + OC_{transportation} + OC_{pollution} + OC_{maintenance}) \quad (44)$$

Both the capital and operation costs were yielded from the correlations of their rated thermal, electricity, and hydrogen-generating modules' capacities and flow rates, namely  $P_{th}$  and  $P_{el}$  (kW),  $Q$  (kg/h), compressor outlet pressure  $P_{out}$  and inlet pressure  $P_{in}$ , taking into account their times of use,  $\tau_{el}$ ,  $\tau_{th}$  and  $\tau_{hy}$  for electrical, thermal and hydrogen modules respectively. (Boukherroub et al. 2016 ; Croteau et al. 2015 ; Rivarolo et al. 2013 ; Sartor et al. 2014 ; Tol et al. 2015 ; Vallios et al. 2009).

$$CC_{thermal\ module} = CC_{Boiler\ module} = (840P_{th}^{0.6}) \quad (45)$$

$$CC_{electrical\ module} = CC_{gas\ turbine\ module} = (2420P_{elc}^{0.872}) \quad (46)$$

$$CC_{Compressor} = 650,000 \left(\frac{Q}{50}\right)^{0.66} + 600,000 \left(\frac{Q}{30}\right)^{0.66} \left(\frac{P_{out}}{P_{in}}\right)^{0.25} \left(\frac{P_{out}}{1}\right)^{0.25} \quad (47)$$

$$CC_{electrolyzer} = 2498 * Q^{0.925} \quad (48)$$

The costs were annualized using net present worth analysis after considering the interest rate of 3.25% and a system lifetime equal to 30 years (Bank of Canada -2020 annual report).

Operation costs for biomass purchase cost and biomass transportation were those used in equations (34) and (35). Pollution cost was taken into consideration based on equations (23) and (24) for deriving emitted pollution in tons. Pollution cost per ton was equal to 30 CAD/ton (Canadian Biomass Magazine). Operation cost for maintenance was assumed to be 1% of the annual capital cost of power plant systems. It was assumed less than second module because installing such a hybrid system with hydrogen requires availability of the maintainers and as such the average cost for maintenance could be decreased. Because of the lack of data for the hydrogen-generating module, the maintenance cost for such a module was considered wholly to be 5% of its initial capital cost. Considering the maintenance interval for electrical and thermal modules and their associated use times, the following equations were obtained:

$$\begin{aligned} OC_{maintenance} = & OC_{thermal\ module\ maintenance} + \\ & OC_{electrical\ module\ maintenance} + OC_{hydrogen\ module\ maintenance} = \\ & \frac{\tau_{th}}{T_{mth}} * 0.01 * CC_{thermal\ module} + \frac{\tau_{el}}{T_{mel}} * 0.01 * CC_{electrical\ module} + 0.05 * (CC_{electrolyzer} \\ & + CC_{Compressor}) \end{aligned} \quad (49)$$

Income costs were calculated as per electricity selling price to the grid and hydrogen selling prices set to 0.3 CAD/kWh and 4 CAD/kg respectively. (NREL 2010, ETC 2023)

$$\text{Income from electricity selling: } (P_{el} - Q * 33.33 / \eta_{electrolyzer}) * 0.3 \quad (50)$$

$$\text{Income from selling hydrogen: } Q * \tau_{hyd} * 4 \quad (51)$$

Total capital and operational costs in CAD were summed up and divided by the whole energy provided by the system to deliver the final cost in CAD/kWh.

After optimization of the cost based on the optimal performance parameters and reliability and maintainability indicators such as  $MTBF_{el}$  and  $MTBF_{th}$  maintenance interval parameters  $T_{mel}$  and  $T_{mth}$  were derived for thermal and electrical modules. These were the result of the optimization of electrical and thermal modules, respectively.

### **3.4 Summary of the Proposed and Developed Methods**

The general methodology was based on developing the cost objective functions as correlations of fuel chemical elements and module technical parameters, coupled with and constrained by a reliability distribution function via an optimization decision parameter, which was modules' use time. The cost function incorporated the initial or capital cost, fuel purchase cost, and pollution cost subjected to raised income from electricity or hydrogen. Sensitivity analyses were conducted using scenario-based approaches for addressing the impact of fuels and feedstock locations (logistics and transportation issues) on the optimality of the system's design and operation. The methodology was first developed to examine its use and capability to fit the energy generation scenarios and configurations of a hybrid bio-geo system intended for supplying heat to a single building. Then, this methodology was extended progressively for the next systems delivering heat, electricity, and finally hydrogen. The RAM parameters were included as constraints to deliver the optimal values for objective functions and technical parameters.

From a global viewpoint, this methodology could be described as an enviro-economic optimization in which the optimization process is carried out using a nonlinear optimization process for minimizing system cost as an optimization objective function, constrained by a nonlinear reliability function that is supposed to be maximized. Objective and constraint functions were both nonlinear because the correlations were compatible and flexible enough to be solved by various software codes and diverse optimization methods such as gradient-based or GA methods.

The methodology enhances existing approaches by adopting a more comprehensive RAM-Optimization framework rather than relying solely on traditional optimization methods and it reduces computational complexity through modular system configurations and stepwise optimization. It excels in validation of results through use of a mix of optimization algorithms and decision-making techniques (which are suitable for finding global optimum values via heuristic and stochastic methods, and for dynamically generating solution populations). It also includes comparison of optimization algorithm results and explicit consideration of biomass energy production and pollutant emissions based on biomass chemical composition. Validation can be further strengthened through the integration of expert feedback and the application of optimization methods.

The methodology is applied progressively to increasingly complex systems, ranging from simple heat-only configurations to CHP and trigeneration approaches. This progression both verifies and validates the results of earlier models. Using validated results from earlier models ensures that more complex models are developed with reliable input data. The summary of the developed models and methodology is illustrated in Figure 14.

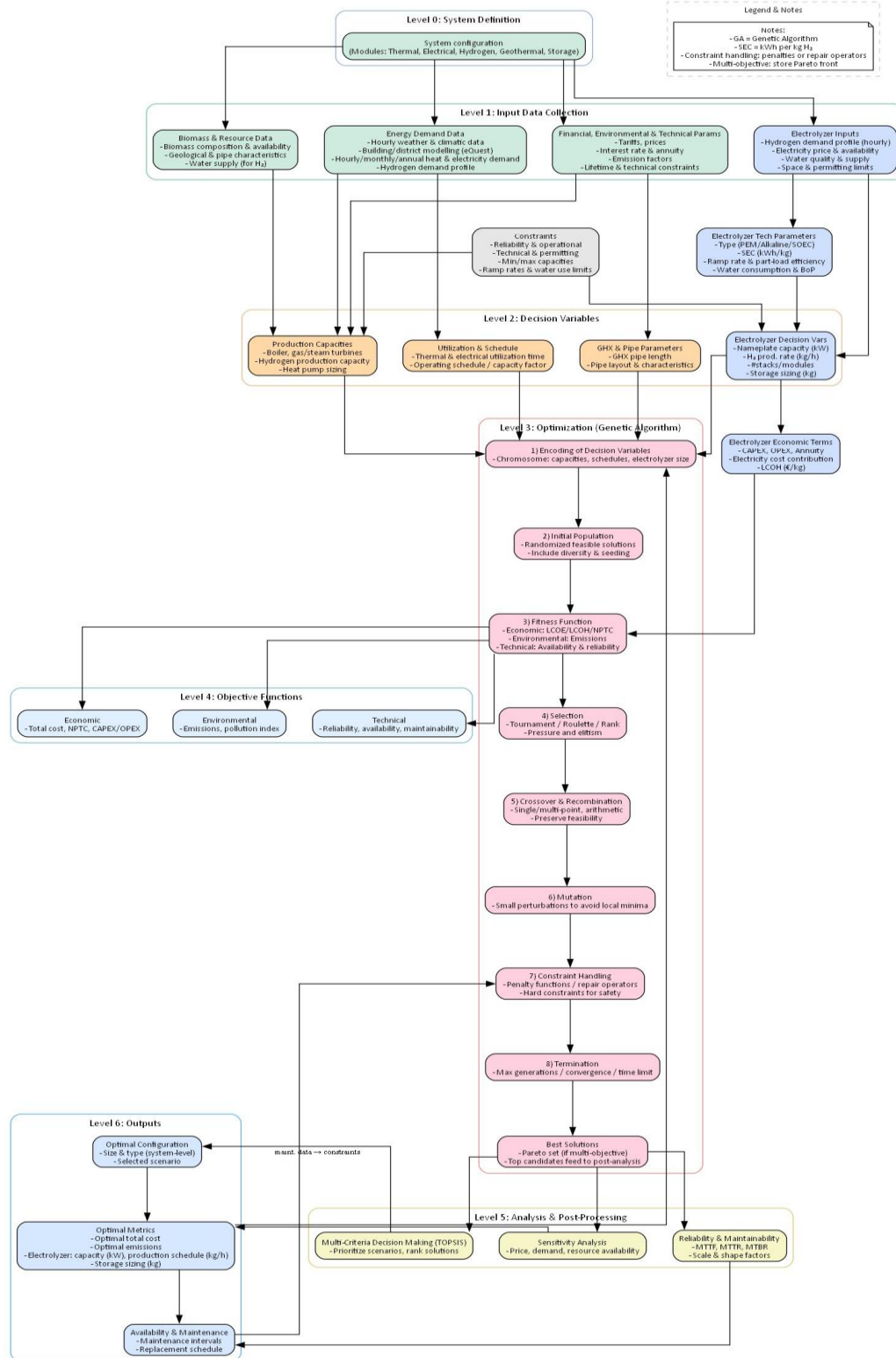


Figure 14

Summary of the proposed and developed methodology

## 4 Chapter 4: Case Studies, Results, and Discussions

This chapter presents the results of three case studies derived from the models developed in Chapter 3, illustrating the progressive application of the joint RAM-Optimization methodology across biomass-powered energy systems. The case studies examine not only the optimality of hybridizing biomass resources and products in an enviro-economical context but also the systematic integration of RAM indicators within the optimization framework.

The three case studies include:

1. A hybrid bio-geothermal (Bio-Geo) energy system for heat-only applications in Northern Canada under harsh climatic conditions.
2. A biomass-based combined heat and power (BCHP) system designed for district-level energy supply in Northern Canada.
3. An integrated hydrogen, heat, and power (BCHP- hydrogen) system, also intended for district-level applications in the same region.

### Case 1: Bio-Geo Hybrid System – Heat-Only Approach for an Office Building

The first case study considers the integration of biomass and geothermal modules for heat production, establishing an initial platform for RAM-Optimization under a single energy-generation approach. Since meeting heating demand is a fundamental requirement across all three case studies, the first step in the optimization process focuses on quantifying building-level energy demand. This involves evaluating hourly, monthly, and annual heating loads for a representative building modeled in eQuest software, located in Kuujuaq, Québec, Canada. These building-level demands are then extrapolated to the district scale, enabling assessment of system performance under district-level operating conditions. This scaling approach allows comparative evaluation of system configurations, ranging from a single building served by a Bio-Geo hybrid

system to multi-building districts supplied by B CHP or trigeneration systems. In this case, two separate objective functions are defined: cost and pollution minimization.

#### Case 2: B CHP System with RAM Analysis for District Heating Supply

The second case study expands the optimization framework to include both heat and electricity generation from biomass for a district of buildings in Northern Canada. Probabilistic RAM functions and associated metrics—such as mean time to failure (MTTF), mean time to repair/restore (MTTR), maintenance intervals, and system availability—are embedded as constraints in the optimization process. Unlike the first case, this and the third case employ a single objective function constrained by time-dependent reliability requirements.

#### Case 3: B CHP with Hydrogen Production and RAM Analysis

The third case study extends the methodology to incorporate hydrogen production, demonstrating the modularity of the framework and its applicability to advanced trigeneration systems for district-level applications in Northern Canada. RAM metrics continue to be embedded in the optimization, supporting evaluation of system performance under harsh environmental and economic conditions.

Throughout the chapter, the case studies are analyzed not only in terms of cost and pollution performance but also in terms of system reliability, maintainability, and operational robustness. By progressively addressing the research objectives, these case studies collectively validate the joint RAM-Optimization methodology and highlight its potential to inform both building-level and district-level energy system design trade-offs.

## 4.1 District Heating Load Calculation

The northern part of the Quebec province of Canada, namely north of the 55th parallel, is called Nunavik. It has a surface area of 443,685 km<sup>2</sup>, and it is made up of 18 communities,

primarily with Inuit inhabitants, as described in Table 11. The 18 communities are being served by a decentralized energy system, primarily based on diesel. Diesel, as the main source of the energy required for building heating, is subsidized by the Hydro Quebec and Makivik Corporation (Hydro Quebec, Atlas of Canada). All the residents of Nunavik, whether in residential, commercial, or institutional buildings, benefit from the subsidies provided according to the agreement between the Quebec and local government. This program has been applied since 1994. Hydro Quebec pays the subsidies. The price of diesel for Nunavik varies depending on the location. Electricity is generated by diesel generators, while building heating is supplied by private boilers or furnaces (Karanasios et al. 2017, Atlas of Canada). The inhabitants are largely settled across a region which is surrounded by Hudson Bay to the west, Hudson Strait to the north, and Ungava Bay to the east. Kuujjuaq, Kangiqsualujjuaq, Puvirnituq, Akuliviq, and Umiujaq are among the regions occupied by the native inhabitants (Figure 15).

Except for the Nunavik nickel mine, which generated electricity at diesel cost prices equal to about 0.77 \$ per liter, for other communities, the diesel price was declared to be 1.4 \$ CAD per liter (CAD/l). According to Belzile (2017), on average, 1.93 CAD/l was declared as the real diesel price in Nunavik. To obtain the cost of diesel consumed for electricity generation, Hydro-Quebec in 2011 showed that the average price for electricity generation was estimated on an average of about 0.43 CAD/kWh. This was succeeded by another estimate that was equal to 0.59 CAD/kWh in 2014 (Atlas of Canada, Nunatsiaq). The price went up to 0.86 CAD/kWh according to other researchers (Karanasios et al. 2017). Northern Quebec is recognized as a low enthalpy area with a low average heat flow density ( $40 \pm 9 \text{ MW/m}^2$ ) that is typical of the Canadian Shield (Figure 16).

**Table 11***Northern Quebec Communities' Demographic Statistics*

Community	Community status	Classification	Category	Population	Power	Provider	MWh/yr
Umiujaq	Single community off-grid	Indigenous	Inuit	442	Diesel	Hydro-Quebec	2989
Akulivik	Single community off-grid	Indigenous	Inuit	633	Diesel	Hydro-Quebec	3801
Aupaluk	Single community off-grid	Indigenous	Inuit	209	Diesel	Hydro-Quebec	1905
Inukjuak	Single community off-grid	Indigenous	Inuit	1757	Diesel	Hydro-Quebec	10269
Ivujivik	Single community off-grid	Indigenous	Inuit	414	Diesel	Hydro-Quebec	2373
Kangiqsualujuaq	Single community off-grid	Indigenous	Inuit	942	Diesel	Hydro-Quebec	4675
Kangiqsujuaq	Single community off-grid	Indigenous	Inuit	750	Diesel	Hydro-Quebec	4815
Tasiujaq	Single community off-grid	Indigenous	Inuit	369	Diesel	Hydro-Quebec	2508
Puvirnituq	Single community off-grid	Indigenous	Inuit	1779	Diesel	Hydro-Quebec	11962
Quaqtaq	Single community off-grid	Indigenous	Inuit	403	Diesel	Hydro-Quebec	2863
Salluit	Single community off-grid	Indigenous	Inuit	1483	Diesel	Hydro-Quebec	8326
Kangirsuk	Single community off-grid	Indigenous	Inuit	567	Diesel	Hydro-Quebec	3601
Kuujuaq	Single community off-grid	Indigenous	Inuit	2754	Diesel	Hydro-Quebec	20333
Kuujuarapik	Multicommunity local microgrid	Indigenous	Inuit	686	Diesel	Hydro-Quebec	12257
Whapmagoostui	Multicommunity local microgrid	Indigenous	First Nation	984	Diesel	Hydro-Quebec	null
Kawawachikamach	Multicommunity local microgrid	Indigenous	First Nation	601	Hydro	Hydro-Quebec	null
Raglan Mine	Single community off-grid	Nonindigenous	null	400	Diesel	Independent	null
Nunavik Mine	Single community off-grid	Nonindigenous	null	500	Diesel	Independent	101000

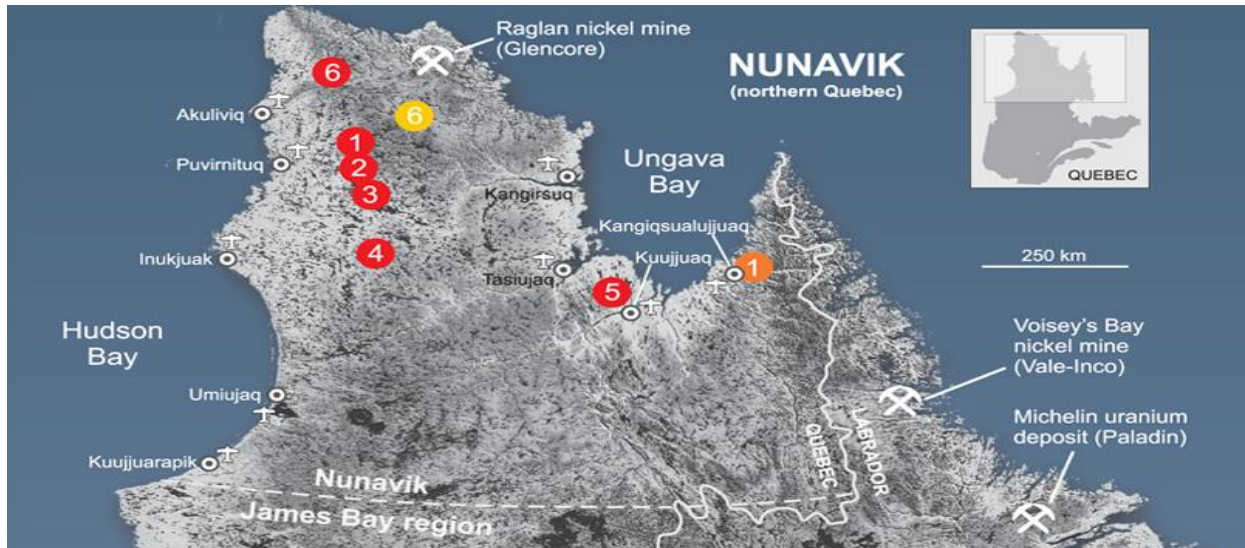


**Figure 15**

*Map and Location of the Nunavik Region in Quebec Province (Nunatsiaq, Atlas of Canada)*



**Figure 16**

*Canadian Shield Map, Natural Resource Canada*

Based on a data analysis of Northern Quebec's geography, climate, weather, infrastructure, power grid, routes, and transportation infrastructure, the bio-geo system was intended to be optimized for use in Kuujjuaq. The main reasons were as follows:

- a) Kuujjuaq is the most important and populated community center of Nunavik. It also has airport facilities.
- b) It has discontinuous and sporadic permafrost, unlike the deep continuous permafrost in other communities.
- c) It has an annual mean weather temperature between  $-6^{\circ}\text{C}$  and  $-7^{\circ}$ , making it suitable for using huge amounts of stored energy in shallow layers.
- d) It benefits from moderate thermal conductivity between 2 and 3 W/m (higher values rather than other areas).
- e) To obtain a better idea of the geological and geotechnical characteristics of the Northern Quebec and Kuujjuaq districts, their climatic and geological characteristics were provided.

#### ***4.1.1 Kuujjuaq Weather***

Kuujjuaq is located at ( $58^{\circ} 06' \text{ N}$ ,  $68^{\circ} 24' \text{ W}$ ) alongside the Koksoak River, southern Ungava Bay (Figure 17).

Kuujjuaq's soil and rock characteristics such as ground surface and underground layer temperatures, thermal conductivity, specific or volumetric heat capacities, and diffusivities necessary for sizing GSHP and the bio-geo system are summarized as follows:

- a) Heat flow density:  $(49 \pm 5 \text{ MW/m}^2)$
- b) Kuujjuaq ground surface mean annual temperatures:  $-2$ — $5^{\circ}\text{C}$
- c) Permafrost depth: 10–30 m
- d) Permafrost category: Discontinuous but scattered



**Figure 17**

*Geographical Location of Kuujuaq* (Source: <http://www.studentsonice.com>)

- e) Underground soil/rock thermal conductivity: 2.6–3 W/k.M
- f) Underground temperature at 50 m depth: -2–0°C
- g) Underground temperature at 250 m depth: 1–3°C
- h) Underground temperature at 3,500 m depth: No exact data but probably 50–75°C
- i) Underground temperature at 6,500 m depth: No exact data but probably 75–80°C
- j) Underground temperature at 10,000 m depth: No exact data but probably 125–150°C
- k) Transportation: Air transport

It is clear that Kuujuaq is a low enthalpy region that is suitable for heat pump technologies.

A building's envelope separates the outdoors and indoors for the comfort of its occupants and must follow clearly stated construction rules. Kuujjuaq is in a region with an average annual heating degree day of more than 7,000. It requires strict construction preparations for building and district modeling compared to Southern Quebec's regions. To comply with the requirement of building and district modeling in Kuujjuaq, the *Nunavik Construction Manual-Société d'Habitation du Québec* was examined. Necessary information for building construction and energy demand profiles was sought in the manual. The information obtained is summarized as follows:

- a) Number of heating degree days: All between 8,200 and 9,200 in Nunavik's villages.
- b) The building should have a raised roof, namely above-grade floors between 0.6 and 1.2 m.
- c) Twenty to thirty percent of heat loss in the northern climate is attributed to the raising of buildings.
- d) Roofs can be flat or of low pitch to provide aerodynamic qualities, thereby letting the wind pass freely under and over the house.
- e) A square layout with a low-pitched roof is the most preferable layout for buildings to reduce insulation, heat loss, air infiltration, and leaks.

Table 12 shows the total thermal resistances of the building components.

**Table 12.**

*Building Energy Modeling Criteria*

Building component	Total thermal resistance
Roof or ceiling separating a heated space from an unheated space or from the exterior air	9.00

Wall above grade except a foundation wall separating a heated space from an unheated space or from the exterior air	5.11
Insulated floor raised above grade level	5.2
Foundation wall separating a heated space from an unheated space, the exterior air, or contiguous soil Foundation wall of which more than 50 percent of the surface is exposed to exterior air. The part of the foundation wall framed in wood must have a total thermal resistance equal to that required for an above-grade wall	2.99
Floor separating a heated space from an unheated space or exterior air	5.20

Minimal resistance of the thermal break will vary from RSI 0.53 to RSI 1.76 depending on the type of framing (wood or steel) and the stud spacing.

Wood framing:

- a) At least RSI 0.7: Where wood framing is spaced less than 600 mm o.c.
- b) Other cases: RSI 0.53

Metal framing:

- a) At least RSI 1.76 where framing is spaced less than 600 mm
- b) At least RSI 1.32 in other cases

Concrete construction:

- a) At least RSI 0.88 in all cases

Standard exterior wall composition:

- a) Reinforced gypsum panels are a recommended finish for all building partitions in Nunavik

Roof insulation

- a) Gypsum panel is recommended as the finish material for ceilings

Resilient flooring:

- a) Resilient flooring such as vinyl, composite, rubber, and linoleum, in tiles or sheets
- b) Reinforced gypsum panels are a recommended finish for all building partitions in Nunavik

Exterior doors:

- a) Polyurethane core
- b) Maximum total thermal transmission coefficient (U) for doors without lights: 0.8
- c) Maximum total thermal transmission coefficient (U)/Minimum energy efficiency ratio of
- d) Windows: 2.0 / 25
- e) Doors with lights: 1.6 / 17
- f) Low emission sealed double glass with inert gases are allowed
- g) Insulated steel door in a wooden frame is preferable

Windows:

- a) Maximum total thermal transmission coefficient (U) for windows: 1.2
- b) Maximum total thermal transmission coefficient (U) for skylights: 2.7
- c) Aluminum is a preferred material
- d) Window-to-wall area: 0.2

Lighting:

- a) Office area: 9.7 w/m<sup>2</sup>

Air permeability:

- a) 0.03 L/s.m<sup>2</sup>

Mechanical ventilation:

- a) Includes a heat recovery ventilator (HRV)
- b) Heat recovery efficiency (HRE) is at least 60%

- c) Each dwelling should have an individual HRV located in the utility room
- d) Fresh air replacement in dwelling unit: 0.3 air change (volume) per hour (ACH)
- e) Minimum flow rates: 5 liter/s

HVAC system:

- a) HVAC system 3
- b) Single zone packaged rooftop unit with baseboard heating
- c) Constant-volume fan control, air-cooled direct expansion
- d) Fuel-fired furnace
- e) Hot water with fuel-fired boiler

#### 4.1.2 Building Modeling

Based on the gathered data for weather, climate, and building construction requirements in Kuujuaq, a building was modeled in eQuest software to calculate energy demand, especially for heating and cooling needs. A three-story office building with a 20 m \* 30 m footprint area at one level above grade was intended to be modeled as shown in Figures 18 and 19.

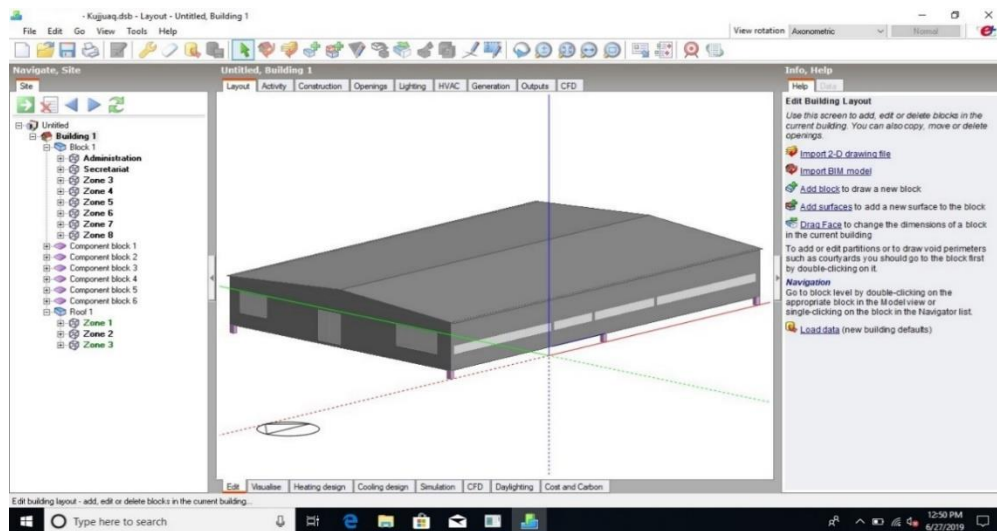


**Figure 18**

*Schematic of the Modeled Office Building*

The following assumptions were made in eQuest during building and district thermal load simulations:

- a) Standard or user-defined insulation levels for walls, windows, roofs, and floors
- b) Assumed thermal mass for materials (e.g., concrete, brick) to model heat storage and release
- c) Assumed window U-values and glazing properties (e.g., coatings, tinting)
- d) Air leakage and infiltration modeled based on a constant rate (e.g., ACH)
- e) Occupancy profiles (number of people and activity levels) affecting heat gain
- f) Typical lighting power densities based on room type and occupancy
- g) Assumed plug load (electrical appliances) based on room function
- h) HVAC load profiles based on system type and operation
- i) Standard efficiencies for HVAC components (chillers, boilers, fans)
- j) Control strategies like thermostat set points, operational schedules, and load limits
- k) Distribution losses from ducts and pipes, typically modeled using standard insulation values
- l) Standard air handling and ventilation rates (e.g., based on ASHRAE 62.1)
- m) Use of typical weather data files (e.g., TMY) for the building location
- n) Solar gains calculated based on building orientation, window types, shading devices, and obstructions
- o) Wind effects modeled based on weather file data, affecting infiltration/ heat loss
- p) Typical operating hours for building activities (e.g., office hours, weekends, etc.)
- q) Constant thermal set points for heating/cooling, with night setbacks or dead bands
- r) Assumed occupant behavior (lighting control, equipment usage, temperature preferences)

- s) Heat recovery systems (e.g., economizers, ERVs) may be modeled with predefined efficiencies
- t) Thermal storage assumptions, including capacity and charge/discharge cycles, when applicable
- u) Equipment operation schedules (start-up, shutdown, fan/pump operation)
- v) HVAC system sizing based on thermal load or industry standards
- w) Compliance with indoor air quality and comfort standards (e.g., ASHRAE 55)
- x) Internal gains from appliances, equipment, and lighting, varying by season/occupancy
- y) Time step for calculations (typically hourly or subhourly)
- z) Simulation period (e.g., 1 year) to capture seasonal variations in thermal loads
- aa) Compliance with local building codes and energy performance regulations (e.g., ASHRAE 90.1)
- bb) Standard utility rates for electricity, gas, and water

These assumptions were used to simplify and standardize the simulation process, though more detailed configurations can be made when needed.

#### **4.1.3 Building Energy Analysis**

Based on input data for Kuujjuaq, energy demands including sensible, total, or annual monthly heating and cooling demands were derived after building modeling as depicted in Figures 20, 21, and 22. From the monthly loads illustrated in Figure 17, it was concluded that January and August were the targeted months for system energy sizing because they had the highest monthly heating and cooling loads. Despite the availability of data on monthly energy demands, hourly demands were used for system sizing. Table 13 shows a sample of the results for hourly load data.

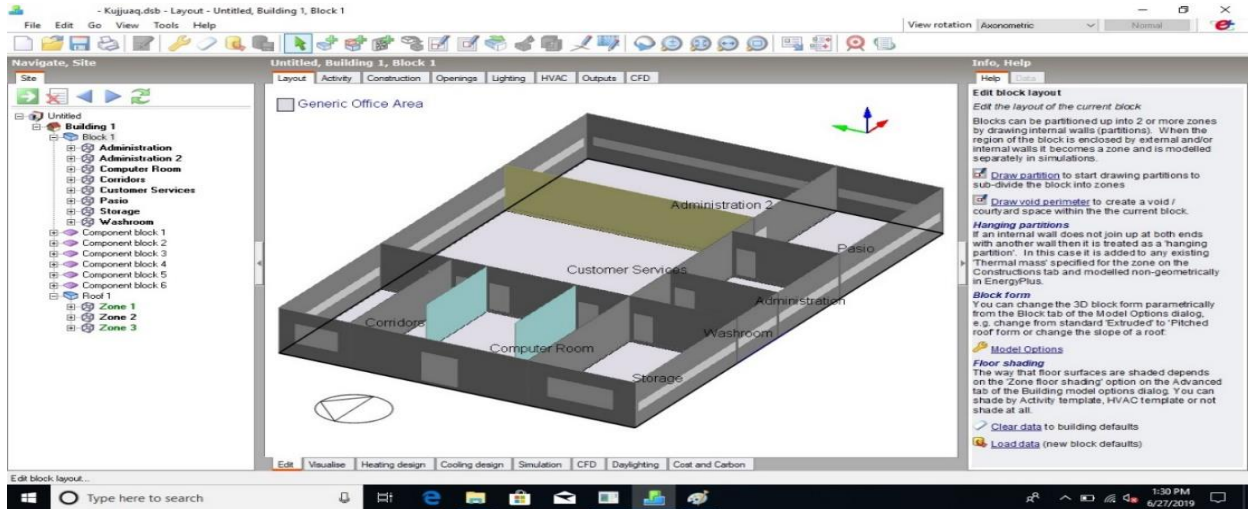


**Figure 19**  
*Modeled Office Building Zoning and Partitioning*

The maximum hourly (heating or cooling) load should be considered for energy system sizing. The maximum hourly load of the building is for heating that occurs at 10 a.m. on February 14 and is equal to 171.16 kW. This heat demand is used as a base for sizing and optimization of the system.

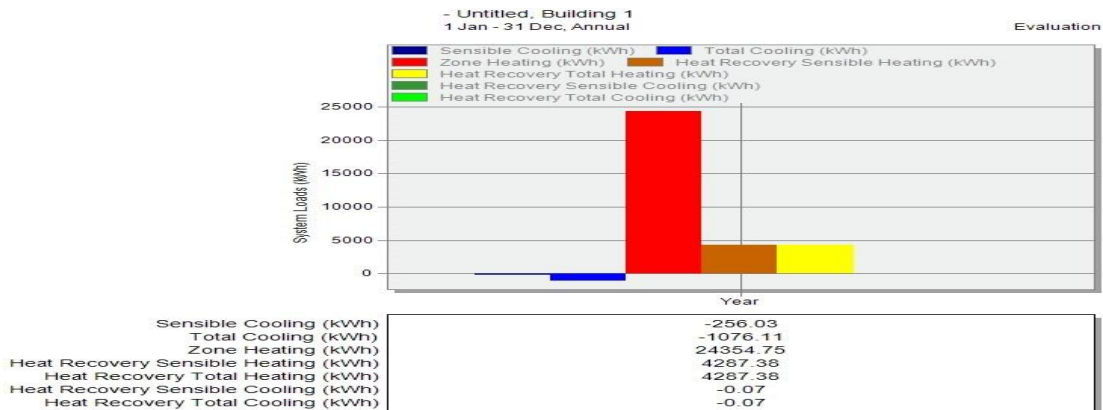


**Figure 20**  
*Annual Zone Heating and Cooling Loads of the Modeled Building*

The values denoted by  $H_{max}$  will be supplied from the bio-geo system modules, namely biomass boiler and geothermal GSHP, as  $P_{bio} + P_{geo} = P_{max}$ .

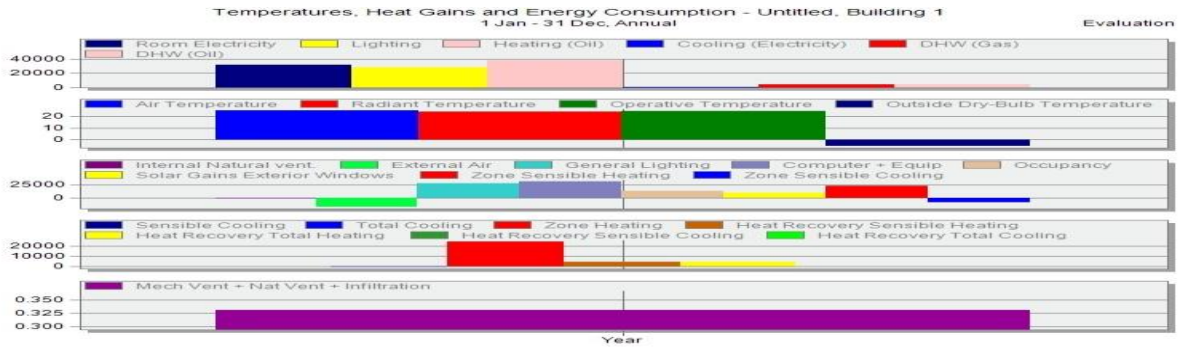


**Figure 21**

*Annual Energy Consumptions Based on Contributing Sources*

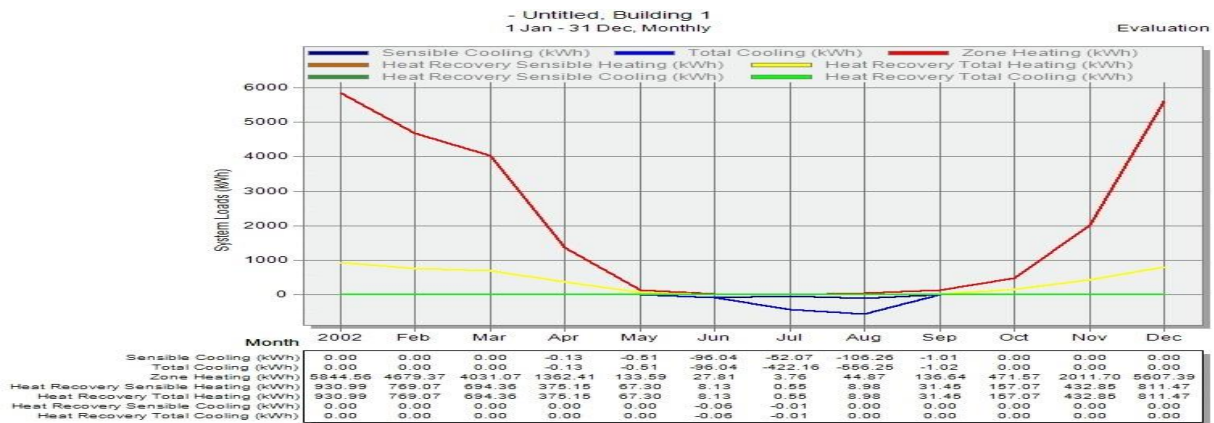


**Figure 22**

*Monthly Zone Heating and Cooling Loads of Modeled Building*

There are two main configurations for GHX design: vertical and horizontal configurations. The total length required for the design of a geothermal system depends on many parameters such as soil characteristics, heat demand, and configurations.

Despite being less expensive because the horizontal configuration is more susceptible to daily and monthly temperature variations, it is more prone to unexpected damage and needs relatively large areas for installation. Therefore, the vertical configuration was considered, and the cost associated with this configuration was derived as mentioned in equation (26).

**Table 13***Sample of Modeled Building Hourly Load Data*

Date/Time	Zone Heating kW	General Lighting kW	Computers equip kW	Occupancy kW	Solar Gains kW	Zone Sensible Heating kW	Zone Sensible Cooling kW
<b>1/14/2022 10:00</b>	163.194981	8.862906	11.775	8.781364	0.6887701	29.97447	0
<b>1/21/2022 10:00</b>	169.165441	8.862906	11.775	8.646608	1.177624	26.25759	0
<b>1/10/2022 10:00</b>	169.69777	8.862906	11.775	7.560055	0.6825536	26.19286	0
<b>1/9/2022 10:00</b>	169.24334	8.862906	11.775	7.459712	0.9798678	25.77122	0
<b>1/7/2022 10:00</b>	158.54815	8.862906	11.775	8.691823	0.9259194	25.76661	0
<b>1/14/2022 9:00</b>	153.927791	8.862906	5.21582	4.816465	0.5781837	23.27344	0
<b>1/14/2022 8:00</b>	152.85382	8.862906	5.21582	4.628792	0	22.85382	0
<b>1/14/2022 11:00</b>	155.632581	8.862906	11.775	8.452162	0.9988254	22.62395	0
<b>1/16/2022 10:00</b>	144.067991	8.862906	11.775	7.634447	0.3495047	21.39355	0
<b>1/10/2022 9:00</b>	141.37566	8.862906	5.21582	3.637557	0.57147	20.65602	0
<b>1/9/2022 9:00</b>	141.02395	8.862906	5.21582	3.541906	0.4928783	20.30283	0
<b>1/8/2022 10:00</b>	143.13202	8.862906	11.775	7.501423	0.9920589	20.23186	0
<b>1/21/2022 9:00</b>	140.63612	8.862906	5.21582	4.713651	0.8459882	19.96985	0
<b>1/7/2022 9:00</b>	140.54087	8.862906	5.21582	4.757381	0.4415127	19.88385	0
<b>1/10/2022 11:00</b>	142.80672	8.862906	11.775	7.261723	0.9494922	19.5061	0
<b>1/2/2022 10:00</b>	142.15754	8.862906	11.775	7.172135	0.7629257	19.41069	0
<b>1/18/2022 10:00</b>	142.22223	8.862906	11.775	7.107672	1.164562	19.33986	0
<b>1/10/2022 8:00</b>	159.25707	8.862906	5.21582	3.566283	0	19.25706	0
<b>1/21/2022 8:00</b>	159.01652	8.862906	5.21582	4.551052	0	19.01652	0
<b>1/7/2022 8:00</b>	158.94815	8.862906	5.21582	4.587653	0	18.94815	0
<b>1/9/2022 8:00</b>	168.89945	8.862906	5.21582	3.476112	0	18.89944	0
<b>1/9/2022 11:00</b>	162.1563	8.862906	11.775	7.158823	1.332161	18.88493	0
<b>1/14/2022 12:00</b>	161.7971	8.862906	11.775	8.177848	1.085243	18.83251	0

## 4.2 Case 1: Bio-Geo Hybrid System for Only Heating Approach

This case focused on the use of GSHPs, known as geothermal energy, in combination with a biomass-powered energy system, intended for generating heat only, to supply the building energy demands of a community in Northern Quebec, Canada. This remote region has extremely cold areas and is totally off-grid with no rail or road transportation. GSHPs have shown appropriate performance in extreme climate regions and are economically and technically feasible, as demonstrated by their implementation in Nordic countries. A case study was conducted on an office building in Kuujuaq, Northern Quebec. Building energy demand modeling was performed to size, and the GEX, GSHP, and biomass modules were configured.

The eQuest software result for building energy modeling was used to specify the hourly, monthly, and yearly loads. Based on the maximum heat demand required for February, the bio-geo system would provide 171.22 kW for heating. Two-step optimization was carried out first. A full set of results of Pareto front for a specific case of MHV-250km is shown in Figure 23, whereas a sample of these results after applying TOPSIS is tabulated in Table 14. The scenarios were represented with biomass type-distance notation that showed the biomass types and the distance from the mills. As Figure 23 shows, the second meta-heuristic technique (hunting search) showed very similar solutions to the results of the GA technique, raising confidence in the accuracy of the other scenarios.

Table 15 demonstrates the final optimal operating and performance parameters for all scenarios and categorizes the optimum scenarios with their performance parameters. Each scenarios' code was run 60 times to find the average of the optimal values for each scenario.

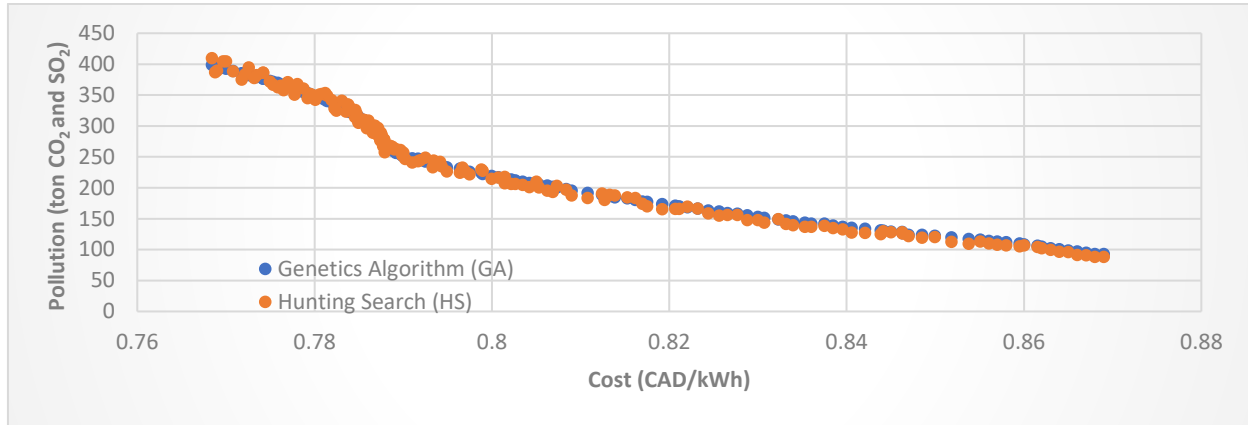


**Figure 23**

*Pareto Front for MHV-250km Scenario*

**Table 14**

*Sample Optimized Solutions Derived for the MHV-250km Scenario*

Cost (CAD/kWh)		Pollution (tons)	$P_{bio}$ (kW)	$P_{geo}$ (kW)
<i>bio</i>	<i>geo</i>			
0.405	0.299	238.146	95.4	76.8
0.402	0.303	236.669	95	77.2
0.400	0.305	236.246	94.8	77.4
0.397	0.308	235.116	94.5	77.7
0.394	0.311	234.109	94.2	78
0.382	0.323	231.895	93.3	78.9
0.473	0.331	229.598	93.5	78.7
0.357	0.349	228.125	92.3	79.9
0.314	0.391	224.895	90.9	81.3

**Table 15**

*Final Optimal Operating and Performance Parameters for All Scenarios- Average Yearly Basis*

	Distance (km)	Cost (CAD/kWh)			$P_{bio}$ $P_{geo}$ (kw)		Bio load (kWh)	Geo load (kWh)	Total load (kWh)
		<i>bio</i>	<i>geo</i>	<i>total</i>					
HHV	50	0.04	0.28	0.32	78	94	619650	418600	1038250
	150	0.19	0.31	0.5	81	91	621800	455470	1077270
	250	0.32	0.29	0.61	89	83	661700	448214	1109914
	350	0.48	0.32	0.8	83	89	661900	499630	1161530
MHV	50	0.03	0.32	0.35	95	77	745960	315058	1061018
	150	0.25	0.34	0.59	85	86	664000	439660	1103660
	250	0.41	0.3	0.71	95	77	681700	438741	1120441
	350	0.59	0.4	0.99	98	74	713780	471255	1185035
LHV	50	0.02	0.3	0.32	90	82	681700	338582	1020282
	150	0.16	0.32	0.48	82	89	657640	402725	1060365
	250	0.32	0.28	0.6	85	87	625560	473572	1099132
	350	0.39	0.4	0.79	85	87	691900	438984	1130884

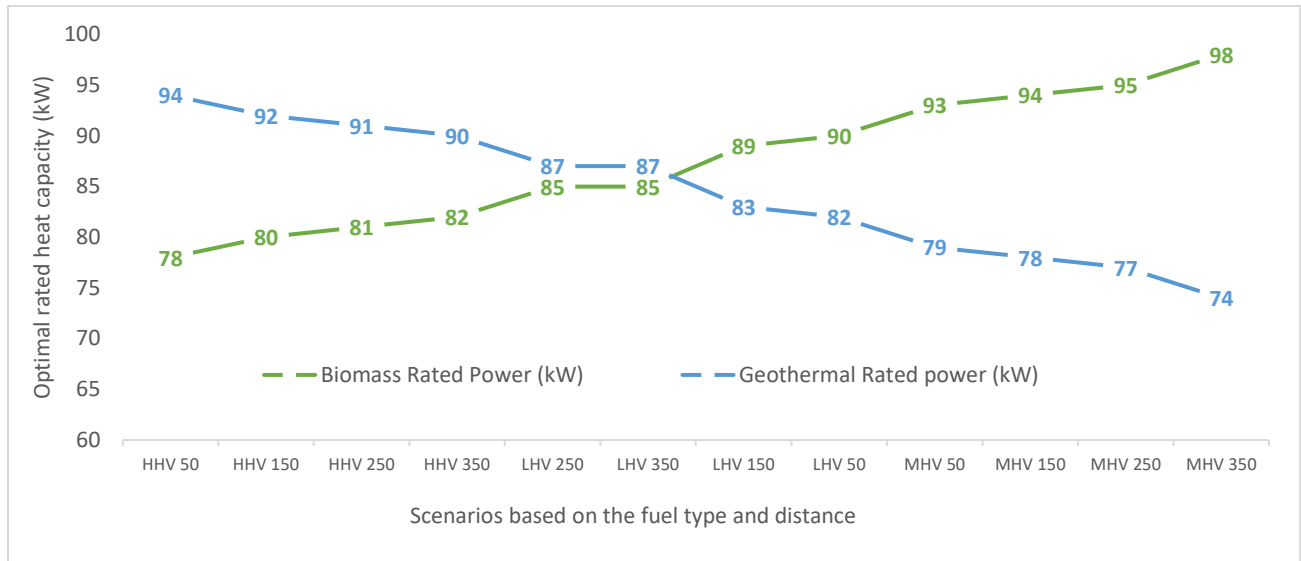


**Figure 24**

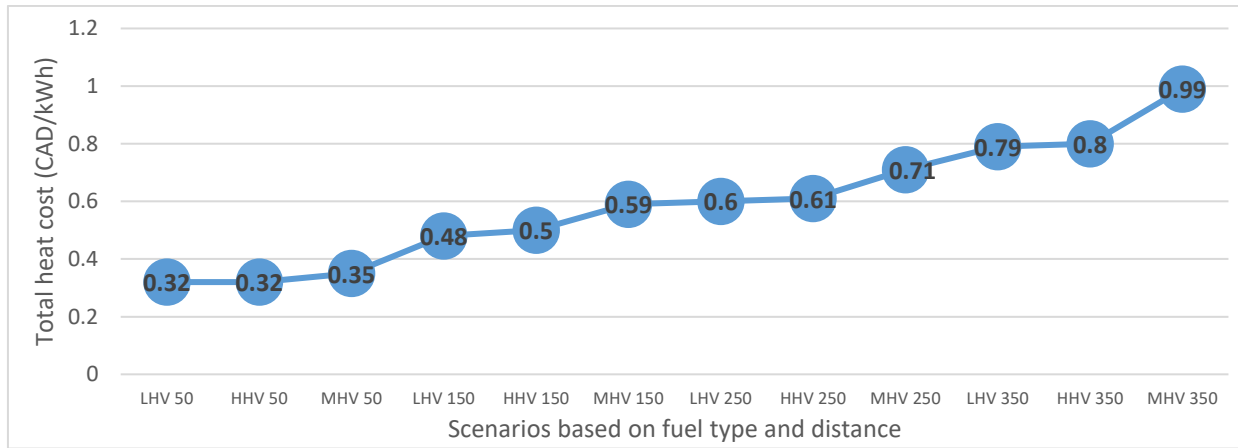
*Optimized Sizing of Each Subsystem for All Scenarios- Average Yearly Basis*

Figure 24 details the optimum sizing of biomass and geothermal subsystems. The HHV-50 scenario had the lowest contribution for the biomass and the highest shares for the geothermal module, equal to 78 and 94 kW rated capacities, respectively.

Conversely, the MHV-350 scenario had the lowest share for the geothermal subsystem and the highest share for the biomass subsystem.

Additionally, scenarios with HHV woods were geothermal dominated, whereas MHV scenarios were biomass dominated. The share of the biomass subsystem increased with distance for HHV and MHV woods, whereas the share of the biomass subsystem decreased for LHV wood when the distance increased. On average, increasing the distance up to 350 km caused a 5% change in the optimal capacities for each system.

Unlike the rated capacities of modules, in all scenarios, the total loads supplied from the biomass subsystem outweighed the total loads from the geothermal modules. This was attributed to the heat pump cost correlation, which resulted in a much lower use time of the geothermal subsystems. Figure 25 illustrates the total heat cost for all scenarios.



**Figure 25**

*Total Cost for the Heat Generation in All Scenarios- Average Yearly Basis*

The cost sensitivity to transportation distance was more than the biomass purchase types. Briefly, the variation of cost to the biomass for the same distance was much less than the variation of cost to distance for the same fuel. The highest costs were for the MHV, HHV, and LHV scenarios, respectively. Although the purchase price of HHV was higher than that of MHV, the HHV within the same distance had a lower total cost than MHV.

Figure 26 shows the variation of the total cost and total heat generation for all scenarios. The total cost was affected by heat generation. Additional heat generation, when constrained by minimum pollution, increases the geothermal share of heat generation, which in turn increases the final cost because of larger capital costs. The total cost and total load in all scenarios could be linearly correlated with each other. To derive a correlation between the heat cost and its generation, the biomass purchase prices for LHV, MHV, and HHV were considered within variations from the initial values with incremental steps. The sensitivity of the results to the purchase price uncertainty was examined, and the results were screened. The correlation between total cost and total load can be formulated as follows:

$$C_{tot} = 0.0042Q_{tot} - 4.0595 \quad (52)$$

$$Q_{tot} = 225.73C_{tot} + 964.54$$

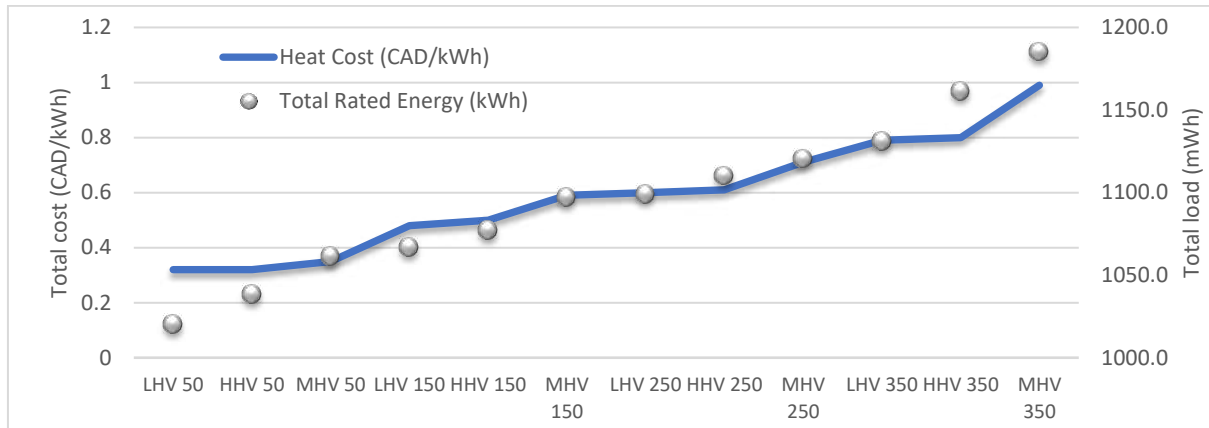


**Figure 26**

*Total Cost and Total Load for 12 Scenarios- Yearly Basis*

The 12 preferred optimal scenarios illustrated in Table 15 were subject to TOPSIS. The scenarios were ranked based on the three predefined favorable criteria, namely heat cost, use times, and boiler efficiencies. Table 16 summarizes the results.

Considering pollution as cost resulted in prioritizing more distant scenarios, such as LHV-350 at higher costs, than less distant scenarios, such as MHV-250.

**Table 16**

*Ranking of 12 Optimal Scenarios With Their GHX and Pollution*

No	Wood pellet type- Distance from mill	Total pipe length	Total Pollution (tons) in 30 years)
1	LHV-50	2749	15728
2	HHV-50	2692	16547
3	MHV-50	2861	23711
4	LHV-150	2805	14315
5	HHV-150	2815	18469
6	LHV-250	2688	14576
7	HHV-250	2667	18960
8	MHV-150	2695	21327
9	LHV-350	2600	15033
10	MHV-250	2584	23814
11	HHV-350	2340	17666
12	MHV-350	2324	24494

### 4.3 Case 2: CHP From Biomass

For integrated optimization and reliability approaches to generating both heat and electricity, scenarios were characterized based on biomass types and employed technologies to generate energy. Six defined scenarios including the combination of HHV woods (HHVW), MHV woods (MHVW), and LHV woods (LHVW) with two technologies, namely ST and GT, are presented as: HHVW-GT, HHVW-ST, MHVW-GT, MHVW-ST, LHVW-GT, LHVW-ST

Based on the reliability and failure distribution function formulations addressed in equations (10), (11), and (14), and after applying the derived values from optimization for maintenance intervals, the reliability function behavior of electrical and thermal modules in each scenario was obtained.

To better understand the comparison of the reliability and failure functions of the two different generators (STs and GTs), results are presented for both modules of HHVW-GT and HHVW-ST scenarios in Figure 27.

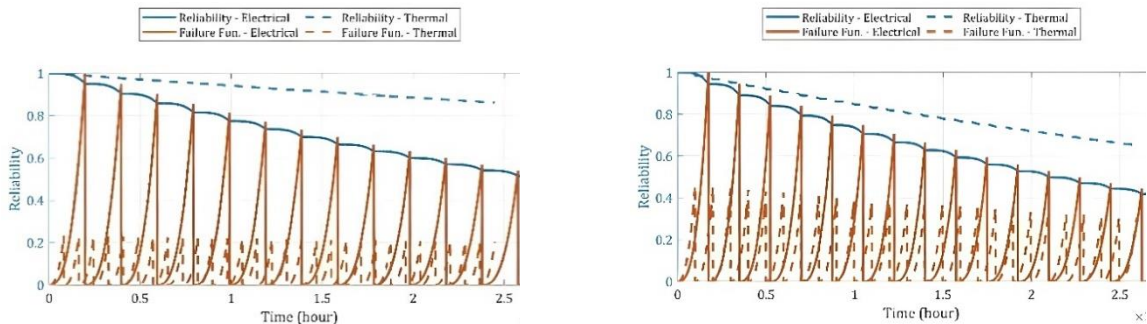


**Figure 27**

*Reliability and Failure Functions Over Time for HHVW-GT (Left) and HHVW-ST (Right) Scenarios*

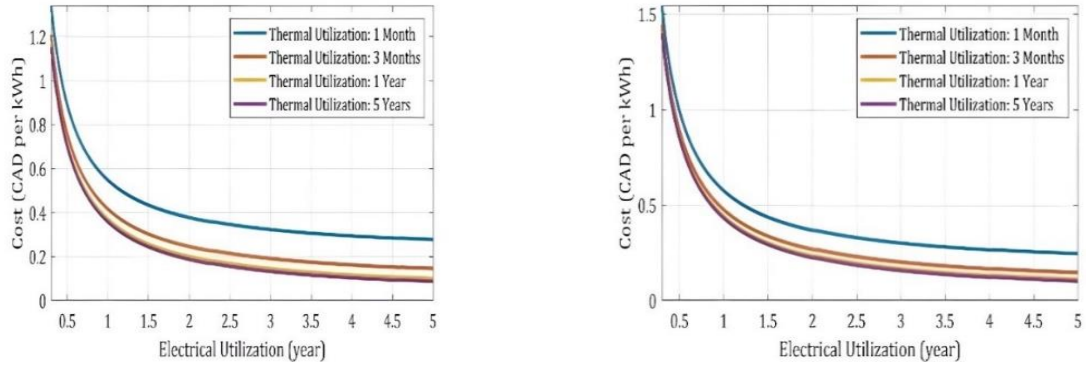
The increasing leaps in reliability for both modules coincided with the carried-out maintenance on the modules, which resulted in decreasing jumps in failures for both units. This demonstrated and addressed the impact of performing maintenance at regular intervals.

As illustrated in Figure 27, maintenance improved reliability values by decreasing failure rates. Nevertheless, despite dropping failure rates and rising reliability values at maintenance times, the overall reliability and failure values at every time step between maintenance were less than in previous intervals. In both scenarios, the reliability levels of thermal modules were higher than those of electrical units, whereas the failure rates of thermal units were lower than those of electrical units. This meant that optimization of the energy costs required that the failure rates of thermal modules be lower than those of electrical ones to yield higher reliability levels.

In both scenarios, the failure function of thermal modules increased more rapidly than the failure function of electrical modules, which resulted in shorter maintenance intervals, higher failure rates, and lower reliability levels in the absence of maintenance. For all scenarios, the final cost was mitigated by increasing both the electrical and thermal use times. Nevertheless, the sensitivity of the cost to electrical use times was much greater than that of the thermal module.

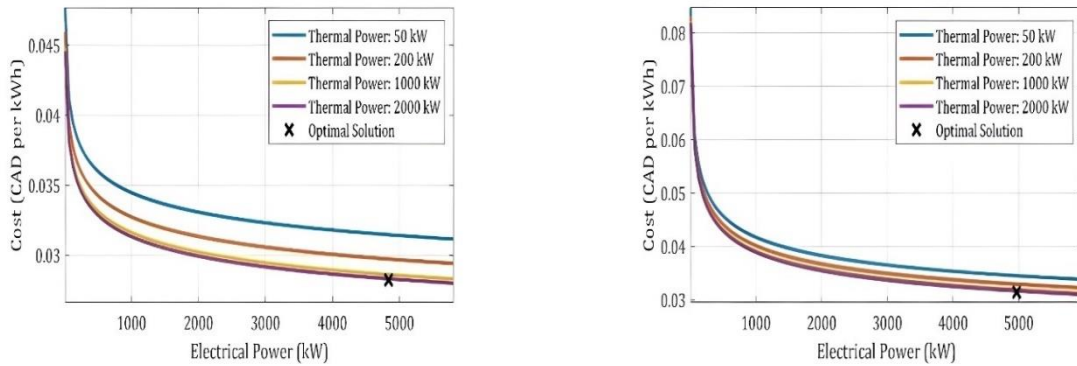
Cost variations per electrical use time for both scenarios are illustrated in Figure 28 for four thermal use times of 1 month, 3 months, 1 year, and 5 years. The cost variations for 1- and 5-year thermal use times were very close. This trend became dominant so that for thermal use times greater than 1 year, the cost profiles almost overlapped. This meant that for thermal use times greater than 1 year, just use times of electrical modules govern the optimal values for cost.

Figure 29 depicts the impacts of the thermal and electrical rated capacities on the final cost. Similar to use time, the higher the rated capacity for both thermal and electrical modules, the lower the final cost. The sensitivity of cost to electrical rated capacity was greater than that to thermal capacity. For thermal rated power greater than 2 MW, the cost variation depended on the electrical rated capacities for both scenarios. The higher values for electrical rated capacities of HHVW-ST refer to the lower exponential power of electricity capacity in the cost correlation function compared to that of GTs.



**Figure 28**

*Cost per Electrical and Thermal Use (Utilization) Time for HHVW-GT (Left) and HHVW-ST (Right) Scenarios*



**Figure 29**

*Cost per Electrical and Thermal Rated Capacity for HHVW-GT (Left) and HHVW-ST (Right) Scenarios*

Although not considerably higher, the cost values of the HHVW-ST scenario were generally higher than the cost values of the HHVW-GT. This could be explained by a much higher capital cost correlation for the electrical module in the HHVW-ST. Figure 30 illustrates the sensitivity of cost to the reliability of thermal and electrical units for these two scenarios. As before, cost sensitivity to electrical module reliability was greater than thermal reliability. It was

interesting to know that, for some time intervals, decreasing reliability did not significantly impact cost reduction. For example, lowering the reliability level from 88% to 80% in the HHHV-GT scenario caused the cost to decline by 0.1%. MTTF decreased with increasing maintenance intervals. As Figure 31 shows, MTTF for both thermal and electrical modules decreased with increasing maintenance intervals. For both scenarios, MTTF of the electrical module was greater than that of the electrical module. Moreover, scenarios were distinct in a way that MTTF for HHVW-ST was almost 10 times larger than that for HHVW-GT. Furthermore, MTTF in the HHVW-GT scenario decreased more sharply in regard to time than MTTF in the HHVW-GT scenario.

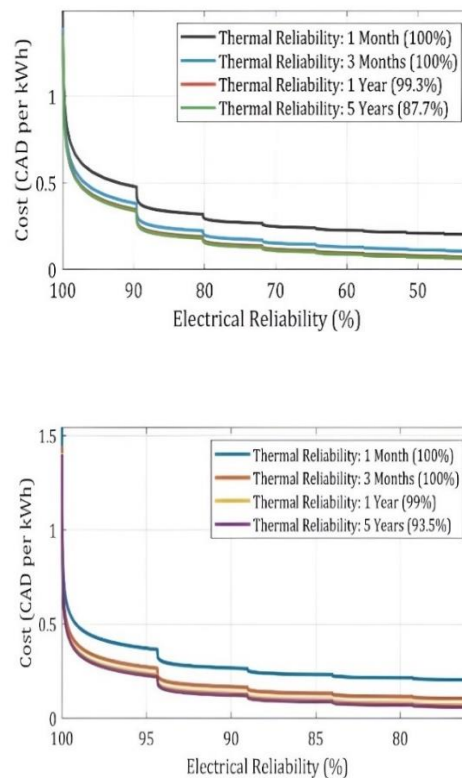


**Figure 30**

*Cost per Electrical and Thermal Reliability for the HHVW-GT (Top) and HHVW-ST (Bottom)*

*Scenarios*

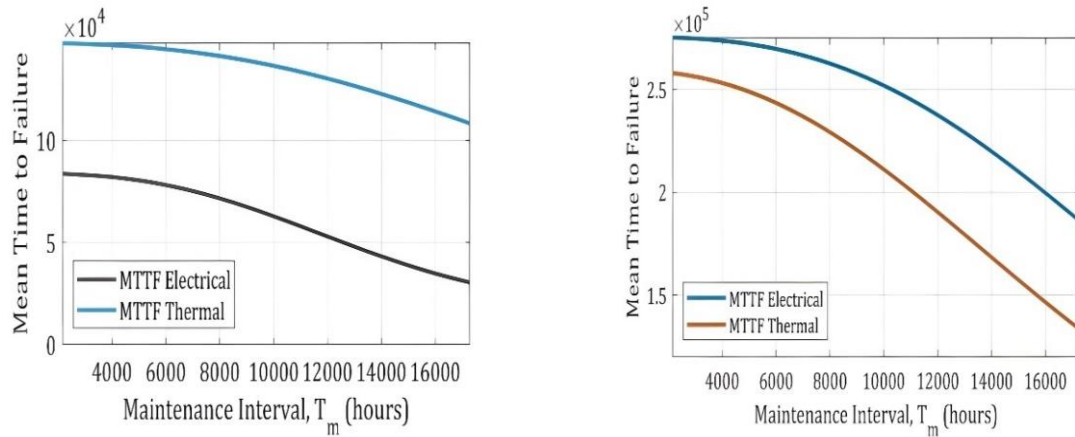


**Figure 31**

*Mean Time to Failure of Electrical and Thermal Modules According to Maintenance Intervals for the HHVW-GT (Left) and HHVW-ST (Right) Scenarios*

To understand the impact of technology on the most preferred optimal values for cost, reliability, and maintainability parameters and to determine the impact of biomass and sensitivity of cost, performance, reliability, and maintainability parameters to biomass variations, four other scenarios for two other biomasses, namely MHVW and LHVW, were analyzed. Figures 32–35 show the results for the three scenarios of HHVW-ST, MHVW-ST, and LHVW-ST.

The cost per electrical and thermal use times for all scenarios followed the same trend, and the cost variations were less than 4%. The cost for the LHVW-ST scenario was higher than that for other scenarios, up to a maximum of 10%. As in the HHVW scenario, by increasing the use times for all scenarios, the cost profile differences became negligible. As Figure 33 shows, the same trend was witnessed for cost variation per rated capacity. Thus, it can be argued that the cost variation per rated capacity for both electrical and thermal modules became negligible for rated capacities greater than 5 MW.

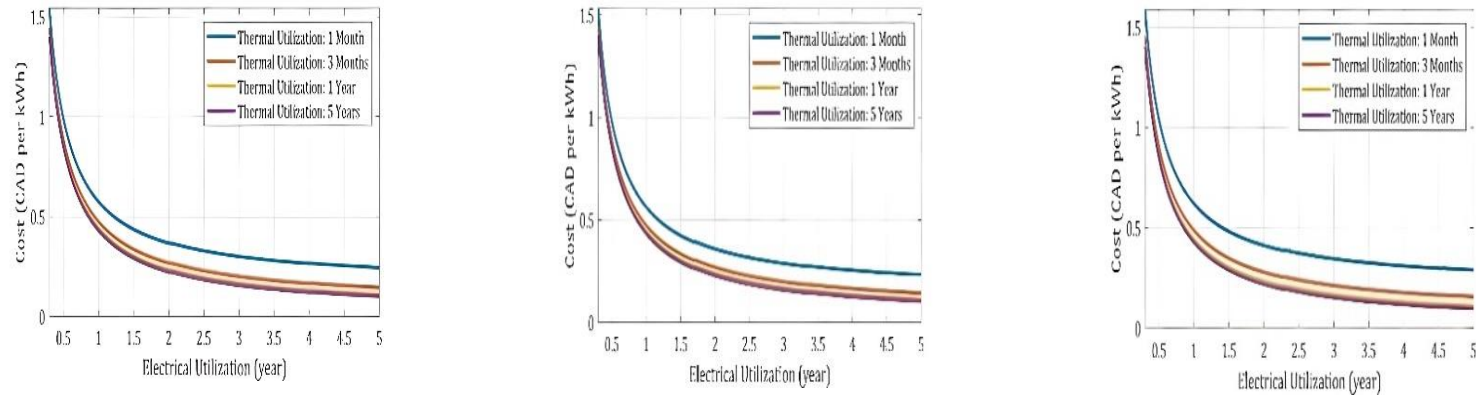


**Figure 32**

*Cost per Electrical and Thermal Use Time for HHVW-ST (Left), MHVW-ST (Middle), and LHVW-ST (Right) Scenarios*

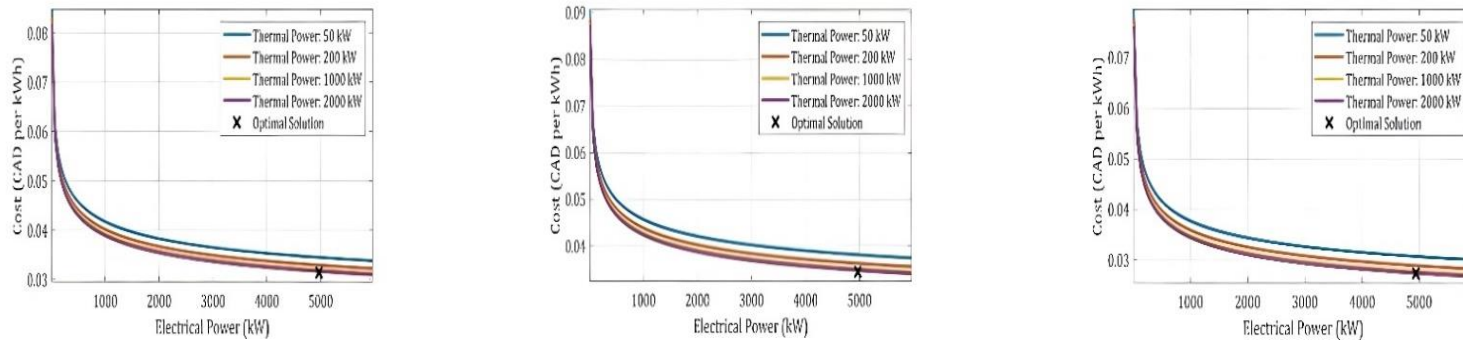


**Figure 33**

*Cost per Electrical and Thermal Rated Capacities for HHVW-ST (Left), MHVW-ST (Middle), and LHVW-ST (Right) Scenarios*

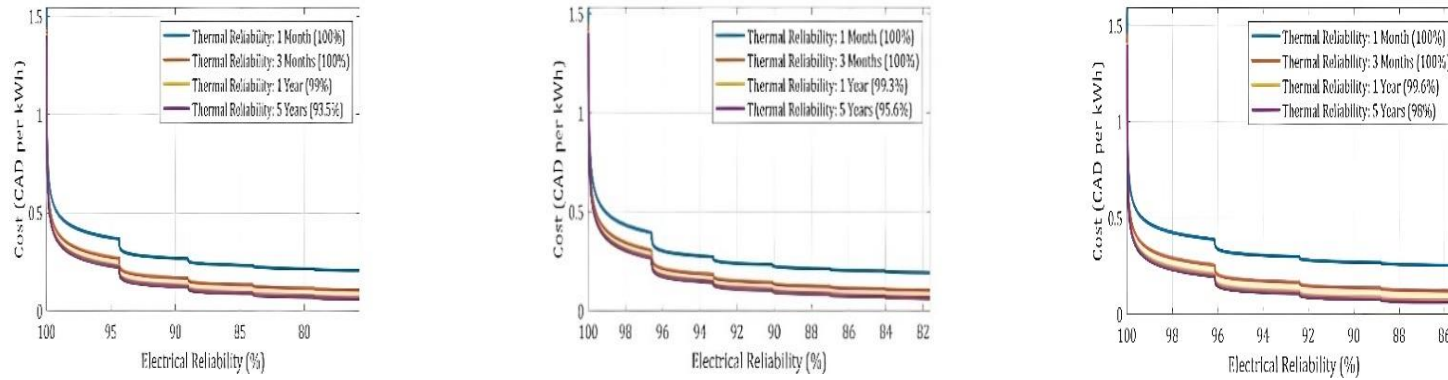


**Figure 34**

*Cost per Electrical and Thermal Reliability for HHVW-ST (Left), MHVW-ST (Middle), and LHVW-ST (Right) Scenarios*

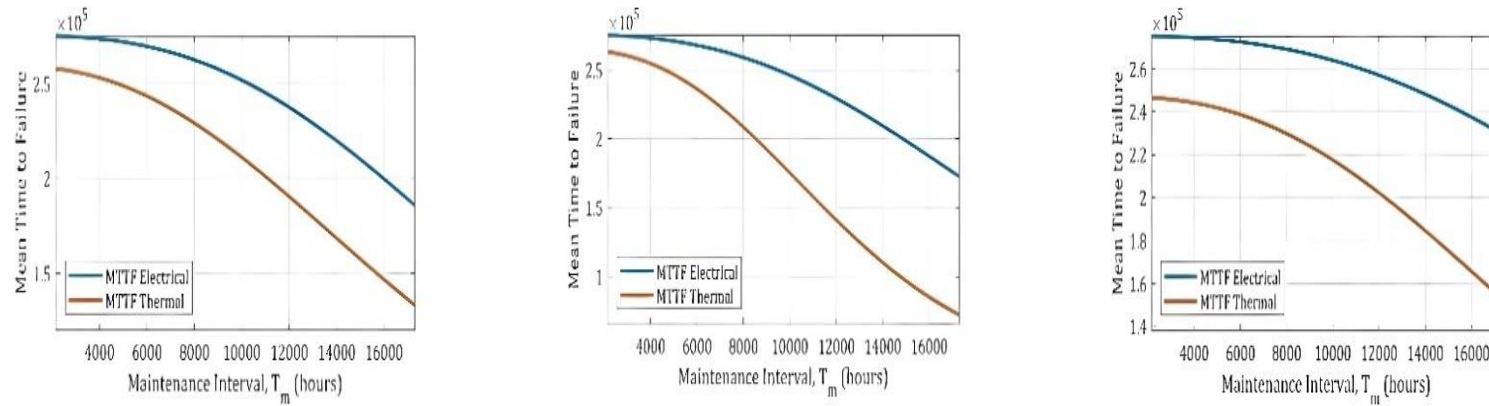


**Figure 35**

*Mean Time to Failure of Electrical and Thermal Units According to Maintenance Intervals for HHVW-ST (Left), MHVW-ST (Middle), and LHVW-ST (Right)*

Figure 34 again highlights that biomass type change had a negligible impact on the cost profile versus thermal and electrical module reliability, particularly after 5 years of use time. As depicted in Figure 35, for all scenarios, MTTF of the electrical module was higher than MTTF of the thermal module. However, unlike cost profiles, variation of MTTF versus maintenance interval was considerable, and these variations were identifiable for three scenarios. Among them, LHVW-ST had higher electrical module MTTF values compared to the other scenarios.

Tables 17 and 18 show the optimal values for each scenario performance parameter to have the minimum achievable cost.

**Table 17**

*Optimal Performance Values for Thermal and Electrical Modules*

Scenario	Cost (\$/kWh)	$P_{th}$ (kW)	$P_{el}$ (kW)	$\tau_{el}$ (h)	$\tau_{th}$ (h)
HHV-ST	0,031	4884,6	4970,9	2,74E+05	2,60E+05
HHV-GT	0,028	6448,8	4976,6	2,75E+05	2,72E+05
MHV-ST	0,033	6936,6	4997,8	2,76E+05	2,75E+05
MHV-GT	0,030	6925,4	4976,9	2,76E+05	2,71E+05
LHV-ST	0,027	4144,1	4947,6	2,75E+05	2,62E+05
LHV-GT	0,024	5423,4	4842,3	2,77E+05	2,40E+05

As tabulated in Table 17, for all scenarios, the optimal value for electrical rated capacities and usage times were 5 MW (+/- 3%) and 2,76E+05 hours. For thermal performance parameters such as rated capacities and use times, the optimal values ranges were wider and spanned from 4,1 MW up to 6,9 MW for rated capacities and from 2,40E+05 to 2,75E+05 hours.

In Table 18, the most preferred optimal values of thermal and electrical modules' reliability parameters for scenarios are listed. In all scenarios, maintenance intervals for the thermal module were less than those for the electrical module, which meant a higher maintenance frequency and MTTF for the thermal module. The variation of values for reliability parameters, namely the scale and shape factors,  $\alpha$  and  $\beta$ , are given in Table 18. The reliability parameters including shape and scale parameters for both units were almost the same at the same scale,  $3 \text{ E} + 04 < \alpha < 4.5 \text{ E} + 04$  and  $3 < \beta < 4$ .

**Table 18***Optimal Values of Reliability Parameters for Thermal and Electrical Modules*

Scenario	$\alpha_{el}$	$\alpha_{th}$	$\beta_{el}$	$\beta_{th}$	$T_{mel}$ (h)	$T_{mth}$ (h)	$MTTF_{el}$ (h)	$MTTF_{th}$ (h)	$N_{el}$	$N_{th}$
HHV-ST	36675	33587	3,84	3,37	17492	9981	1,84E+05	2,11E+05	11	21
HHV-GT	47147	40726	3,76	3,54	18389	12425	2,26E+05	2,33E+05	12	19
MHV-ST	44355	37023	3,71	3,66	18398	12514	2,12E+05	2,26E+05	12	18
MHV-GT	48491	36875	3,37	3,85	19703	12467	2,03E+05	2,32E+05	10	19
LHV-ST	39183	29981	3,87	3,69	18356	9019,6	1,93E+05	2,22E+05	10	25
LHV-GT	44373	44516	3,62	3,43	18460	7322,4	2,07E+05	2,32E+05	11	32

By having optimal values for MTTF of both thermal and electrical modules, it was possible to provide the optimal values for the MTTR of modules and keep the CHP system at predefined availability levels. Tables 19 and 20 list the optimal MTTR for scenarios at availability levels equal to 99%, 99.9%, 99.99%, and 99.999%.

**Table 19***MTTR of Electrical Modules for Alternative Availability Levels of the CHP System*

Scenario	$MTTF_{el}$ (h)	Availability			
		99%	99.9%,	99.99%	99.999%
		$MTTR_{el}$ (h)			
HHV-ST	1,84E+05	1855,35354	183,863864	18,369837	1,83681837
HHV-GT	2,26E+05	2279,59596	225,905906	22,570257	2,25682257
MHV-ST	2,12E+05	2144,44444	212,512513	21,2321232	2,12302123
MHV-GT	2,03E+05	2053,93939	203,543544	20,3360336	2,03342033
LHV-ST	1,93E+05	1946,56566	192,902903	19,2729273	1,92711927
LHV-GT	2,07E+05	2090,90909	207,207207	20,7020702	2,0700207

**Table 20***MTTR of Thermal Modules for Alternative Availability Levels of the CHP System*

Scenario	$MTTF_{th}$ (h)	Availability			
		99%	99.9%,	99.99%	99.999%
		$MTTR_{th}$ (h)			
HHV-ST	2,11E+05	2135,15152	211,591592	21,140114	2,11382114
HHV-GT	2,33E+05	2350,40404	232,922923	23,2713271	2,32692327
MHV-ST	2,26E+05	2286,46465	226,586587	22,6382638	2,26362264
MHV-GT	2,32E+05	2339,89899	231,881882	23,1673167	2,31652317
LHV-ST	2,22E+05	2244,74747	222,452452	22,2252225	2,22232222
LHV-GT	2,32E+05	2341,31313	232,022022	23,1813181	2,31792318

Tables 19 and 20 show the times assigned to maintenance activities to maintain the availability levels of the system based on the optimal values for MTTF and maintenance interval times.

In addition to the same trends that were discussed for the first scenario and that were witnessed in the other five scenarios, from the obtained results, it could be concluded that scenario change had no remarkable impact on the electrical module features and performance parameters such as use times and rated capacities. In contrast, for the thermal module, optimal values for rated capacities and use times were influenced by scenario changes.

#### 4.4 Case 3: Heat, Power, and Hydrogen Triple Generation

As indicated in the methodology section of Chapter 3, the third case was intended for economic optimization of biomass-gasification-driven combined heating, hydrogen, and electricity systems considering reliability and maintenance parameters.

The most preferred optimal values for the total cost, hydrogen and electrical module incomes, their rated capacities, use times, reliability and maintainability indicators such as MTTF, and maintenance intervals for different modules were derived, discussed, and compared in this case. Figures 36 and 37 illustrate the thermal and hydrogen module costs based on electricity (el) module-rated capacities and use. As can be seen by increasing the rated capacities of electricity modules, the cost of thermal modules increased and the income from hydrogen modules decreased.

Assigning more capacity to electricity generation normally results in allocating less capacity for hydrogen modules to profit more from selling electricity to the grid. However, the sensitivity of hydrogen modules to electrical module rated capacity was not as considerable as electricity module use time. In other words, the sensitivity of hydrogen module cost to electricity-rated capacity was greater than its use time. Figures 38 and 39 depict the behavior of the thermal (ther) module. The thermal module net cost decreased by increasing the thermal module rated capacities; however, increasing rated capacities caused the total cost of the system to rise by decreasing the share of electricity and hydrogen modules and subsequently their associated incomes. Net cost per kWh was calculated as the total final cost divided by the whole system load delivered by thermal and electrical modules. Unlike with the electricity module, it could be concluded that the sensitivity of the system's total cost to thermal rated capacity was more than its use times.

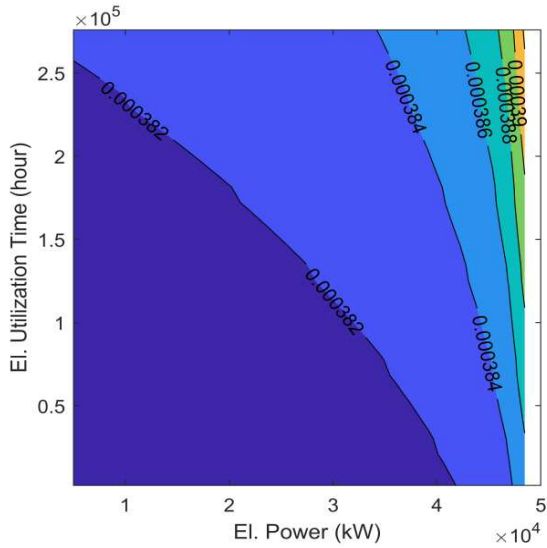


**Figure 36**

*Thermal Module Cost (Curves on the Graph) versus Electrical Module Rated Capacity (Horizontal Axis) and Electrical Module Usage (Utilization) Time (Vertical Axis)*

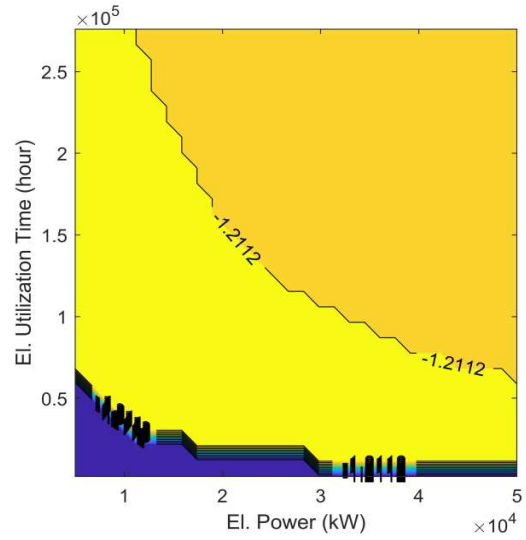


**Figure 37**

*Hydrogen Module Cost (Curves on the Graph) Versus Electrical Module Rated Capacity (Horizontal Axis) and Electrical Module Usage (Utilization) Time (Vertical Axis)*

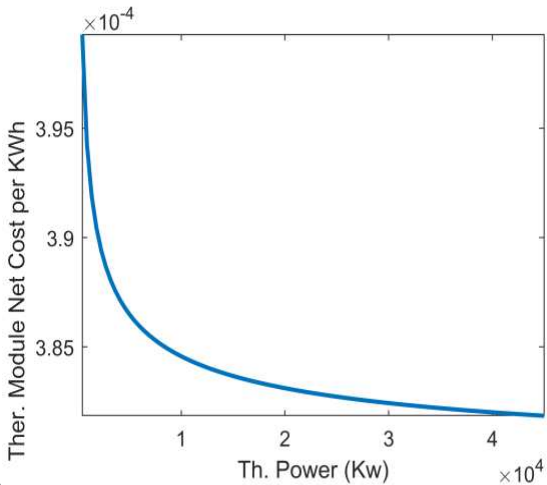


**Figure 38**

*Thermal Module Net Cost (Vertical Axis) versus the Thermal Module Rated Capacity (Horizontal Axis)*

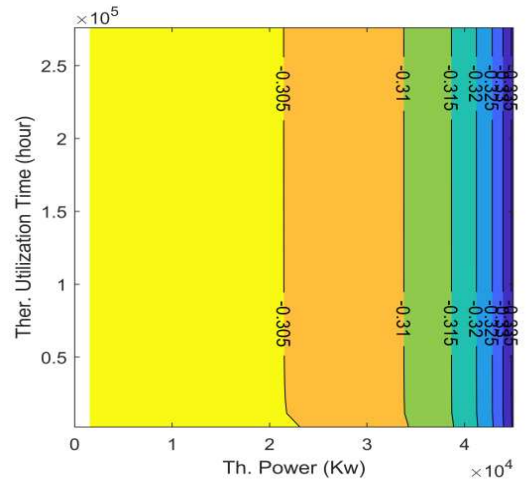


**Figure 39**

*Total Cost of the System Versus Thermal Module Rated Capacities and Usage (Utilization) Time*

As seen in figure 40, biomass fuel costs increased linearly by increasing the thermal module-rated capacities. The variation of biomass cost versus thermal module rated capacity and use time is illustrated in Figure 41. It was concluded that biomass supply cost is influenced by thermal modules' rated capacity and use time and raising both causes the total cost to rise. The same trend is seen in Figures 42 and 43 for this cost versus electrical module.

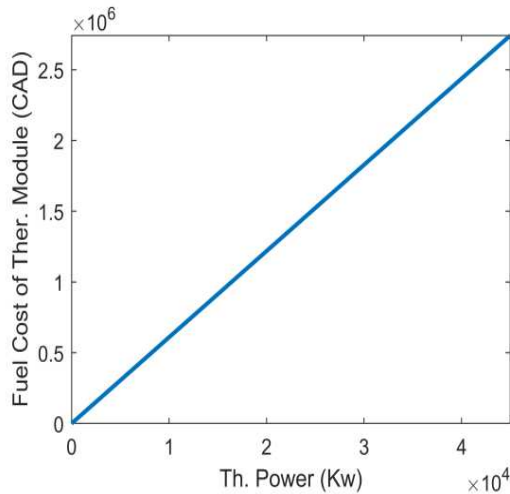


**Figure 40**

*Biomass Supply Cost of the Thermal Module (Vertical Axis) Versus the Thermal Module Rated Capacity (Horizontal Axis)*

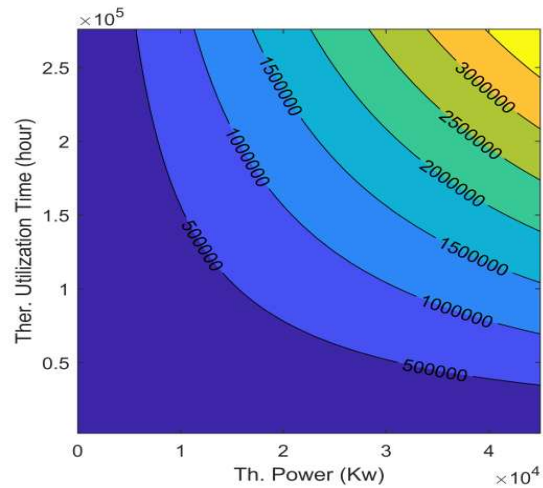


**Figure 41**

*Biomass Supply Cost of Thermal Module (Curves on the Graph) Versus Thermal Module Rated Capacity (Horizontal Axis) and Thermal Module Usage (Utilization) Time (Vertical Axis)*

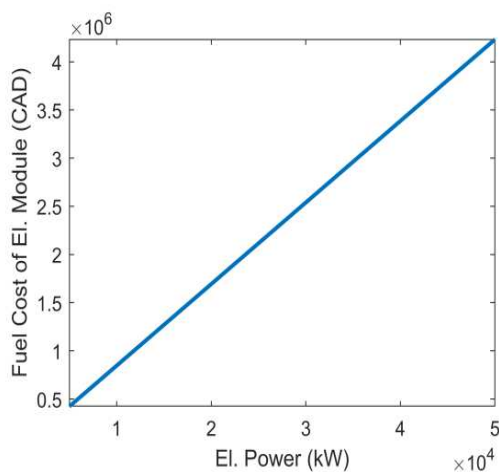


**Figure 42**

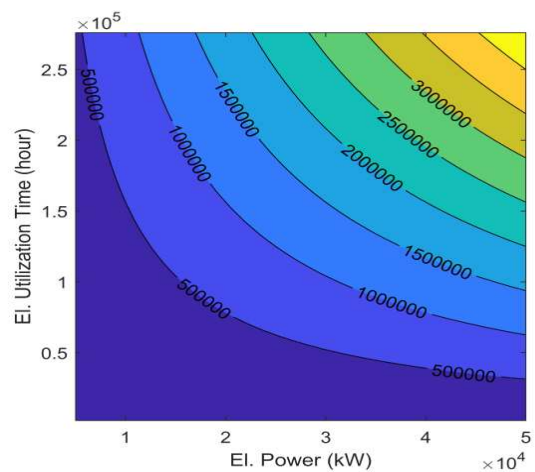


**Figure 43**

*Biomass Supply Cost of the Electrical Module (Vertical Axis) Versus the Electrical Module Rated Capacity (Horizontal Axis)*

*Biomass Supply Cost of the Electrical Module (Curves on the graph) Versus the Electrical Module Rated Capacity (Horizontal Axis) and Electrical Module Usage (Utilization) Time (Vertical Axis)*

However, as can be seen in Figures 44 and 45, the cost of the biomass assigned for electricity generation decreased after the thermal module rated capacity was increased. This cost was exclusively sensitive to thermal module rated capacities but not to its use time.

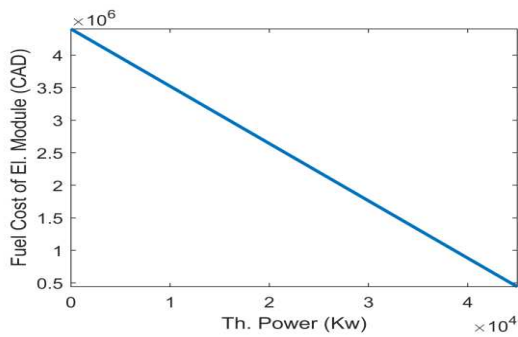


**Figure 44**

*Biomass Supply Cost of the Electrical Module (Vertical Axis) Versus the Thermal Module Rated Capacity (Horizontal Axis)*

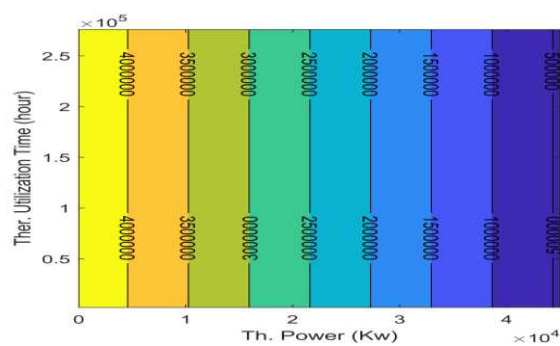


**Figure 45**

*Biomass Supply Cost of Electrical Module (Curves on the graph) Versus the Thermal Module Rated Capacity (Horizontal Axis) and Thermal Module Usage (Utilization) Time (Vertical Axis)*

Figures 46 and 47 depict the behavior of the hydrogen module by presenting the most economic values of the electrolyser versus its and electrical module performance parameters. Figure 46 confirms the behavior of the model with regard to delivering the most preferred optimal values. It demonstrated the direct relation between electrolyser capital cost and its capacity based on the variations of electrolyser flow rates. Figure 47 depicts the dependency of

this module income on the electrical module rated capacity and use time. Model behavior presenting the total cost of the system versus electricity and hydrogen modules' performance parameters is shown in Figures 48 and 49. The values for the total cost of the system studied are illustrated in various scenarios. The figures show that more income and less cost of the system occurred by devoting less rated capacities and use times to electricity modules in favor of increasing the hydrogen module use times and flow rates. The sensitivity of the total cost to the electricity module use time was less than its rated capacities. Figure 50 and Figure 51 illustrate the variation of system total costs versus hydrogen and thermal modules performance parameters, namely electrolyser use time and thermal rated capacities and use time.

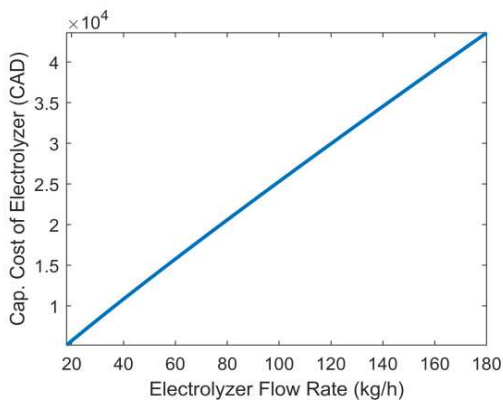


**Figure 46**  
*Hydrogen Module Capital Cost (CAD) Versus Electrolyser Hydrogen Flow Rate*

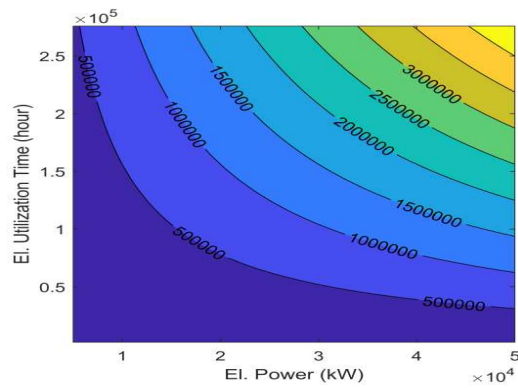


**Figure 47**  
*Electrolyser Module Income (CAD) Illustrated as Curves Versus Electrical Module Rated Capacity (Horizontal Axis) and Electrical Module Usage (Utilization) Time (Vertical Axis)*

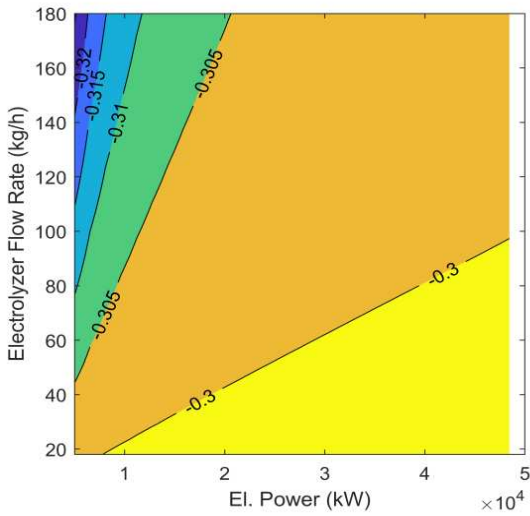


**Figure 48**

*System Total Cost (Curves on the graph) Versus Hydrogen Module Flow Rate (Vertical Axis) and Electrical Module Rated Capacity (Horizontal Axis)*

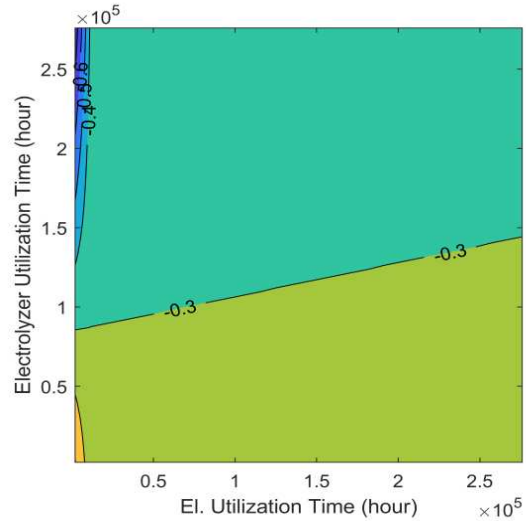


**Figure 49**

*System Total Cost (Curves on the Graph) Versus Hydrogen Module Utilization Time (Vertical Axis) and Electrical Module Utilization Time (Horizontal Axis)*

It is evident that in both cases, increasing the hydrogen module use time decreased the total cost. Moreover, increasing the capacity for heat and hydrogen generation resulted in less total cost. The sensitivity of the system's total cost to the thermal module use time was less than that to the hydrogen module use time, particularly after 10,000 hours of operation.

It can be concluded from Figures 48 to 51 that increasing the rated capacities for the electricity module resulted in more total cost for the thermal module. Further, increasing the potential for hydrogen generation, either by increasing the use time or flow rate, is profitable.

To verify this result, the variation of cost versus thermal and electrical module

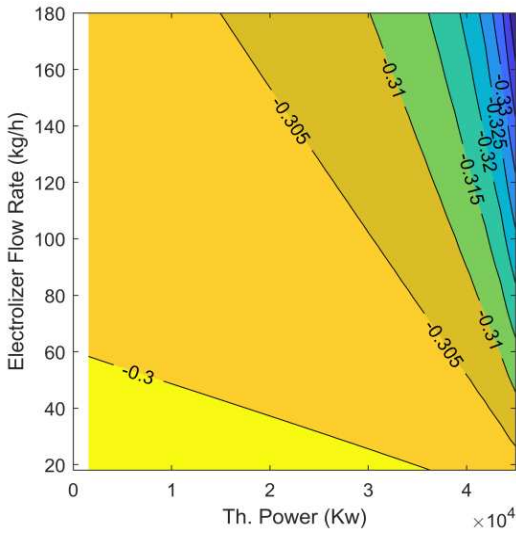


**Figure 50**

*System Total Cost (Curves on the Graph) Versus Hydrogen Module Flow Rate (Vertical Axis) and Thermal Module Rated Capacity (Horizontal Axis)*

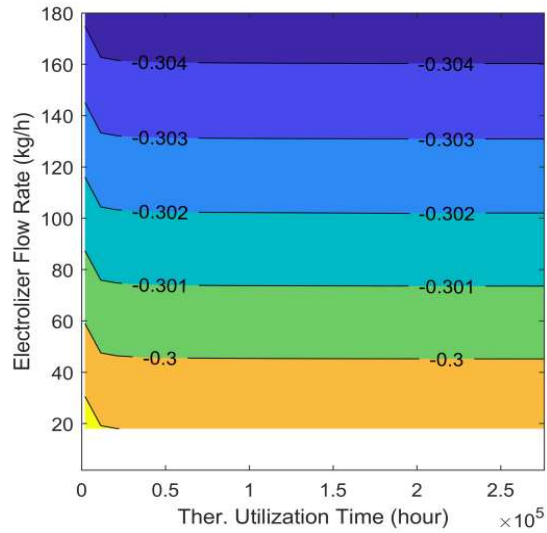


**Figure 51**

*System Total Cost (Curves on the Graph) Versus Hydrogen Module Flow Rate (Vertical Axis) and Thermal Module Utilization Time (Horizontal Axis)*

Three modules' performance parameters were compared in Figures 52 and 53. The results confirmed the results of Figures 50 and 51 by demonstrating that when a hydrogen generation opportunity exists in the integrated system, devoting more shares to hydrogen generation instead of electricity generation is more beneficial. Based on Figures 52 and 53, for fixed values of both electricity and thermal modules rated capacities, raising more income and decreasing cost required more use time for the operation of the hydrogen module. However, at fixed values for hydrogen generation use times, the highest income and lowest cost were yielded in lower electrical modules' rated capacities.

The same results were obtained for larger rated capacities of the thermal module. This confirmed that allocating more capacity to heat generation even at lower flow rates of hydrogen generation could be more profitable than assigning more capacity for electricity generation.

To analyze the impact of maintenance parameters on delivering the most preferred optimal values for all three modules, Figures 54 and 55 present the electrical module income and

the integrated system total cost based on electrical module performance and maintenance parameters, that is, rated capacities and maintenance intervals. At first glance, it seems that income caused by increasing either the size (capacity) and maintenance interval time was favorable as the optimal result. It seemed that it produced more income by selling electricity to the grid and/or through the hydrogen module.

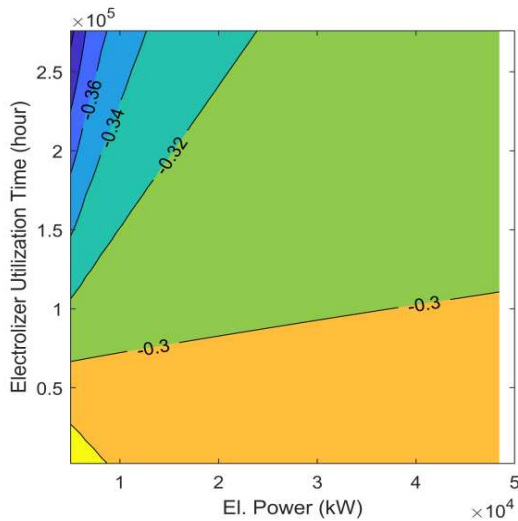


**Figure 52**  
*System Total Cost (Curves on the Graph) Versus Hydrogen Module Utilization Time (Vertical Axis) and Electrical Module Rated Capacity (Horizontal Axis)*

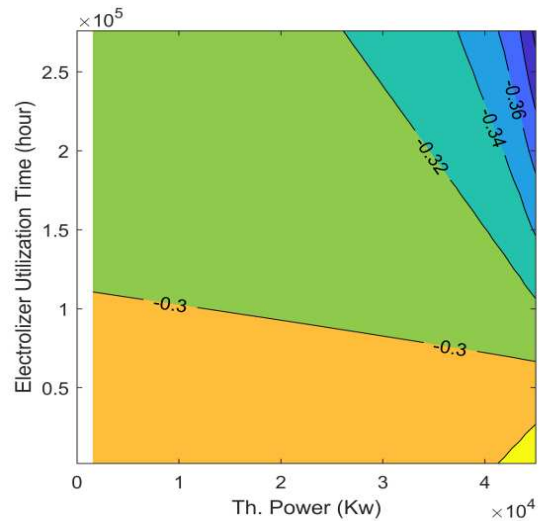


**Figure 53**  
*System Total Cost (Curves on the Graph) Versus Hydrogen Module Utilization Time (Vertical Axis) and Thermal Module Rated Capacity (Horizontal Axis)*

However, after considering the total cost, even though increasing the electrical module capacity increased the module income, the increased income may not compensate (counteract) the capital cost increase, the operating costs such as the biomass fuel purchase, and other costs related to the electrical module. As a result, an unbounded increase in the size of an electrical module would eventually lead to more total cost, and there exists an optimal size for the electrical module. The results showed that income raised from the hydrogen module was greater than that from selling electricity from the electrical module to the grid. The main reason for attributing more capacity for the electrical module was hydrogen generation.

This trend was reversed for the maintenance interval time because increasing the maintenance interval time for the electricity module resulted in less total cost due to decreased maintenance costs and more electricity income.

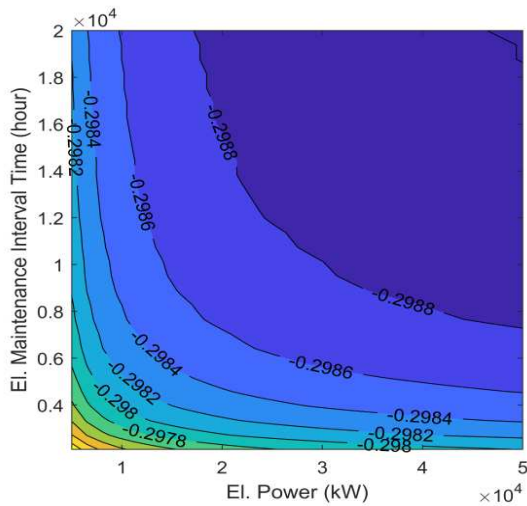


**Figure 54**

*Electrical Module Income (Curves on the Graph) Versus Electrical Module Maintenance Interval Times (Vertical Axis) and Electrical Module Rated Capacity (Horizontal Axis)*

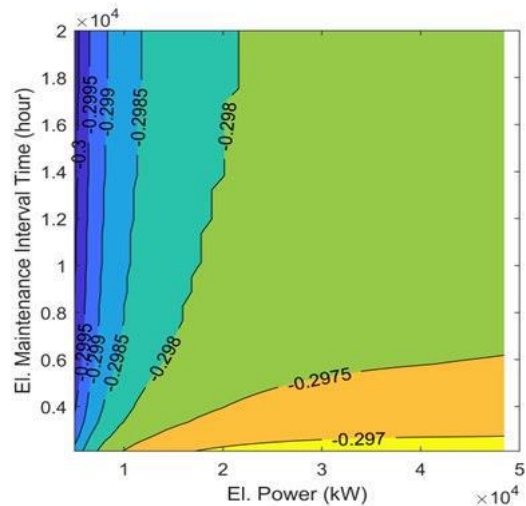


**Figure 55**

*System Total Cost (Curves on the Graph) Versus Electrical Module Maintenance Interval Times (Vertical Axis) and Electrical Module Rated Capacity (Horizontal Axis)*

Figures 56 and 57 show the sensitivity of the thermal module and system total cost to thermal module maintenance interval times and rated capacities. Raising the thermal module rated capacities decreased the thermal module and system total costs. However, the maintenance interval time of the thermal module had no considerable impact on both module cost and the whole system total cost.

The cost profiles of the thermal module, unlike the electrical modules, were not sensitive to maintenance intervals and the thermal module rated capacities. This fact was confirmed in Figure 58, which illustrates variation of system total cost versus thermal and electrical modules maintenance interval times. As is visible in Figure 54, total cost (income) was a function of electrical module maintenance interval times.

Regarding the reliability behavior of such a system, as depicted in Figure 59, the reliability levels for both thermal and electrical modules remained above 55% thanks to the maintenance activities. This confirms that the most preferred optimal values of the total cost, performance, and maintenance parameters for modules and the whole system were achieved by meeting the predefined minimum reliability level for both modules.

This also indicated that after obtaining the most preferred optimal values for the cost, the decrease in the reliability levels was still above those accepted minimum levels during the design phase. The improvements due to the maintenance activities in Figure 59 were addressed by sharp falls in the failure functions for both modules. Maintenance intervals for the thermal module were shorter than those for the electrical module mainly due to the sharper increase of the thermal module failure function compared to the electrical one. It also implied the greater criticality of thermal modules for their operation due to the lower MTTF and higher hazard rates.

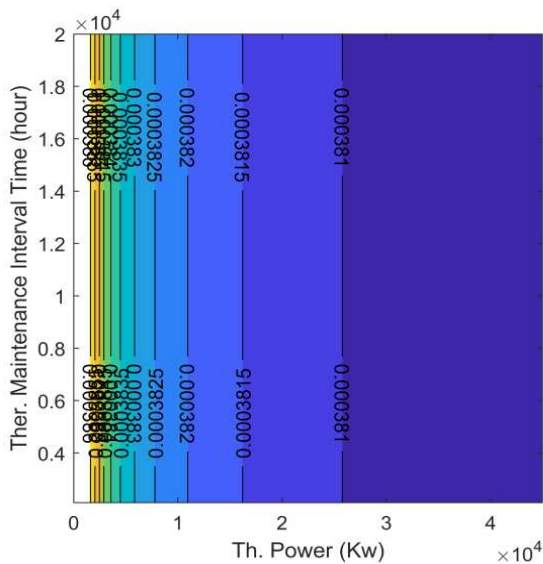


**Figure 56**  
*Thermal Module Cost (Curves on the Graph) Versus Thermal Module Rated Capacity (Horizontal Axis) and Maintenance Interval Times (Vertical Axis) and Thermal Module Rated Capacity (Horizontal Axis)*

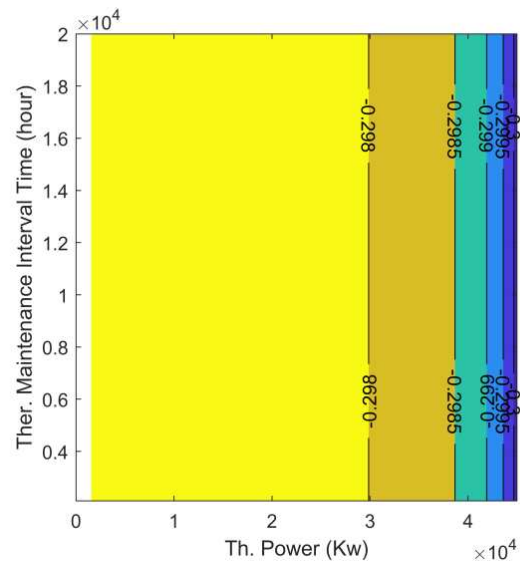


**Figure 57**  
*System Total Cost (Curves on the Graph) Versus Thermal Module Maintenance Interval Times (Vertical Axis) and Thermal Module Rated Capacity (Horizontal Axis)*

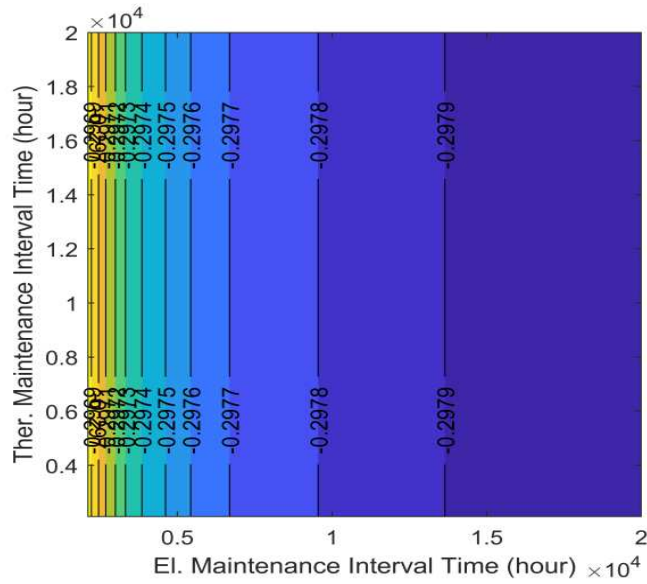


**Figure 58**

*Variation of the System Total Cost (Curves on the Graph) Versus Thermal Modules Maintenance Interval Time (Vertical Axis) and Electrical Module Maintenance Interval Times (Horizontal Axis)*

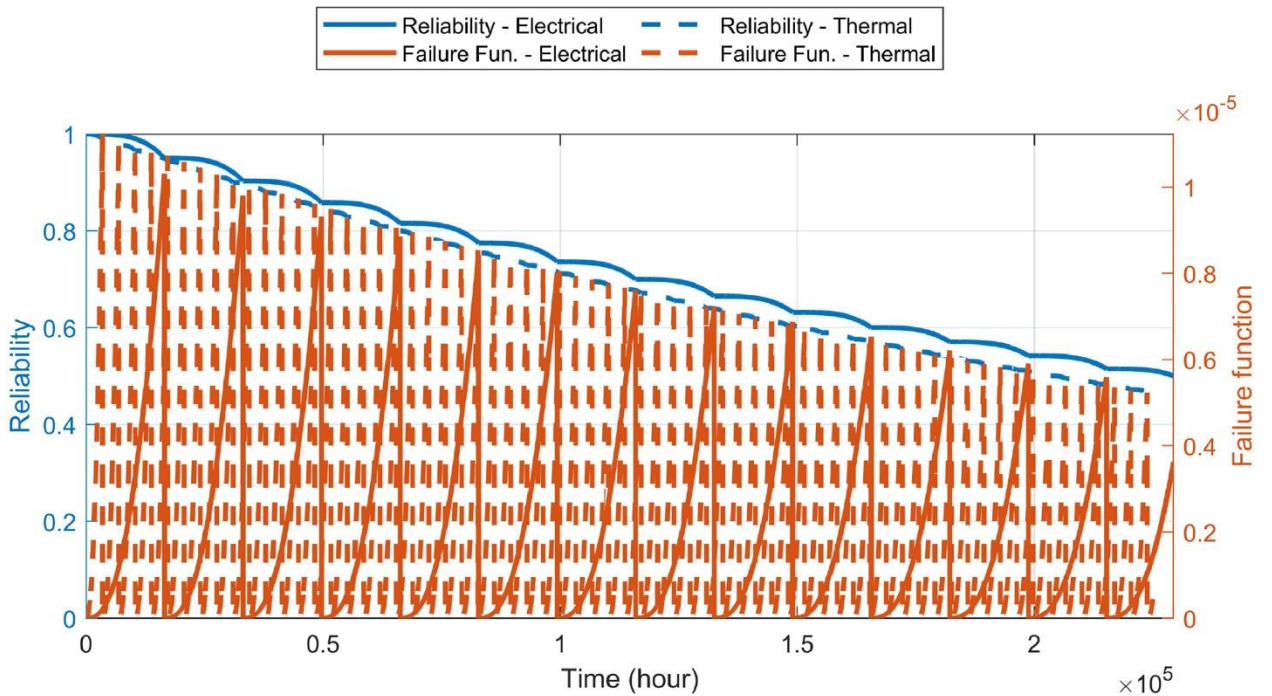


**Figure 59**

*Reliability and Failure Function Variation Versus Time for Electricity and Thermal Modules*

As is obvious from Figure 44 and in line with Figure 43, MTTF of the thermal module was lower than the electrical module, demonstrating its need for fewer maintenance intervals than an electrical module. By increasing maintenance interval, MTTF of both modules decreased. However, increasing the maintenance intervals for the thermal module resulted in a greater reduction of MTTF for the thermal module compared to the electrical module.

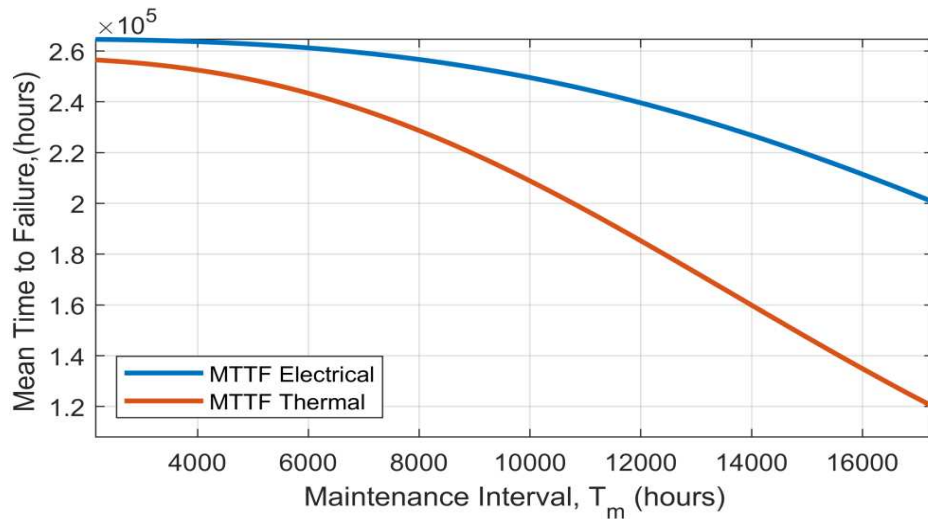


**Figure 60**

*Variation of MTTF of Both Electrical and Thermal Modules Versus Maintenance Interval Times*

#### 4.5 Chapter Summary

As a summary, unlike traditional approaches, which typically optimize for cost or energy efficiency alone, this case—based on the proposed model—incorporates two separate objective functions: cost and pollution, considering biomass chemical composition, pollutant constituents, and the sizing of geothermal modules. This enables the optimization to balance economic and environmental performance as distinct objectives using MCDM methods within a scalable framework, rather than treating emissions as a secondary or simplified factor. Moreover, this case presents how the proposed model optimizes the partitioning of heat generation between biomass and geothermal modules, considering system modularity, borehole sizing, fuel transportation, etc.

Existing methods often assess energy supply sources separately or rely on fixed apportionment strategies, whereas this case can adjust the share of various sources to achieve optimal trade-offs. The proposed model for this case considers real-world constraints (borehole sizing, transportation, fuel costs) more accurately than conventional models that might simplify these aspects. Unlike conventional methods that focus primarily on cost or energy output, this case—based on the proposed BHP model—optimizes a single objective function. Probabilistic RAM function is embedded as a constraint to objective function to deliver simultaneously with system optimal performance parameters, optimal values for RAM metrics such as mean time to failure (MTTF), mean time to repair/restore (MTTR), maintenance intervals, and system availability. This approach allows the optimization to identify operationally reliable and cost-effective configurations for district-level heat and electricity supply, explicitly accounting for system reliability over time rather than treating it as an afterthought.

This case further extends the BHP model by integrating hydrogen generation, evaluating the modularity and scalability of the proposed methodology. The model optimizes a single objective function subject to reliability constraints and operational considerations. This approach enables an integrated assessment of trigeneration systems, considering costs and revenues under reliability constraints.

The research improves validation through several means, including expert feedback, the use and comparison of optimization algorithms (GA and gradient-based methods), MCDM analysis, and the integration of RAM metrics into the optimization framework. Together, these steps ensure that the solutions are not only cost-effective but also operationally robust.

To improve the validity of the optimization results, GA and gradient-based methods were applied, and by comparing the results of these two approaches—one heuristic and population-based, the other derivative-based—it was possible to verify that the results were coherent and

credible. The convergence of results across these methods strengthens the validity of the methodology, models, and their results, confirming that the identified solutions are reliable.

Validation is further reinforced through the progressive application of the methodology to increasingly complex systems, ranging from a single-building heat-only model to district-level configurations, and from simple heat-only systems to CHP and trigeneration systems. This progression both verifies and validates the results of earlier models and demonstrates that the methodology remains robust when scaled and diversified.

Finally, the cases and models are designed to be modular, scalable, and flexible, allowing the integration of multiple energy sources and products, and supporting applications across different scales—from individual buildings to district systems. These characteristics ensure generalizability across diverse energy systems, operating scales, and climates, making the methodology a versatile tool for hybrid energy system optimization and design.

## 5 Chapter 5: Conclusions

### 5.1 Summary

In this thesis, a methodology is developed to be used for modeling a biomass-powered energy system that can be integrated into DHS and be hybridized for energy resources and products such as hydrogen to deliver the optimal performance parameters for minimum cost and pollution after considering biomass chemical compositions and reliability constraints. The reliability indicator is incorporated as a constraint to the cost objective function to satisfy the availability levels for such system operation. In other words, the cost optimization is modeled mathematically by considering a distributed reliability function as a constraint for the nonlinear cost correlation functions of system module performance parameters.

The developed methodology has the potential to be adopted for optimization of every hybridized biomass-powered energy system under reliability constraints by considering the cost correlations of the adopted technologies, biomass chemical compositions, and pollution elements.

Hybridization of biomass-powered systems either by hybridization of the resources (e.g., solar, geothermal) or byproducts (hydrogen) to deliver competitive prices with acceptable levels of availability and reliability could be feasible even in remote areas with harsh climates. The best optimal values for minimum cost of proposed configurations and for delivering multiple outputs with assured minimum reliability levels and optimal values for maintenance intervals are in the range of 0.295 to 0.298 CAD/kWh if the system is devoted to only heat and electricity generation.

The results show the very low sensitivity of the optimal configurations of the system to biomass resource types. This could be attributed to the cost-to-heat content ratio of biomasses that are relatively close to each other. In other words, by increasing the heat content of biomass,

or processing it to burn more efficiently, the biomass feedstock purchase price also increases, resulting in inconsiderable differences in final energy costs. The sensitivity of cost to biomass transportation is more than the biomass purchase cost. This demonstrates that in-place biomass feed stocks are very important for having an economic biomass-powered energy system.

When pollution and transportation supply costs are added to the biomass purchase cost to yield the final biomass cost, this cost is found to be further sensitive to the thermal module than the electricity module. Biomass cost is influenced by both the thermal module's rated capacity and use time, and increasing each one causes the cost to rise.

Electricity generation in the CHP-biomass system is not justified for generating electricity to be sold in large volumes to the electric grid. Although increasing capacity for electricity generation could result in more income for the electricity module, the total income of the whole energy system (including the hydrogen module income) decreases and causes rising system total cost. This is mainly attributed to larger electrical module capital costs and lower energy conversion efficiencies.

Increasing hydrogen module rated capacities and use times decrease system total cost considerably, notably if this is accompanied by sacrificing the electrical module generation capacity to the hydrogen module. In all cases, even by not increasing the hydrogen module rated capacity, rising hydrogen module use time can cause system total cost reduction. This supports the finding that if there are opportunities to sell hydrogen, it is advantageous to integrate hydrogen modules into CHP applications.

Increasing thermal module rated capacities and use times, unlike with electrical modules, result in system total cost reduction. This is primarily due to much lower thermal module capital costs compared to the electrical module and relatively low pollution costs that cannot justify

limiting the huge amount of heat generation over assigning more potential to electricity generation that produces less pollution but has larger module capital cost.

Supplying large volumes of electricity into the grid is justified either by improving the electrical modules' efficiency or increasing the electricity buy-back rates to higher rates, putting competitiveness at risk.

Maintenance interval times of electrical modules are more than those of thermal modules. This characteristic of electrical module, largely due to its higher costs, causes more MTTF to be required for this module. The redundancy for electrical modules is highlighted by this result because less maintenance check times make electrical modules less flexible for maintenance compared to thermal ones. In addition to redundancy, more frequent inspections or doing technical reliability analyses to determine critical item lists helps ensure reliable optimal performances.

## 5.2 Contributions

The novelty of this research is its more comprehensive joint RAM-optimization methodology. Despite being defined as a biomass-powered hybridized energy generation system, its structure and flowchart can be developed further to define more specific methodologies that adopt other fuels (even fossil fuels) and energy conversion technologies, and cost constraints and pollution elements, by replacing the cost correlations, economic factors, and the chemical composition of fuels or pollutions. Implied sensitivity analysis is possible in these methodologies by defining various scenarios as demonstrated in the cases studied in this research.

Another novelty of this research is the integration of RAM analysis for optimization in a mathematical approach that considers the impact of reliability constraints on the most preferred optimal costs, system performance parameters, and RAM.

The reliability functions have been formulated as optimization constraints to cost objective functions. In this way, on the one hand, the optimal values for cost and performance parameters (rated powers, use times) are obtained. On the other hand, the optimal values for reliability and maintainability parameters (time to failure and time to repair or restorations) are yielded to assure system availability at accepted levels. Such outputs of integrated optimization-reliability methodology assist in system operation and maintenance planning.

Another contribution of this research is introducing modularized optimization in which the impact of each module on the optimal technical parameters, minimum cost, or accepted reliability of the system is traceable. For example, the impact of the maintenance activities on the improvement of the reliability of each module at the end of each maintenance interval could be monitored by controlling the extent of the reliability increase. It can help in choosing the better-fit functions for modeling the reliability and planning the maintenance activities.

For cost analysis, just replacing the replaced module cost correlation with a new replacement module is possible without any other modification in methodology to provide the most preferred optimal and reliable parameters for the new system.

### **5.3 Limitations**

Scope of System Boundaries: The proposed methodology and associated models are limited to enviro-economic and techno-economic analyses and do not constitute a life-cycle cost assessment, due to the lack of parameters for administrative costs, service downtimes and delays costs, site construction costs (e.g., land purchase), and biomass processing costs.

Moreover, although the methodology is modular and allows the inclusion or exclusion of various concepts, modules, fuels, and products, the scope is still constrained to energy-related modules such as biomass, borehole geothermal modules, and hybrid CHP configurations. Urban

energy interactions (e.g., integration with other urban sectors) are not considered, which limits the applicability of results in holistic smart city or grid contexts.

**Data Availability and Uncertainty:** The quality and reliability of the methodology outputs are constrained by the uncertainties in data related to the areas of implementation, including the seasonality of renewable resources, future energy demands, national or regional environmental policies (e.g., pollution costs), and the certainty, availability, and accuracy of input data. The proposed methodology and models rely on cost correlations of technical, chemical, and logistics parameters, as well as probabilistic reliability and maintainability data. They can be applied in different regions; however, such correlations must be available and adjusted accordingly to account for uncertainties. For example, the results of this research are specific to Northern Quebec, Canada, where data on biomass purchase, inflation, and interest rates were available at the time of research development.

**Variability of Economic Data:** The optimization framework incorporates cost parameters for fuels and energy products in a fixed manner and does not consider the volatility of electricity and hydrogen selling prices or the seasonality of biomass feedstock driven by market fluctuations, policy incentives, and regional supply-demand conditions. The sensitivity of costs to variations in pollution costs or biomass seasonality, and their impacts on optimal values, were not analyzed due to lack of reliable data.

**Model Complexity and Computational Burden:** The integration of multiple modules, fuels, and technologies within a modular optimization framework significantly increases model complexity. While the methodology supports stepwise optimization and multi-level decomposition to mitigate computational challenges, the execution of large-scale problems remains computationally intensive.

Generalizability and Practical Implementation: The proposed approach has been developed in a research-oriented context, which facilitates methodological innovation but may limit immediate industrial adoption. Implementation in real-world projects may require adaptation to specific regulatory, economic, and operational constraints.

#### 5.4 Future Research Directions

Understanding the low impact of biomass type can help obtain more benefits from generating heat and hydrogen given the current pollution penalty rates and the relatively expensive technologies for electricity generation. It is proposed to focus on optimization-reliability approaches for design and application of biomass-powered energy systems in cold climate regions with a large abundance of biomass feed stocks that are in urgent need of heat and can provide hydrogen for export as income. Hydrogen is highlighted because of its skyrocketing rate of use for various purposes around the world. This makes it a viable option to render whole biomass-powered energy systems more economical and competitive.

The electricity required for these applications can be supplied from solar, wind, or geothermal sources based on their availability or affordability in those regions. Therefore, the proposed future work is enviro-economic optimization of a hybrid BCHP-hydrogen system using biomass modules for heat and hydrogen generation and solar, wind, or geothermal modules for electricity generation. To adapt such systems for smart cities or off-grid applications, considering the energy storage components is of most importance.

In case one has access to reliable data or technical specifications of modules, detailed RAM analyses such as FMECA and FTA could be done on the whole system level or at the module level to enable designers and operators to identify critical items and systems or spare parts necessary for optimization of the maintainability.

Using life-cycle assessment is suggested to scrutinize the environmental aspects of the hybrid system with biomass as the main driver. Because the life-cycle assessment of bioenergy-based systems is complex and faces significant uncertainty, considering reliability and availability is suggested. Moreover, the prediction of biomass is essential when considering the operation of the hybrid system in the future. It is suggested to incorporate a prediction method to improve prediction reliability by including the following four steps:

1. using a simple accounting framework.
2. using a robust selection of probability density functions.
3. using a probabilistic propagation of uncertainty; and
4. using a sensitivity analysis to identify key variables contributing to uncertainty of the overall heating, power, and hydrogen production system.

Furthermore, extending the methodology to include more real-time and transient dynamic scheduling considering energy market sharing and the demand in smart cities for energy exchange and hybridization of BCHP with other renewables and technologies such as wind, fuel cell etc. are suggested for future works.

## 6 References

- A. Al-abidi, Sohif Bin Mat, K. Sopian, M. Y. Sulaiman, Abdulrahman Th. Mohammed, CFD applications for latent heat thermal energy storage: A review, *Renewable and Sustainable Energy Reviews*, 20, 353-363, 2013.
- A. Arsad, M. Hannan, A. Q. Al-Shetwi, M. Mansur, K. Muttaqi, Z. Dong, and F. Blaabjerg, Hydrogen energy storage integrated hybrid renewable energy systems: A review analysis for future research directions, *International Journal of Hydrogen Energy*, 47 (39), 17285-17312, 2022.
- A. Benonysson, B. Bohm and H.F. Ravn, Operational optimization in a district heating system, *Energy Conversion and Management*. 1995; 36; 297-314
- A. H. Schrottenboer, A. A. Veenstra, M. A. uit het Broek, and E. Ursavas, A Green Hydrogen Energy System: Optimal control strategies for integrated hydrogen storage and power generation with wind energy, *Renewable and sustainable energy reviews*, (168), 112744, 2022.
- A. Mazhar, Shuli Liu, Ashish Shukla, A state of art review on the district heating systems, 2018, *renewable and sustainable Energy reviews*, (96), 420-439, 2018.
- A. Nieto-Morote, F. Ruz-Vlila, F. Canovas-Rodríguez, Selection of a trigeneration system using a fuzzy AHP multi-criteria decision-making approach, *Energy Research*. 2011; 35 (9): 781–794
- A. Nuorkivi, Remote control and optimization system of district heating network. *International Symposium on District Heat Simulation*, Reykjavik (1989).

- A. Sharma, V.V. Tyagi, C. R. Chen, D. Buddhi, Review on thermal energy storage with phase change materials and applications, *Renewable and Sustainable Energy Reviews*, 13(2), 318–345, 2009.
- A. Silvennoinen, Computer-Aided operation of district heating systems. The Energy Research Cooperation of the Nordic Council of Ministers 1990.
- A. Uotila, Energy management system (EMS). International Symposium on District Heat Simulation, Reykjavik, April 13-16, 1989.
- A. V. Novo, Joseba R. Bayon, Daniel Castro-Fresno, Jorge Rodriguez-Hernandez, Review of seasonal heat storage in large basins: Water tanks and gravel–water pits, *Applied Energy*, (8)7, Issue 2, 390-397, 2010.
- Aamot, H. and G. Phetteplace, Long distance heat transmission with steam and hot water. 1st International Total Energy Congress, Copenhagen, 4-8 October 1976; 517-549.
- Adams PWR, McManus MC. Small-scale biomass gasification CHP use in industry: energy and environmental evaluation. *Sustainable Energy Technologies and Assessments* 2014:129-140.
- Agyenim F, Hewitt N, The development of a finned phase change material (PCM) storage system to take advantage of off-peak electricity tariff for improvement in cost of heat pump operation, *Energy and Buildings*, 42(9), 2010, Pages 1552-1560.
- Ahmadi MH, Sameti M, Pourkiaei SM, et al. Multi-objective performance optimization of irreversible molten carbonate fuel cell–Stirling heat engine–reverse osmosis and thermodynamic assessment with ecological objective approach. *Energy Science & Engineering*, 2018, 6:783–796.
- Ahmadi P, Dincer I, Rosen MA. Development and assessment of an integrated biomass-based multi-generation energy system. *Energy*, 2013, 56:155–166.

- Al-Abbasi, O.; Abdelkefi, A.; Ghommem, M. Modeling and assessment of a thermochemical energy storage using salt hydrates. *Energy Research*, 41, 2149–2161, 2017.
- Alajmi, A. and Wright, J., 2014. Selecting the most efficient genetic algorithm sets in solving unconstrained building optimization problem. *International Journal of Sustainable Built Environment*, 3(1), pp.18-26.
- Aste N, Caputo P, Del Pero C, et al. A renewable energy scenario for a new low carbon settlement in northern Italy: biomass district heating coupled with heat pump and solar photovoltaic system. *Energy*, 2020, 206:118091.
- Atlas of Canada, Remote Communities Energy Database, Natural Resource Canada. 2019
- AURI. Agricultural renewable solid fuels data. Retrieved from Agricultural Utilization Research Institute Fuels Initiative, [www.auri.org](http://www.auri.org).
- Ayyappan S, Mayilsamy K, Sreenarayanan VV. Performance improvement studies in a solar greenhouse drier using sensible heat storage materials. *Heat and Mass Transfer*, 2016, 52:459–467.
- B. Wei, S.-L. Wang, L. Li Fuzzy comprehensive evaluation of district heating systems, *Energy Policy*, 2010(38), 5947-5955.
- Barbieri ES, Spina PR, Venturini M. Analysis of innovative micro-CHP systems to meet household energy demands. *Applied Energy* 2012; 97:723–33.
- Basu P. Biomass gasification, pyrolysis, and torrefaction: practical design and theory. Academic Press; 2013.
- Belzile, P., Comeau, F.A, Raymond, J., Lamarche, L, *Revue technologique: efficacité énergétique et énergies renouvelables au nord du Québec*. INRS, Centre Eau Terre Environnement, QC, Research Report R1716, 2017.

- Biomass Combined Heat and Power Catalog of Technologies, United states Environmental protection agency, September 2007.
- Boukherroub, T., LeBel, L., Lemieux, S., Woody Biomass Supply Chain Development in Eastern Canada: A case study in Quebec, CIRRELT 24, 1-23. 2016.
- Brandoni C, Renzi M. Optimal sizing of hybrid solar micro-CHP systems for the household sector. *Applied Thermal Engineering* 2015, 75:896–907.
- Buoro D, Pinamonti P, Reini M. Optimization of a distributed cogeneration system with solar district heating. *Applied Energy*, 2014, 124:298–308.
- Böhm, B. On the optimal temperature level in new district heating networks. *Fernwärme International*, 1986; 15: 301-306.
- C. Weber, N. Shah, Optimization based design of a district energy system for an eco-town in the United Kingdom, *Energy* 36 (2011) 1292-1308.
- C.S. Goh, M. Junginger, M. Cocchi, D. Marchal, D. Thran, C. Hennig, et al., Wood pellet market and trade: a global perspective, *Biofuel, Bioproducts and Biorefinery* 2013; 7: 24-42.
- Cao, Y., Dhahad, H. A., Hussien, H. M., Anqi, A. E., Farouk, N., & Issakhov, A. Development and tri-objective optimization of a novel biomass to power and hydrogen plant: a comparison of fueling with biomass gasification or biomass digestion. *Energy*, 238, 122010, 2022.
- Caputo P, Ferla G, Ferrari S. Evaluation of environmental and energy effects of biomass district heating by a wide survey based on operational conditions in Italy. *Energy*, 2019, 174:1210–1218.
- Carine Tran, Luyi Xu, J. Ignacio Torrens Galdiz, Jan L. M. Hensen, Vincent Lemort, Model-based assessment of cost-effective retrofit solutions for a District Heating System extension, *Proceedings of the 15th IBPSA Conference San Francisco, CA, USA, 2017.*

- Casisi M, Pinamonti P, Reini M. Optimal lay-out and operation of combined heat & power (CHP) distributed generation systems. *Energy*, 2009, 34:2175–2183.
- Chen F., Duic N., Manuel Alves L., Carvalho, M., da Graça., *Renewislands—Renewable energy solutions for islands.*, *Renewable and Sustainable Energy Reviews*, 2007, 1888-1902,
- Coelho B, Oliveira A, Schwarzbözl P, et al. Biomass and central receiver system (CRS) hybridization: integration of syngas/ biogas on the atmospheric air volumetric CRS heat recovery steam generator duct burner. *Renewable Energy*, 2015, 75:665–674.
- Connolly D, Lund H, Mathiesen B, Leathy M. A review of computer tools for analyzing the integration of renewable energy into various energy systems. *Applied Energy* 2010; (87) 1059-1082.
- Cormos, C. C. Green hydrogen production from decarbonized biomass gasification: An integrated techno-economic and environmental analysis. *Energy*, 270, 126926, 2023.
- Croteau, R., Gosselin, L., Correlations for cost of ground-source heat pumps and for the effect of temperature on their performance, *Energy Research*. 39, 3015, 433–438.
- D. Gao, D. Jiang, P. Liu, Z. Li, S. Hu, and H. Xu, An integrated energy storage system based on hydrogen storage: Process configuration and case studies with wind power, *Energy*, (66), 332-341, 2014.
- D. N. Dewangan, Manoj Kumar Jha, Y. P. Banjare, Reliability Investigation of Steam Turbine Used In Thermal Power Plant, *Innovative Research in Science, Engineering and Technology*, (3), 2014, 7.
- D.G. Luenberger, Y. Ye, *Linear and Nonlinear Programming*, Springer, US, 2008.
- D.W. Wu, R.Z. Wan, Combined cooling, heating, and power: A review, *Progress in Energy and Combustion Science* 32 (2006) 459–495

- De Gracia A, Oró E, Farid M, Cabeza L, Thermal analysis of including phase change material in a domestic hot water cylinder, *Applied Thermal Engineering*, 31 (17-18), 2011, 3938-3945.
- de Jong E, Higson A, Walsh P, et al. Bio-based Chemicals, Value Added Products from Biorefineries. Wageningen: IEA Bioenergy, Task 42 Biorefinery, 2012, 34.
- De Paepe M, D’Herdt P, Mertens D. Micro-CHP systems for residential applications. *Energy Convers Management* 2006; 47:3435–46.
- Del Barrio E, Godin A, Duquesne M, Daranlot J, Jolly J, Alshaer, W, Kouadio, T, Sommier, A, Characterization of different sugar alcohols as phase change materials for thermal energy storage applications, *Solar Energy Materials and Solar Cells*, 159, 560-569, 2017.
- Demirbas, A. Combustion characteristics of biomass fuels. *Progress Energy Combustion Science*, 30, 2004, 219–230.
- Drescher, U., Bruggemann, D., 2007. Fluid selection for the Organic Rankine Cycle (ORC) in biomass power and heat plants. *Applied Thermal Engineering*. 27 (1), 223-228.
- Duffie, J.A.; Beckman, W.A. *Solar Engineering of Thermal Processes*, Wiley & Sons, Inc.: Hoboken, NJ, USA, 2013.
- Energy-Transition Commission. (2023). Accelerating clean hydrogen in an Electrified economy – Technical Annex.
- F. Wu, R. Gao, C. Li, and J. Liu, A comprehensive evaluation of wind-PV-salt cavern-hydrogen energy storage and utilization system: A case study in Qianjiang salt cavern, China, *Energy Conversion and Management* (277), 116633, 2023.
- Fazlollahi S, Marechal F. Multi-objective, multi-period optimization of biomass conversion technologies using evolutionary algorithms and mixed integer linear programming (MILP). *Applied Thermal Engineering*, 2013, 50:1504–1513.

- Felea, I., Secui, C., Ciobanca, A., & Goia, E. Study on Operational Reliability of Steam Boilers from Oradea CHP Plant. 2023 International Conference on Power Energy, 59-63, 2013
- Fernando Jesus Guevara Carazas and Gilberto Francisco Martha de Souza, Availability Analysis of Gas Turbines Used in Power Plants Thermodynamics (12) 1, 2009, 28-37
- Franco A, Versace M. Multi-objective optimization for the maximization of the operating share of cogeneration system in district heating network. Energy Conversion and Management, 2017, 139:33–44.
- Franco A, Versace M. Optimum sizing, and operational strategy of CHP plant for district heating based on the use of composite indicators. Energy, 2017, 124:258–271.
- Frederiksen, S. Thermodynamic analysis of district heating. Doctoral Dissertation. Lund, Sweden: (1982) Lund Institute of Technology.
- Gerber L, Fazlollahi S, Marechal F. A systematic methodology for the environomic design and synthesis of energy systems combining process integration, life cycle assessment and industrial ecology. Computers & Chemical Engineering, 2013 (59) 2-16.
- Ghaebi H, Bahadori MN, Saidi MH. Performance analysis and parametric study of thermal energy storage in an aquifer coupled with a heat pump and solar collectors, for a residential complex in Tehran, Iran. Applied Thermal Engineering, 2014, 62:156–170.
- Giordano, N., Miranda. M., Kanzeri, I., Dezayes, C., Raymond, J., Shallow geothermal resource assessments for the northern community of Kuujjuaq, Québec, Canada. IGCP636 conference Annual Meeting, Santiago de Chile, 2017.
- Girones V, Moret S, Peduzzi E, et al. Optimal use of biomass in large-scale energy systems: insights for energy policy. Energy, 2017, 137:789–797.
- Golla A, Geis J, Loy T, et al. An operational strategy for district heating networks: application of data-driven heat load forecasts. Energy Informatics, 2020, 3:1–11.

- Gregory D. Williams, Jan C. Jofriet, Kurt A. Rosentrater, Biomass Storage and Handling: Status and Industry Needs, 2008 ASABE Annual International Meeting, Rhode Island June 29 – July 2, 2008.
- Gunasekara SN, Pan R, Chiu JN, et al. Polyols as phase change materials for surplus thermal energy storage. *Applied Energy*, 2016, 162:1439–1452.
- H. Eriksson, on the operation of district heating systems, Department of Energy Conversion, Chalmers University of Technology, Gothenburg April 13-16, 1988.
- H. Li, B. Qin, Y. Jiang, Y. Zhao, and W. Shi, Data-driven optimal scheduling for underground space based integrated hydrogen energy system, *IET Renewable Power Generation*, vol. 16(12), 2521-2531, 2022.
- H. Madsen, H. T. Sogaard, O. P. Palsson, and K. Sejling, Models and methods for optimization of district heating systems. The Energy Research Program of the Danish Ministry of Energy 1990.
- H. Song, H. Guo, Y. Wang, J. Lao, H. Zhu, L. Tang, and X. Liu, A novel hybrid energy system for hydrogen production and storage in a depleted oil reservoir, *International Journal of Hydrogen Energy*, (46)34, 18020-18031, 2021.
- H. T. Lurid, Methods for operational optimization of district heating systems. The Energy Research Cooperation of the Nordic Council of Ministers April 13-16, 1989.
- H. T. Sogaard, Identification and adaptive control of district heating systems. The Institute of Mathematical Statistics and Operations Research, Technical University of Denmark 1988.
- H. Yavuz, Modelling and simulation of a heaving wave energy converter-based PEM hydrogen generation and storage system, *International Journal of Hydrogen Energy*, (45), 50, 26413-26425, 2020.

- Haeseldonckx D, Peeters L, Helsen L, D'haeseleer W. The impact of thermal storage on the operational of residential CHP facilities and the overall CO<sub>2</sub> emissions, *Renewable and Sustainable Energy Reviews*.2007 (11), 1227–1243.
- Hammer A, Reinalter J, Reinplan F. Biomass (district) heating plants. Important technical aspects. prepared for the BIOHEAT seminar Pichl, February 2004.
- Haoshan Ge, Haiyan Li, Shengfu Mei, Jing Liu. Low melting point liquid metal as a new class of phase change material: An emerging frontier in energy area, *Renewable and Sustainable Energy Reviews* (21) 331-346, 2013.
- Hassan A, Shakeel Laghari M, Rashid Y. Micro-encapsulated phase change materials: a review of encapsulation, safety, and thermal characteristics. *Sustainability*, 2016, 8:1046.
- Hassan N.S, Jalil A.A, Hitam C.N.C, et al. Biofuels and renewable chemicals production by catalytic pyrolysis of cellulose: a review. *Environmental Chemistry Letters* 2020, 18:1625–1648.
- Hosseini, S. E., Abdul Wahid, M., Jamil, M. M., Azli, A. A., & Misbah, M. F. A review on biomass-based hydrogen production for renewable energy supply. *International journal of energy research*, 39 (12), 1597-1615, 2015.
- Housing construction in Nunavik, guide to good practices, SOCIÉTÉ D'HABITATION DU QUÉBEC. Government of Quebec, First Edition, 2017.
- International Energy Agency (IEA). *Energy Conservation through Energy Storage (ECES) Programme; Brochure*, International Energy Agency: Paris, France, 2016.
- Invernizzi CM, Iora P, Bonalumi D, et al. Titanium tetrachloride as novel working fluid for high temperature Rankine cycles: thermodynamic analysis and experimental assessment of the thermal stability. *Applied Thermal Engineering*, 2016, 107:21–27.

- J. Cihlar, D. Mavins, and K. Van der Leun, Picturing the value of underground gas storage to the European hydrogen system, Guide house: Chicago, IL, USA, p. 52, 2021.
- J. Li, X. Zhang, H. Pawlak-Kruczek, W. Yang, P. Kruczek, W. Blasiak, Process simulation of co-firing torrefied biomass in a 220 MWe coal-fired power plant, *Energy Conversion Management*. 84, 503-511, 2014.
- Jie P, Zhu N, Li D. Operation optimization of existing district heating systems. *Applied Thermal Engineering*, 2015, 78:278–288.
- Jing YY, Bai H, Wang JJ. Multi-objective optimization design and operation strategy analysis of BCHP system based on life cycle assessment. *Energy*, 2012, 37:405–416.
- Joseph, A. Kabbara, M. Groulx, D. Allred, P. White, M.A, Characterization and real-time testing of phase-change materials for solar thermal energy storage. *Energy Research*, 40, 61–70, 2016.
- Ju, H., Badwal, S., & Giddey, S. A comprehensive review of carbon and hydrocarbon assisted water electrolysis for hydrogen production. *Applied energy*, 231, 502-533. 2018.
- J. Heier, Chris Bales, Viktoria Martin, Combining thermal energy storage with buildings – a review, *Renewable and Sustainable Energy Reviews*. 42, 1305-1325, 2015.
- K. Brown, S. Minett, History of CHP developments and current trends, 1996, 11-22.
- K. Svensson, Cost-optimization in district heating systems. *International Symposium on District Heat Simulation*, Reykjavik, April 13-16, 1989.
- Kalina J. Complex thermal energy conversion systems for efficient use of locally available biomass. *Energy*, 2016, 110:105–115.
- Kalinci, Y., Hepbasli, A., & Dincer, I. Biomass-based hydrogen production: a review and analysis. *International journal of hydrogen energy*, 34 (21), 8799-8817, 2009.

- Karschin I, Geldermann J. Efficient cogeneration, and district heating systems in bioenergy villages: an optimization approach. *Journal of Cleaner Production*, 2015, 104:305–314.
- Kaushal P, Tyagi R. Advanced simulation of biomass gasification in a fluidized bed reactor using Aspen Plus. *Renewable Energy*, 2017, 101:629–636.
- Kaygusuz A., Keles C., Alagoz B.B, Karabiber A., Renewable energy integration for smart sites, *Energy and Buildings* 2013 (64) 456–462.
- Kayo G, Hasan A, Siren K. Energy sharing and matching in different combinations of buildings, CHP capacities and operation strategy. *Energy and Buildings* 2014 (82) 685–695.
- Kays, W.M. and A.L. London, Compact Heat Exchangers, *Journal of Applied Mechanics*. 1960, 27(2): 377
- Kenisarin M, Mahkamov K. Passive thermal control in residential buildings using phase change materials. *Renewable and Sustainable Energy Reviews*, 2016, 55:371–398.
- Konstantinos Karanasios, Paul Parker, Recent Developments in Renewable Energy in Remote Aboriginal Communities, Québec, Canada, *Papers in Canadian Economic Development*, 2017; 16; 98-108
- Koskelainen, L. Optimal dimensioning of district heating networks. *Fernwärme International*, 1980; 9(2):84-90.
- Krajačić, G., Duić, N., Tsikalakis, A., Zoulias, M., Caralis, G., Panteri, E., Carvalho, M., da Graça. Feed-in tariffs for promotion of energy storage technologies, 2011, 1410-1425.
- L. A. Chidambaram, A. S. Ramana, G. Kamaraj, R. Velraj, Review of solar cooling methods and thermal storage options, *Renewable and Sustainable Energy Reviews* 15 (6), 3220-3228, 2011.

- L.J.R. Nunes, J.C.O. Matias, J.P.S. Catalao, A review on torrefied biomass pellets as a sustainable alternative to coal in power generation, *Renewable and Sustainable Energy Reviews* 40 (2014) 153-160.
- L. Zhang, N. Gari, L.V. Hmurcik, Energy management in a microgrid with distributed energy resources, *Energy Conversion Management*. 78, 297–305, 2014.
- Laszlo Sikos, New trends in reliability, availability and maintenance optimization of waste thermal treatment plants. PhD thesis. University of Pannonia. 2010.
- Li H, Wang B, Yan J, et al. Performance of flue gas quench and its influence on biomass fueled CHP. *Energy*, 2019, 180:934–945.
- Li H, Zhang X, Liu L, et al. Proposal and research on a combined heating and power system integrating biomass partial gasification with ground source heat pump. *Energy Conversion and Management*, 2017, 145:158–168.
- Lian ZT, Chua KJ, Chou SK. A thermoeconomic analysis of biomass energy for trigeneration. *Applied Energy*, 2010, 87:84–95.
- Lin, C. Y., Nguyen, T. M. L., Chu, C. Y., Leu, H. J., & Lay, C. H. Fermentative biohydrogen production and its byproducts: A mini review of current technology. developments. *Renewable and Sustainable Energy Reviews*, (82), 4215-4220, 2018.
- Liu M., Steven Tay N., Bell S., Belusko M., Jacob R., et. al., Review on concentrating solar power plants and new developments in high temperature thermal energy storage technologies, *Renewable and Sustainable Energy Reviews*, (53), 1411-1432, 2016.
- Lund H, Duic N, Østergaard PA, et al. Smart energy systems and 4th generation district heating. *Energy*, 2016, 110:1–4.
- Lund H, Moller B, Mathieson BV, Dryland A. The role of district heating in future renewable energy systems. *Energy* 2010; 35: 1381-1390.

- Lund H, Østergaard PA, Chang M, et al. The status of 4th generation district heating: research and results. *Energy*, 2018, 164:147–159.
- Lythcke-Jørgensen C, Ensinas AV, Münster M, et al. A methodology for designing flexible multigeneration systems. *Energy*, 2016, 110:34–54.
- M. Mahmoud, M. Ramadan, S. Naher, K. Pullen, M. A. Abdelkareem, and A. G. Olabi, A review of geothermal energy-driven hydrogen production systems, *Thermal Science and Engineering Progress*, (22),100854, 2021.
- M.Noro, R.M.Lazzarin, F.Busato, Solar cooling and heating plants: An energy and economic analysis of liquid sensible vs phase change material (PCM) heat storage. *International Refrigeration*, 39, 104-116, 2014.
- M. Okundamiya, Size optimization of a hybrid photovoltaic/fuel cell grid connected power system including hydrogen storage, *international journal of hydrogen energy*, (46), 59, 30539-30546, 2021.
- M. Rivarolo, A. Greco, A.F. Massardo, Thermo-economic optimization of the impact of renewable generators on poly-generation smart-grids including hot thermal storage, *Energy Conversion and Management*, 2013 (65) 75–83.
- M. Valdma, m. Keel, h. Tammoja, k. Kilk, Reliability of electric power generation in power systems with thermal and wind power plants, *oil shale*, 2007, (24) 2, 197–208.
- M.H. Ahmadi, M.A. Ahmadi, F. Pourfayaz, H. Hosseinzade, E. Acıkkalp, I. Tlili, M. Feidt. Designing a powered combined Otto and Stirling cycle power plant through multi-objective optimization approach, 2016 (62), 585-595
- M.L. Ferrari, A. Traverso, M. Pascenti, A.F. Massardo, Real time optimization and experimental validation of a smart poly-generation grid with thermal storage device. 5th International Conference on Applied Energy ICAE, Pretoria, South Africa, July 1-4, 2013.

- M. Rezaei, M. Sameti, F. Nasiri, Biomass-fuelled combined heat and power: integration in district heating and thermal-energy storage *Clean Energy*, 2019, 5(1), 44–56.
- M. Rezaei, M. Sameti, F. Nasiri, An enviro-economic optimization of a hybrid energy system from biomass and geothermal resources for low-enthalpy areas, *Energy and Climate Change*, 2, 2021, 100040.
- M. Rezaei, M. Sameti, F. Nasiri, An enviro-economic RAM-based optimization of biomass-driven combined heat and power generation, *Biomass Conversion and Biorefinery*, 2024 (14), 24427–24442
- M. Rezaei, M. Sameti, F. Nasiri, Design optimization for an integrated tri-generation of heat, electricity, and hydrogen powered by biomass in cold climates, *International Journal of Thermofluids*, 2024 (22), 100618.
- Maghanki MM, Ghobadian B, Najafi G, Galogah RJ. Micro combined heat and power (MCHP) technologies and applications. *Renewable and Sustainable Energy Reviews* 2013 (28) 510–24.
- Majorowicz, J.A., Minea, V., 2015, Shallow and deep geothermal energy potential in low heat flow/cold climate environment: northern Quebec, Canada, case study. *Environmental Earth Sciences*, 74, 2015, 5233–5244.
- Marconcini, R. and G. Neri, Numerical simulation of a steam pipeline network. *Geothermics*, 1979; 7:17-27.
- Martinez S, Michaux G, Salagnac P, et al. Micro-combined heat and power systems (micro-CHP) based on renewable energy sources. *Energy Conversion and Management*, 2017, 154:262–285.

- Mavrou P, Papadopoulos AI, Stijepovic MZ, et al. Novel and conventional working fluid mixtures for solar Rankine cycles: performance assessment and multi-criteria selection. *Applied Thermal Engineering*, 2015, 75:384–396.
- McDonald, C.L. and C.H. Bloomster, The geocity model: Description and application. Battelle Pacific Northwest Laboratories, (1977); BNWL-SA-6343.
- Milovanovic N. Zdravko, Modified Method for Reliability Evaluation of Condensation Thermal Electric Power Plant, *Journal of Safety Engineering* 2012, 1(4): 57-67
- Moharamian A, Soltani S, Rosen MA, et al. A comparative thermoeconomic evaluation of three biomass and biomass- natural gas fired combined cycles using Organic Rankine Cycles. *Journal of Cleaner Production*, 2017, 161:524–544.
- Mongibello L, Capezzuto M, Graditi G. Technical and cost analyses of two different heat storage systems for residential micro-CHP plants. *Applied Thermal Engineering*, 2014, 71:636–642.
- Moradi MH, Hajinazari M, Jamasb S, Paripour M. An energy management system (EMS) strategy for combined heat and power (CHP) systems based on a hybrid optimization method employing fuzzy programming. *Energy*, 49: 86–101, 2013.
- Moret S, Peduzzi E, Gerber L, et al. Integration of deep geothermal energy and woody biomass conversion pathways in urban systems. *Energy Conversion and Management*, 2016, 129:305–318.
- Morofsky, E.L. and V. Verma, District Energy System Analysis (DESA) analytical manual. Publics Works Canada, Guidelines Series 1979; 29.
- Mudasar R, Aziz F, Kim MH. Thermodynamic analysis of organic Rankine cycle used for flue gases from biogas combustion. *Energy Conversion and Management*, 2017, 153:627–640.

- Murugan S, Horák B. A review of micro combined heat and power systems for residential applications. *Renewable and Sustainable Energy Reviews*, 2016, 64:144–162.
- Nemés M, Nemés A, Kasperski J, et al. Thermo-hydraulic analysis of heat storage filled with the ceramic bricks dedicated to the solar air heating system. *Materials*, 2017, 10:940. 1-20.
- Noussan M, Abdin GC, Poggio A, et al. Biomass-fired CHP and heat storage system simulations in existing district heating systems. *Applied Thermal Engineering*, 2014, 71:729–735,
- NREL, National Renewable energy Laboratory. 2010. Hydrogen Production: Fundamentals and Case Study Summaries
- Nussbaumer T, Thalmann S. Influence of system design on heat distribution costs in district heating. *Energy*, 2016, 101:496–505.
- Oleg Borisovich Shonin, Roman Alekseyevich Salov, Improvement of energy efficiency, reliability and environmental safety of power plants based on associated petroleum gas, *Journal of Ecological Engineering*, 18, (3), 2017, 91–96.
- Ondeck AD, Edgar TF, Baldea M. Optimal operation of a residential district-level combined photovoltaic/natural gas power and cooling system. *Applied Energy*, 2015, 156:593–606.
- Oner, O., & Dincer, I. A unique solar and biomass-based system for integrated production of electricity, heat, freshwater, hydrogen and ethanol. *Energy Conversion and Management*, 269, 116115, 2022
- Optimal Design of Piping Systems for District Heating. Gary Phetteplace, August 1995.
- Ostro Cornwall, Structural lifetime, reliability and risk analysis approaches for power plant components and systems, VTT publications 775, 2011.
- P. L. Chang, C. W. Hsu, C. Y. Lin, Assessment of hydrogen fuel cell applications using fuzzy multiple-criteria decision making method, *Appl. Energy* 100, 93–99, 2012.

- Paksoy, H., Snijders, A. Stiles, L. State of the art review of aquifer thermal energy storage systems for heating and cooling building. In Proceedings of the Effstock Conference, Stockholm, Sweden, 5–17 June 2009.
- Pantaleo AM, Camporeale SM, Sorrentino A, et al. Hybrid solar-biomass combined Brayton/organic Rankine-cycle plants integrated with thermal storage: techno-economic feasibility in selected Mediterranean areas. *Renewable Energy*, 2020, 147:2913–2931.
- Pfeifer A, Dominković DF, Ćosić B, et al. Economic feasibility of CHP facilities fueled by biomass from unused agriculture land: case of Croatia. *Energy Conversion and Management*, 2016, 125:222–229.
- Phetteplace, G.E. Transient analysis of heat transmission systems. USA Cold Regions Research and Engineering Laboratory, CRREL Report. 1981; 81: (24)
- Philippe, M., Bernier, M., Marchio, D., sizing calculation spreadsheet: vertical geothermal bore fields, *ASHRAE Journal*, 52(7), 2010, 20-28.
- Pirkandi J, Jokar MA, Sameti M, et al. Simulation and multi- objective optimization of a combined heat and power (CHP) system integrated with low-energy buildings. *Building Engineering*, 2016, 5:13–23.
- Postnikov, I. A reliability assessment of the heating from a hybrid energy source based on combined heat and power and wind power plants. *Reliability Engineering & System Safety*, 221, 108372, 2022.
- Powell KM, Kim JS, Cole WJ, et al. Thermal energy storage to minimize cost and improve efficiency of a polygeneration district energy system in a real-time electricity market. *Energy*, 2016, 113:52–63.

- Prakash M, Sarkar A, Sarkar J, et al. Proposal and design of a new biomass-based syngas production system integrated with combined heat and power generation. *Energy*, 2017, 133:986–997.
- Prato A Pini, Strobino F, Broccardo M, Giusino L Parodi. Integrated management of cogeneration plants and district heating networks. *Applied Energy* 2012; 97:590–600.
- Preto, F. Properties of the 13 common biomass fuels in Ontario. Natural Resource Canada (NRCan), Ottawa, ON.
- Proskurina S, Heinimö J, Schipfer F, et al. Biomass for industrial applications: the role of torrefaction. *Renewable Energy*, 2017, 111:265–274.
- Qiu, G., 2012. Selection of working fluids for micro-CHP systems with ORC. *Renewable Energy*, 48, 565-570.
- Ren H, Gao W, Ruan Y. Optimal sizing for residential CHP system. *Applied Thermal Engineering*, 2008 (28) 514–523.
- RETScreen Engineering&Cases Textbook. Biomass Heating Project Analysis, Canada 2001-2005.
- Rivarolo M, A. Cuneo, A. Traverso, A.F. Massardo, Design optimisation of smart poly-generation energy districts through a model-based approach, (25), 291-301, 2016.
- Rolfsman B. Combined heat-and-power plants and district heating in a deregulated electricity market. *Applied Energy* 2004 (78) 37–52.
- Rommel M, Hauer A, van Helden W. IEA SHC Task 42/ECES Annex 29 Compact thermal energy storage. *Energy Procedia*, 2016, 91:226–230.
- Ruan Y, Liu Q, Zhou W, et al. Optimal option of distributed generation technologies for various commercial buildings. *Applied Energy*, 2009, 86:1641–1653.

- S. S. Farahani, C. Bleeker, A. van Wijk, and Z. Lukszo, Hydrogen-based integrated energy and mobility system for a real-life office environment, *Applied energy*, (264), 114695, 2020.
- Sameti M, Haghghat F. A two-level multi-objective optimization for simultaneous design and scheduling of a district energy system. *Applied Energy*, 2017, 208:1053–1070.
- Sameti M, Haghghat F. Hybrid solar and heat-driven district cooling system: optimal integration and control strategy. *Solar Energy*, 2019, 183:260–275.
- Sameti M, Haghghat F. Integration of distributed energy storage into net-zero energy district systems: optimum design and operation. *Energy*, 2018, 153:575–591.
- Sameti M, Haghghat F. Optimization approaches district heating and cooling thermal network. *Energy and Buildings*, 2017, 140:121–130.
- Sameti M, Haghghat F. Optimization of 4th generation distributed district heating system: design and planning of combined heat and power. *Renewable Energy*, 2019, 130:371–387.
- Sarbu, I, Sebarchievici, C, Review: A Comprehensive Review of Thermal Energy Storage, *Sustainability*, 10 (1), 191, 2018.
- Sartor K, Dewallef P. Integration of heat storage system into district heating networks fed by a biomass CHP plant. *Journal of Energy Storage*, 2018, 15:350–358.
- Sartor K, Quoilin S, Dewallef P. Simulation and optimization of a CHP biomass plant and district heating network. *Applied Energy*, 2014, 130:474–483.
- Singh, S., Pandey, G., Rath, G. K., Veluswamy, H. P., & Molokitina, N. Life cycle assessment of biomass-based hydrogen production technologies: A review. *International Journal of Green Energy*, 1-16, 2023.
- Smith A, Mago P, Fumo N, Benefits of thermal energy storage option combined with CHP system for different commercial building types, *Sustainable Energy Technologies and Assessments*, 2013 (1) 3-12,

- Sorrentino A, Pantaleo AM, Le Brun N, et al. Energy performance and profitability of biomass boilers in the commercial sector: a case study in the UK. *Energy Procedia*, 2018, 148:639–646.
- Soumerai, H. *Practical Thermodynamic Tools for Heat Exchanger Design Engineers*. New York: John Wiley and Sons. 1987.
- Stijepovic MZ, Papadopoulos AI, Linke P, et al. Organic Rankine Cycle system performance targeting and design for multiple heat sources with simultaneous working fluid selection. *Journal of Cleaner Production*, 2016, 14:1950–1970.
- Stojiljković MM, Blagojević BD. Multi-objective combinatorial optimization of trigeneration plants based on metaheuristics. *Energies*, 2014, 7:8554–8581.
- Stoner, M. Modeling the steady state pressure-flow response of steam and water systems. In *Proceedings of the Annual Conference of the International District Heating Association*, 1974, 53-69.
- Stritih U, Butala V, Optimization of a thermal storage unit combined with a biomass boiler for heating buildings, *Renewable Energy* 2004, 29 (12) 2011-2022.
- Szepe, S. and J. Calm, Thermal fluid selection for long-distance heat transmission. In *Proceedings of the 14th Intersociety Energy Conversion Engineering Conference*, Boston, Massachusetts, 5-10 August 1979.
- T. E. W. Schumann, Heat transfer: A liquid flowing through a porous prism, *Journal of the Franklin Institute*, 208 (3), 405-416.
- Terhan M, Comakli K. Design and economic analysis of a flue gas condenser to recover latent heat from exhaust flue gas. *Applied Thermal Engineering*, 2016, 100:1007–1015.

- The U.S. Department of Energy, Combined Heat and Power, A vision for the future, ITP  
Industrial Distributed Energy: Combined Heat and Power - A Decade of Progress, A  
Vision for the Future, August 2019.
- Tol, H.I, Dinçer, I., Svendsen, S., (2015) Determining the Optimal Capacities of Renewable  
Energy-Based Energy Conversion Systems for Meeting the Demands of Low-Energy  
District Heating, Electricity, and District Cooling: Case Studies in Copenhagen and  
Toronto. *Progress in Clean Energy*, (2), 777-830.
- Trillat-Berdat V, Souyri B, Fraisse G. Experimental study of a ground-coupled heat pump  
combined with thermal solar collectors. *Energy and Buildings*, 2006, 38:1477–1484.
- Valizadeh, S., Hakimian, H., Farooq, A., Jeon, B. H., Chen, W. H., Lee, S. H., ... & Park, Y. K.  
Valorization of biomass through gasification for green hydrogen generation: A  
comprehensive review. *Bio resource technology*, 365, 128143, 2022.
- Vallios.I, Tsoutsos.T, Papadakis.G, Design of biomass district heating systems, *Biomass and  
Bioenergy* (2009), 33: 659-678.
- Verda V, Coletta F. Primary energy savings through thermal storage in district heating networks.  
*Energy*, 2011, 36:4278–4286.
- Verhaert I, Mulder G, De Paepe M. Evaluation of an alkaline fuel cell system as a Micro-CHP.  
*Energy Conversion and Management*, 2016, 126:434–445.
- Vesterlund M, Dahl J. A method for the simulation and optimization of district heating systems  
with meshed networks. *Energy Conversion and Management*, 2015, 89:555–567.
- Victor, R.A., Kim, J.K., Smith, R., 2013. Composition optimisation of working fluids for organic  
Rankine Cycles and Kalina cycles. *Energy* 55, 114-126.

- Vincent Basecq, Ghislain Michaux, Christian Inard, Patrice Blondeau. Short-term storage systems of thermal energy for buildings: a review, *Advances in Building Energy Research*, 7, 66–119, 2013.
- Volkova A, Latosov E, Siirde A. Heat storage combined with biomass CHP under the national support policy. a case study of Estonia. *Environmental and Climate Technologies*, 2020, 24:171–184.
- Volkova, A., Latõšov, E., Andrijaškin, M., Siirde, A., Feasibility of Thermal Energy Storage Integration into Biomass CHP-Based District Heating System. *Chemical engineering transactions*, (70), 2018, 498-504.
- W. Jiang-Jiang, Z. Chun-Fa, J. You-Yin, Multi-criteria analysis of combined cooling, heating, and power systems in different climate zones in China, *Applied Energy* 2010 87 (4); 1247–1259.
- Wang H, Yin W, Abdollahi E, et al. Modeling and optimization of CHP based district heating system with renewable energy production and energy storage. *Applied Energy*, 2015, 159:401–421.
- Wang JJ, Jing YY, Zhang CF, Shi GH, Zhang XT. A fuzzy multi-criteria decision-making model for trigeneration system. *Energy Policy* 2008 (3), 3823-3832.
- Wang K, Satyro MA, Taylor R, et al. Thermal energy storage tank sizing for biomass boiler heating systems using process dynamic simulation. *Energy and Buildings*, 2018, 175:199–207.
- Weber C, Maréchal F, Favrat D, Kraines S. Optimization of an SOFC-based decentralized poly-generation system for providing energy services in an office-building in Tokyo. *Applied Thermal Engineering* 2006 (26):1409-1419.
- Werner S. International review of district heating and cooling. *Energy*, 2017, 137:617–631.

- Werner, S.E. *The Heat Load in District Heating Systems*. Göteborg, Sweden: Chalmers University of Technology. (1984)
- Windeknecht M, Tzscheutschler P. Optimization of the heat output of high temperature fuel cell micro-CHP in single family homes. *Energy Procedia*, 2015, 78:2160–2165.
- Y. E. Yuksel, M. Ozturk, and I. Dincer, Thermodynamic analysis and assessment of a novel integrated geothermal energy-based system for hydrogen production and storage, *International Journal of Hydrogen Energy*, (43) 9, 4233-4243, 2018.
- Y. Qiu, S. Zhou, J. Wang, J. Chou, Y. Fang, G. Pan, and W. Gu, Feasibility analysis of utilizing underground hydrogen storage facilities in integrated energy system: case studies in China, *Applied energy*, (269), 115140, 2020.
- Y.Tian, C.Y.Zhao, “A review of solar collectors and thermal energy storage in solar thermal applications”. *Applied Energy*, 104, 538-553, 2013.
- Y. Zhang, Q. Hua, L. Sun, and Q. Liu, Life cycle optimization of renewable energy systems configuration with hybrid battery/hydrogen storage: a comparative study, *Journal of Energy Storage*, (30), 101470, 2020.
- Yuan Y, Zhang N, Tao W, et al. Fatty acids as phase change materials: A review. *Renewable and Sustainable Energy Reviews*, 2014, 29:482–498.
- Zajacs A, Bogdanovics R, Borodinecsa A. Analysis of low temperature lift heat pump application in a district heating system for flue gas condenser efficiency improvement. *Sustainable Cities and Society*, 2020, 57:102130.
- Ziebig A, Gladysz P. Optimal coefficient of the share of cogeneration in district heating systems. *Energy*, 2012, 45:220–227.
- Ziher D, Poredos A. Economics of a trigeneration system in a hospital. *Applied Thermal Engineering* 2006 (26) 680–687.

Østergaard PA, Johannsen RM, Lund H, et al. new developments in 4th generation district heating and smart energy systems. *International Journal of Sustainable Energy Planning and Management*, 2020, 27:1–3.

Ünal AN, Ersöz İ, Kayakutlu G. Operational optimization in simple tri-generation systems. *Applied Thermal Engineering*, 2016, 107:175–183.